UC San Diego

UC San Diego Electronic Theses and Dissertations

Title

Improving aircraft endurance through extremum seeking

Permalink

https://escholarship.org/uc/item/7cq8p1n9

Author

Krieger, James Paul

Publication Date

2012

Peer reviewed|Thesis/dissertation

eScholarship.org Powered by the California Digital Library
University of California

UNIVERSITY OF CALIFORNIA, SAN DIEGO

Improving Aircraft Endurance Through Extremum Seeking

A dissertation submitted in partial satisfaction of the
requirements for the degree
Doctor of Philosophy

in

Engineering Science (Aerospace Engineering)

by

James Paul Krieger

Committee in charge:

Professor Miroslav Krstic, Chair
Professor Thomas Bewley
Professor Massimo Franceschetti
Professor David Miller
Professor Michael Todd

2012

Copyright
James Paul Krieger, 2012
All rights reserved.

The dissertation of James Paul Krieger is approved, and it is acceptable in quality and form for publication on microfilm and electronically:

_____

_____

_____

_____

_____

Chair

University of California, San Diego

2012

TABLE OF CONTENTS

LIST OF FIGURES

LIST OF TABLES

ACKNOWLEDGEMENTS

The author expresses his gratitude to Professor Miroslav Krstic and the committee in charge for guiding the research contained herein and to local industry for offering the use of proprietary aircraft simulation software.

The author thanks the San Diego chapter of the ARCS Foundation for their dedication to advancing science in America and for their support of his graduate work at UCSD.

Chapter 2 contains material that appears in the Journal of Guidance, Control, and Dynamics (Krieger, J., and Krstic, M., AIAA, November-December 2011). The authors retain the copyright to this material. The dissertation author was the primary investigator and author of this material.

Chapter 3 contains material that is currently being prepared for submission for publication (Krieger, J., and Krstic, M.). The dissertation author was the primary investigator and author of this material.

Chapter 4 contains material that has been submitted for publication to the Journal of Guidance, Control, and Dynamics (Krieger, J., and Krstic, M.). The dissertation author was the primary investigator and author of this material.

VITA

2000	B.A. in Political Science, Purdue University
2006	B.S. in Mechanical Engineering, University of California, Davis
2007	M.S. in Mechanical and Aeronautical Engineering, University of California, Davis
2007–2012	ARCS Foundation Award Recipient
2012	Ph.D. in Engineering Science (Aerospace Engineering), University of California, San Diego

ABSTRACT OF THE DISSERTATION

Improving Aircraft Endurance Through Extremum Seeking

by

James Paul Krieger

Doctor of Philosophy in Engineering Science (Aerospace Engineering)

University of California, San Diego, 2012

Professor Miroslav Krstic, Chair

The length of time a jet aircraft is capable of remaining airborne can be maximized by flying at the speed that produces the least amount of drag. This speed may be predicted based on wind tunnel models, but the optimal speed for any aircraft in service differs somewhat from the calculated speed. Identifying the optimal speed has the potential to realize fuel savings and improve endurance. Extremum seeking is a non-model based form of real time nonlinear optimization that is suitable for problems such as this; however, traditional extremum seeking involves adding a small periodic perturbation to the control input. In this application, this would mean perturbing the throttle, which could erase the fuel savings otherwise achieved by the optimization process.

To address this problem, a modified form of extremum seeking is developed that uses atmospheric turbulence in place of throttle perturbations. Using stochastic averaging, it is proven analytically that the extremum-seeking controller stabilizes the speed of the aircraft to the minimum-drag speed, with an average offset proportional to the third derivative of the drag curve and the variance of the airspeed. Brief simulation results illustrate the performance of the basic algorithm.

Next, a new form of extremum seeking is introduced that extends a recent development in extremum seeking (called Newton method extremum seeking) to systems using stochastic perturbations. This work is parallel to the work on endurance optimization, but is relevant because the gradient estimator developed herein correctly estimates a two-dimensional gradient with perturbations of different amplitudes in the two dimensions.

This is used in a refinement of the basic endurance optimization algorithm that involves a two-dimensional dependence; lift and drag are treated as functions of not only angle of attack (as implicitly assumed to this point) but also Mach number. Optimization proceeds along a line of constant lift in this two-dimensional plane. Analysis proves similar convergence properties for the refined algorithm, and the algorithm is tested in a high fidelity simulation lent by local industry. Simulation results show improvement over the nominal loiter speed.

Chapter 1

Introduction

In the past decade, a form of real time nonlinear optimization called extremum seeking has experienced a resurgence of academic interest. This has resulted in a number of theoretical extensions and numerous applications. The research contained in this dissertation is motivated by a particular application of extremum seeking: maximizing the length of time for which an aircraft can remain airborne, that is, maximizing aircraft endurance.

This introduction provides general background information on the subject of extremum seeking. The later chapters describe how extremum seeking may be used for the application in question. While the later chapters are designed to stand alone, they are sorted in order of increasing complexity and may be best understood on the foundation of the preceding chapters.

Extremum seeking in its most basic form consists of three components.

1. A periodic perturbation added to the control input of a given system.

2. A gradient estimator in which the output of the system is demodulated by the periodic perturbation.

3. An adaptation law that slowly moves the average control input in a way that drives the gradient estimate to zero.

These three components are shown schematically in Fig. 1.1. The periodic perturbation is $\sin(\omega t)$. It is scaled by some constant a and then added to the input

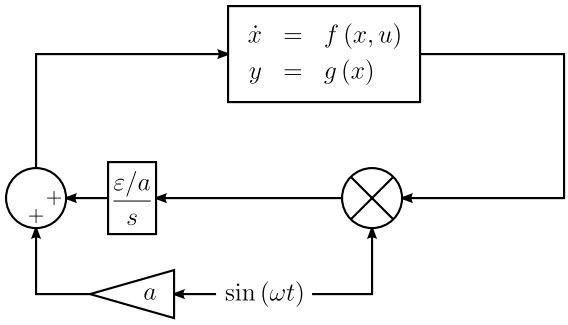

Figure 1.1: Extremum seeking in its most basic form.

to a generic dynamic system. The system is assumed stable (either naturally or through a control system subsumed in the plant model). It is assumed that the steady state output of the system can be minimized by appropriate selection of the control input, and it is the goal of extremum seeking to find this optimal input.

To find this optimal input, the output of the system is measured and multiplied by the same sine wave used to generate the perturbation to the control input. This forms a product which, if averaged over time, is very nearly proportional to the slope of the steady state input-output map of the dynamic system. The nominal control input is then set by slowly integrating this slope estimate. The integral gain is chosen as some number denoted by ϵ (which we all know is small) divided by the amplitude of the perturbation. This division allows the adaptation rate to be independent of the perturbation amplitude. If the gain ϵ is chosen sufficiently small, then the dynamics of the system and the gradient estimator are time-scale separated from the integrator. The results is something very much like a gradient descent to the optimal point of the steady state input-output map. The scheme shown in Fig. 1.1 finds a maximum (assuming ϵ and a are chosen positive), but can be reconfigured to find a minimum by making the integral gain negative and so can in general find an extremum (maximum or minimum) of the system output.

The form of extremum seeking shown in Fig. 1.1 is the most basic and is sufficient for analytical proofs of stability, but the form shown in Fig. 1.2 significantly improves the achievable rate of convergence to the extremum. This is a

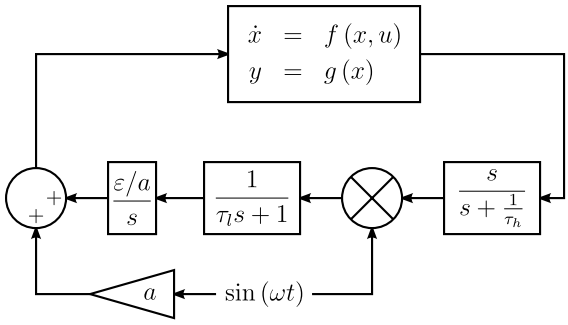

Figure 1.2: Extremum seeking in standard form.

more standard form used in practice and for many simulations. High pass filtering the output serves to extract the DC component of the signal, which greatly reduces the oscillations seen in the gradient estimator. Having a smoother gradient estimate allows the adaptation rate to be increased without causing instability. Note that once the system has converged to the extremum, the control law will tend to produce small oscillations in the estimate of the optimal input, oscillations that remain as long as the extremum seeking algorithm is active. Low pass filtering the gradient estimate serves to reduce the amplitude of these oscillations. For a comprehensive review of extremum seeking, see the text [1] and the survey paper [2].

One additional form of extremum seeking relevant to the following chapters is a stochastic variant. Stochastic extremum seeking is quite similar to standard extremum seeking, only letting the periodic perturbation be a stochastic signal rather than a sinusoid or some other deterministic signal. Stochastic extremum seeking is depicted in Fig. 1.3, which shows the sine wave replaced by the stochastic signal η. Note that the stochastic signal is bounded, here explicitly so by a saturation function. It is included because a bounded signal is necessary for certain proofs of stability based on the stochastic averaging theory presented in [3].

While extremum seeking has traditionally employed an added perturbation signal as a key component of the controller, nothing requires that the signal be generated by the control system. Indeed, any additive disturbance with suitable properties can be used as long as the disturbance is measurable. This concept

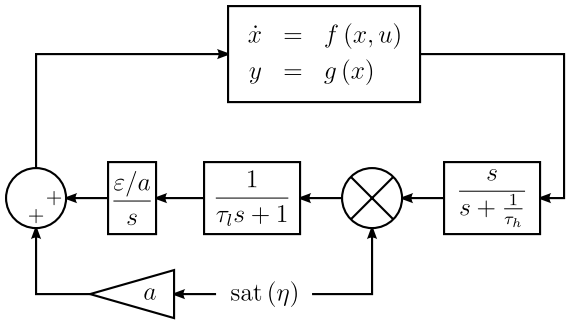

Figure 1.3: Stochastic extremum seeking.

seems to have been first applied only recently in [4]. This is the starting point for the following research.

Chapter 2

Extremum Seeking Based on Atmospheric Turbulence for Aircraft Endurance

Traditional extremum seeking depends on adding a perturbation to the control input, but it is untenable to continuously perturb the throttle in a controller meant to minimize fuel consumption. Inspired by a recent application of extremum seeking to a fusion reactor where internal non-periodic perturbations were employed in the seeking process, a novel variant of extremum seeking is proposed that utilizes naturally occurring stochastic disturbances in lieu of the traditionally-added perturbation signal. Relying on airspeed perturbations from atmospheric turbulence to reveal the local slope of the drag curve, the scheme induces a gradient descent to the minimum drag speed. Using stochastic averaging, it is proven analytically that the extremum-seeking controller stabilizes airspeed to the minimum-drag speed, with an average offset proportional to the third derivative of the drag curve and the variance of the airspeed. Brief simulation results illustrate the performance of the algorithm.

2.1 Nomenclature

A	=	Aspect ratio
a	=	Stochastic disturbance post-saturation scaling factor
B	=	Timescale-shifted and scaled Brownian motion
b	=	Engine thrust proportionality constant
C_2, C_4	=	Averaging constants
C_D	=	Coefficient of drag
C_{D0}	=	Zero-lift drag coefficient
C_{Di}	=	Induced drag coefficient
C_L	=	Coefficient of Lift
D	=	Drag
$\bar{D}$	=	Re-centered drag function
e	=	Oswald efficiency number
		(also base of natural logarithm)
g	=	Acceleration due to gravity
J	=	Jacobian of a system
k_{ES}	=	Extremum-seeking gain
k_i	=	Integral gain
k_p	=	Proportional gain
L	=	Lift
L_u, L_v, L_w	=	Characteristic lengths of turbulence field
		(longitudinal, lateral, vertical)
m	=	Mass of the aircraft
n_0, n_1, n_2	=	Coefficients of the assumed form of $v_{eq}^{e,a}$
q	=	Stochastic disturbance pre-saturation scaling factor
S	=	Reference area
t	=	Time
u	=	Throttle position
U_0	=	Nominal airspeed for turbulence model
V	=	Airspeed
V_S	=	Stall speed
v	=	Ground speed

v_*	=	Minimum drag speed
$\hat{v}_*$	=	Estimate of minimum drag speed
W	=	Standard Brownian motion
ϵ	=	Turbulence time constant
η	=	Wind speed, pre-saturation
$\mu(\mathrm{d}\eta)$	=	Invariant distribution of η
ρ	=	Air density
σ	=	Integrator value
$\sigma_u, \sigma_v, \sigma_w$	=	Root mean square turbulence intensity (longitudinal, lateral, and vertical components)
τ_H	=	Simulation high pass filter time constant
τ_L	=	Simulation low pass filter time constant
$\Phi_{u_g}, \Phi_{v_g}, \Phi_{w_g}$	=	Turbulence spectra (longitudinal, lateral, vertical)
χ	=	Timescale-shifted wind speed
Ω	=	Spatial frequency
ω	=	Temporal frequency

Subscripts

eq	=	Equilibrium value

Superscripts

a	=	Average system variable
e	=	Error variable

2.2 Introduction

Extremum seeking is traditionally performed by adding a perturbation signal to the set-point of a system. The perturbation signal is usually a sinusoid [1, 5, 6] but can also be non-sinusoidal [7] or stochastic [3, 8]. It is also possible to use naturally occurring disturbances in lieu of an added perturbation signal [4]. Here, this approach is taken to optimize the speed of an aircraft for maxi-

mum endurance; that is, to maximize the length of time an aircraft can stay aloft. Convergence to the optimum speed is proven analytically and shown in simulation.

Over the past decade, extremum seeking has been adapted to many different applications, including anti-lock braking [9], particle beam matching [10], axial compressors [11], lean premixed combustion [12, 13], flow control [14], bio-reactors [15], tokamak fusion devices [16], and formation flight [17]. Extremum seeking may also be applied to an aircraft optimizing airspeed for best possible endurance. Aircraft wings have an optimal angle of attack that provides a maximum lift-to-drag ratio. All other factors being equal, a jet aircraft flying at the speed that achieves this angle of attack burns fuel more slowly than when flying either slower or faster than this optimal speed. This optimal speed is calculated during the design of the aircraft based on wind tunnel data; however, the optimal speed for any particular aircraft varies from the calculated value to some degree. The optimal speed varies based on many factors, from manufacturing differences to the condition of the wing. Accumulated bugs, nicks and dents can all change the optimal angle of attack, which changes the airspeed for optimal endurance. Extremum seeking may be used to find the optimal airspeed for the current condition of each individual aircraft as it flies. A recent survey of extremum seeking is given in [2].

While traditional, perturbation-based extremum seeking is a possibility, there are potential disadvantages to using this technique. The first is the possibility that the act of introducing the airspeed perturbation would decrease endurance. Periodically changing the commanded airspeed would cause the throttle command to oscillate, which quite possibly would use more fuel than a more steady throttle command. While finding the optimal airspeed would decrease drag and improve endurance, an oscillating throttle command could use more fuel and hurt endurance.

The second disadvantage to using traditional extremum seeking has less to do with technical performance than aviation administration. It may be seen as undesirable for the speed of an aircraft to be continuously varying. Traditional extremum seeking alters the observable motion of the aircraft, which may act as an impediment to its implementation. Utilized herein is a form of extremum

seeking that relies on naturally occurring disturbances, rather than manually added perturbations, to avoid these disadvantages.

Aircraft in flight on occasion encounter turbulence, which acts as a stochastic disturbance in airspeed. By taking advantage of this, a turbulence-based extremum-seeking algorithm can avoid the disadvantages of traditional extremum seeking. If the throttle is used to control airspeed in response to turbulence, no objection is raised; it is expected that airspeed will be controlled. Doing so does not use any additional fuel. The second disadvantage can be answered similarly; since the aircraft's speed is only being perturbed by turbulence, the observable motion of the aircraft is not altered. These two reasons may make turbulence-based extremum seeking a good fit for this application.

It should be mentioned that steady level flight is not necessarily optimal, but is the only form of flight considered in this paper. Periodic flight consisting of alternating higher-speed climbs and lower-speed glides can achieve endurance superior to steady flight [18, 19, 20, 21]. Since such periodic flight would alter the observable motion of the aircraft even more than traditional extremum seeking, only the case of steady flight at a given altitude is considered.

This paper is organized as follows. First, the relevant aerodynamics are reviewed. Next, the dynamic aircraft model is developed and the extremum-seeking control law is designed. An analysis of the stability of the system is then presented, followed by simulation results. A discussion is given and then lastly, some concluding remarks.

2.3 Aerodynamics

This section presents the simplified aerodynamic model that is used in the following analysis. Additional background can be found in [22]. Readers comfortable with aerodynamics and turbulence modeling may proceed to the control design below, noting that for simplicity the vertical component of turbulence is ignored.

2.3.1 Lift and Drag

To begin, a discussion of lift and drag is presented. Lift is the force on an aircraft perpendicular to the relative wind. The relative wind is the velocity of the air relative to the aircraft. In straight and level flight, lift is the upward force on the aircraft. Drag is the force on an aircraft parallel to the relative wind, acting generally backwards on the aircraft.

Lift is a function of air density, airspeed, a coefficient of lift, and a reference area. The expression for lift is

$$L = C_L \frac{1}{2} \rho V^2 S \ . \tag{2.1}$$

The coefficient of lift is a function of angle of attack, and is roughly linear for small angles. The angle of attack is the angle that the aircraft makes with the relative wind. The angle of attack is typically small during flight, less than five or ten degrees. A typical lift curve is shown in Fig. 2.1.

Drag is calculated similarly, only using a drag coefficient C_D. Drag is calculated as

$$D = C_D \frac{1}{2} \rho V^2 S \ . \tag{2.2}$$

The coefficient of drag is commonly calculated as the sum of two parts: the zero-lift drag coefficient and the induced drag coefficient.

$$C_D = C_{D0} + C_{Di} \tag{2.3}$$

The zero-lift drag coefficient accounts for the part of drag that is the same regardless of how much lift the aircraft is producing. The induced drag coefficient accounts for drag that is created because of the lift the aircraft produces. So the coefficient of drag is some constant C_{D0} plus some function of lift C_{Di}.

Induced drag is commonly approximated as having a quadratic dependence on the coefficient of lift [23]

$$C_{Di} = \frac{C_L^2}{\pi A e} \ . \tag{2.4}$$

The aspect ratio of the wing and the Oswald efficiency number are constants associated with the geometry of an aircraft

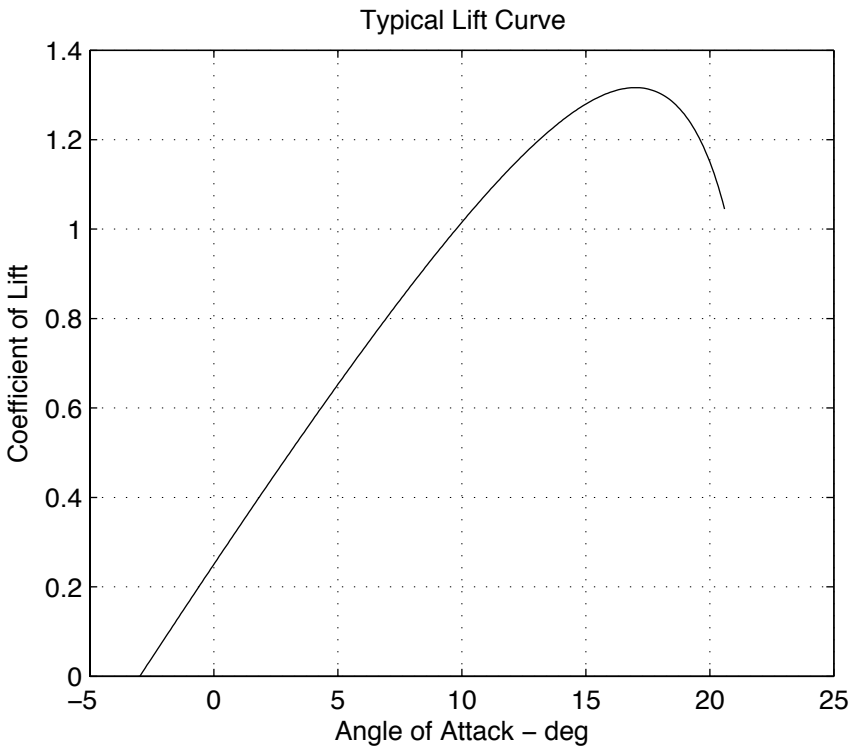

Figure 2.1: Typical coefficient of lift curve $C_L(\alpha)$.

2.3.2 Level Flight

Using these expressions for lift and drag, the case of level flight is analyzed. To maintain a constant altitude, the lift produced by the aircraft must equal the weight of the aircraft. For a given altitude and airspeed, this implies a required value of C_L. This value of C_L is given by

$$C_L = \frac{mg}{\frac{1}{2}\rho V^2 S} \ . \tag{2.5}$$

So, the C_L required for level flight is a function of speed. From (2.3), and (2.4) it is apparent that this implies a certain coefficient of drag. Substituting this coefficient of drag into (2.2) gives the drag for level flight as a function of speed

$$D = C_{D0}\frac{1}{2}\rho V^2 S + \frac{(mg)^2}{\pi A e \frac{1}{2}\rho V^2 S} \ . \tag{2.6}$$

Here, the first term represents the zero-lift drag (also called parasite drag) and the second term is the induced drag. These two terms are plotted along with the total drag in Fig. 2.2.

Note also that because there is a maximum possible C_L, as can be seen in Fig. 2.1, there is a minimum speed necessary for level flight. This speed is referred to as the stall speed. The stall speed is calculated as

$$V_S = \sqrt{\frac{2mg}{(\max C_L)\,\rho S}} \ . \tag{2.7}$$

Because it is not possible to fly slower than V_S, Fig. 2.2 does not show speeds below V_S.

2.3.3 Turbulence

Atmospheric turbulence is conventionally modeled as filtered gaussian white noise. The three components of turbulence (i.e., longitudinal, lateral and vertical) are modeled independently. The Dryden turbulence model is one commonly used atmospheric turbulence model [24]. It specifies the spectra of the three components

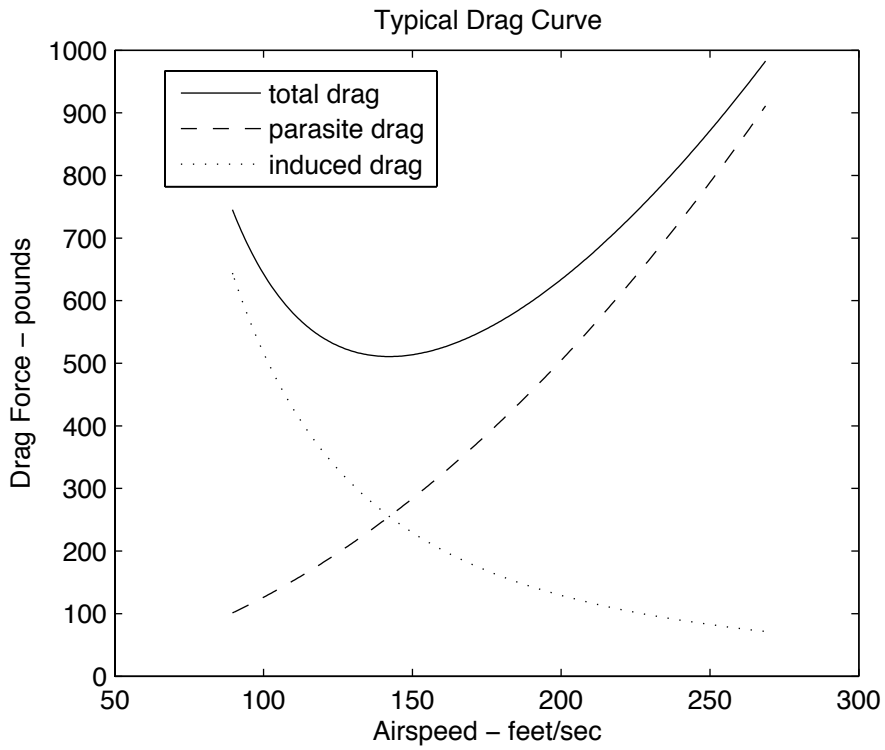

Figure 2.2: Drag $D(V)$ in level flight.

of turbulence as follows:

$$\Phi_{u_g}(\Omega) = \sigma_u^2 \frac{2L_u}{\pi} \frac{1}{1 + (L_u\Omega)^2} \tag{2.8a}$$

$$\Phi_{v_g}(\Omega) = \sigma_v^2 \frac{L_v}{\pi} \frac{1 + 3(L_v\Omega)^2}{\left[1 + (L_v\Omega)^2\right]^2} \tag{2.8b}$$

$$\Phi_{w_g}(\Omega) = \sigma_w^2 \frac{L_w}{\pi} \frac{1 + 3(L_w\Omega)^2}{\left[1 + (L_w\Omega)^2\right]^2} \ . \tag{2.8c}$$

The spectra are given in terms of spatial frequency, which is converted to temporal frequency ω by multiplying by the speed of the aircraft:

$$\omega = \Omega U_0 \ . \tag{2.9}$$

At medium to high altitudes (above 2,000 feet) the turbulence is assumed to be isotropic. The characteristic lengths and the intensities in each direction are equal to each other. A typical characteristic length is 1,750 feet. Intensities are charted as a function of altitude. Moderate turbulence has a root mean square intensity of about 10 ft/sec at 2,000 feet, decreasing roughly linearly to near zero at 60,000 feet.

Whereas lateral turbulence has little effect on the speed of an aircraft, longitudinal turbulence has a direct effect on airspeed. Longitudinal turbulence with a spectrum matching that given in (2.8a) can be obtained by passing white noise through a filter of the form

$$\sigma_u \sqrt{\frac{2L_u}{U_0}} \frac{1}{\frac{L_u}{U_0}s + 1} \ . \tag{2.10}$$

Vertical turbulence has an indirect effect on airspeed, but for this analysis it is ignored.

2.4 Control Design

2.4.1 Dynamic Model

Based on the aerodynamic model presented above, a simple dynamic model is considered: a scalar system perturbed by turbulence. The system is of the form

$$m\frac{\mathrm{d}v}{\mathrm{d}t} = -D(V) + bu \tag{2.11a}$$

$$\epsilon\,\mathrm{d}\eta = -\eta\,\mathrm{d}t + \sqrt{\epsilon}q\,\mathrm{d}W\ . \tag{2.11b}$$

The wind speed is defined as a headwind being positive, so that airspeed is the sum of groundspeed and wind speed. More precisely, airspeed is considered to be given by

$$V = v + a\,\mathrm{sat}\,\eta\ , \tag{2.12}$$

where $a\,\mathrm{sat}\,\eta$ is the wind speed. The saturation function

$$\mathrm{sat}(\eta) = \begin{cases} \eta & \text{if } -1 < \eta < 1 \\ 1 & \text{if } \eta \geq 1 \\ -1 & \text{if } \eta \leq -1 \end{cases} \tag{2.13}$$

is introduced for mathematical convenience. Its sole purpose is to ensure that the wind speed is bounded, which is a requirement for the stochastic averaging results used below. However, it is quite reasonable to bound the wind speed because it is not physically possible for the wind speed to be unbounded. The effect of the sat function can be made negligible by choosing q small with respect to one. The constant a can then be chosen to give the desired wind amplitude. The wind speed is modeled as filtered gaussian white noise, as per the Dryden longitudinal turbulence model. The timescale of the turbulence ($\epsilon \triangleq L_u/U_0$) is taken to be a constant, using an airspeed representative of the range of airspeeds expected to be encountered.

Without loss of generality, the wind speed is taken as zero-mean. If there were a steady-state component to the wind, then v would represent the ground speed plus the steady-state wind component, but the dynamics of the system would remain the same.

The rate of change of v is determined from total drag, engine thrust, and the mass of the aircraft. Engine thrust is modeled as proportional to the control input, namely throttle position. The drag function is taken as a general convex map with a minimum at speed v_*.

It is assumed that a proportional-integral control law is used to control airspeed to a set-point $\hat{v}_*$. The control law is written as

$$u = k_p\left(\hat{v}_* - V\right) + k_i\sigma \tag{2.14a}$$

$$\frac{\mathrm{d}\sigma}{\mathrm{d}t} = \hat{v}_* - V \ . \tag{2.14b}$$

Combining (2.11) and (2.14), the aircraft model is written as follows:

$$m\frac{\mathrm{d}v}{\mathrm{d}t} = -D(V) + b\left[k_p\left(\hat{v}_* - V\right) + k_i\sigma\right] \tag{2.15a}$$

$$\frac{\mathrm{d}\sigma}{\mathrm{d}t} = \hat{v}_* - V \tag{2.15b}$$

$$\epsilon\,\mathrm{d}\eta = -\eta\,\mathrm{d}t + \sqrt{\epsilon}q\,\mathrm{d}W \ . \tag{2.15c}$$

In this model, a, b, k_i, k_p, m, q, $\hat{v}_*$, and ϵ are positive. The airspeed V can be measured by a pitot-static system. It is considered that $\mathrm{d}v/\mathrm{d}t$, the acceleration of the aircraft, can also be measured. Further, it is assumed that the thrust produced by the engine (i.e., bu) and the mass of the aircraft are known. In the control design below, this is utilized.

The aircraft model in (2.15) represents the quasi-steady dynamics of the aircraft with altitude tightly controlled. The underlying assumptions of this model are that altitude is being controlled with the elevator, and that the altitude response is much faster than the airspeed response. The assumptions are chosen to be consistent with a jet aircraft in slow flight. Using elevator to control the airspeed of a jet in slow flight can result in substantial loss of altitude, so altitude is maintained with elevator and throttle is used to control airspeed. The throttle response of a jet aircraft, especially at a low throttle setting, is slow. Because of this, the airspeed controller is assumed to have a much lower bandwidth than the altitude controller.

2.4.2 Turbulence-Based Extremum Seeking

The goal is to optimize endurance. It is assumed that fuel consumption is an increasing function of thrust and that the thrust vector is level with the flight path. Then, optimizing endurance is equivalent to minimizing throttle position.

That is, the cost to be minimized is the control input u. Normally, this would require adding a perturbation to the set point of the system, $\hat{v}_*$. By modulating the cost with this perturbation signal, the rate of change of the cost with respect to $\hat{v}_*$ would be estimated. The set-point of the system would then be updated using an integral control law with a gain proportional to the estimated gradient. It is desired to do the same thing, but without adding a perturbation signal.

Observe that the goal of minimizing u is, more specifically, the goal of minimizing u in steady flight. Note that in steady flight (2.11a) reduces to $D(V) = bu$, so minimizing u in steady flight is equivalent to minimizing $D(V)$. Also, in steady flight (2.14b) reduces to $\hat{v}_* = V$. The goal can then be stated as choosing $\hat{v}_*$ such that $D(\hat{v}_*)$ is minimized.

While drag is not directly measurable, from (2.11a) it is seen that drag is indirectly measureable. Using knowledge of vehicle acceleration, engine thrust, and mass, drag $D(V)$ is calculated as

$$D(V) = bu - m\frac{\mathrm{d}v}{\mathrm{d}t} \ . \tag{2.16}$$

It is desired to demodulate this signal with the perturbation velocity. If the aircraft has a measurement of ground speed, say from an inertial navigation system, and a measurement of airspeed, the difference of the two could serve as a measurement of the perturbation. If the aircraft is not so equipped, it is possible to obtain an approximation of the airspeed perturbation from the error signal feeding the control law, $(\hat{v}_* - V)$. Here, the latter approach is taken. As in traditional extremum seeking, an integral control law is used to update the system and a gain proportional to this demodulated signal is chosen:

$$\frac{\mathrm{d}\hat{v}_*}{\mathrm{d}t} = k_{ES}\left[\hat{v}_* - V\right]\left(bu - m\frac{\mathrm{d}v}{\mathrm{d}t}\right) \ . \tag{2.17}$$

The system and extremum-seeking control law are shown in Fig. 2.3.

2.5 Analysis

In this section, analysis of the closed loop system formed by combining the aircraft model (2.15) with the extremum-seeking control law (2.17) is performed.

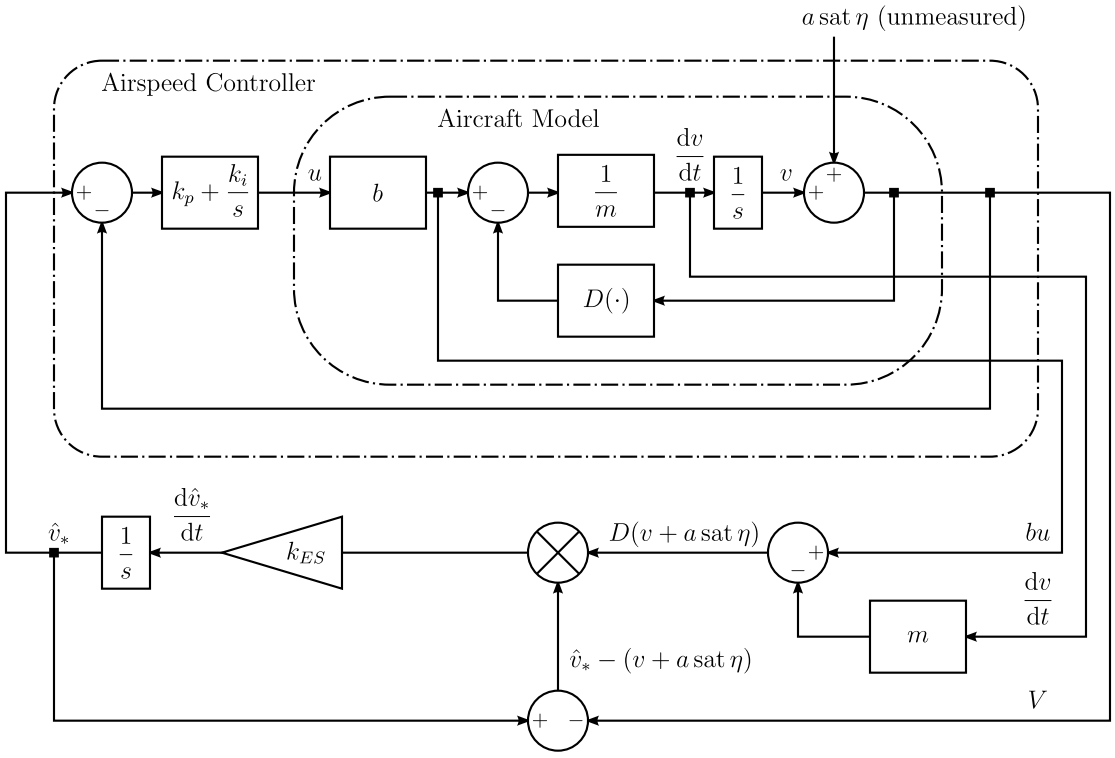

Figure 2.3: Block diagram of system and extremum-seeking feedback. The algorithm uses measurements of $\mathrm{d}v/\mathrm{d}t$, bu, m, and $v + a \sin \eta$, but not of v and η alone.

For analysis, the expression $(bu - m\,\mathrm{d}v/\mathrm{d}t)$ in the control law is written simply as $D(V)$. The expression for V from (2.12) is also substituted throughout. This produces the following set of equations.

$$m\frac{\mathrm{d}v}{\mathrm{d}t} = -D(v + a\,\mathrm{sat}\,\eta) + b\left[k_p\left(\hat{v}_* - (v + a\,\mathrm{sat}\,\eta)\right) + k_i\sigma\right] \tag{2.18a}$$

$$\frac{\mathrm{d}\sigma}{\mathrm{d}t} = \hat{v}_* - (v + a\,\mathrm{sat}\,\eta) \tag{2.18b}$$

$$\frac{\mathrm{d}\hat{v}_*}{\mathrm{d}t} = k_{ES}\left[\hat{v}_* - (v + a\,\mathrm{sat}\,\eta)\right] D(v + a\,\mathrm{sat}\,\eta) \tag{2.18c}$$

$$\epsilon\,\mathrm{d}\eta = -\eta\,\mathrm{d}t + \sqrt{\epsilon}q\,\mathrm{d}W \tag{2.18d}$$

Theorem 1. *Consider system* (2.18) *comprised of the aircraft model* (2.11)–(2.14) *and parameter update law* (2.17)*, where $D(\cdot)$ is a convex map with a minimum at v_*, all constants are positive, and $K_{ES} \in \left(0, bk_p/m\overline{D}_*\right)$, where $\overline{D}_*$ is a known upper bound on minimum drag, $D(v_*)$. Let constants C_2 and C_4 be defined by*

$$C_2(q) \triangleq \frac{q^2}{2}\,\mathrm{erf}\,\frac{1}{q} - \frac{q}{\sqrt{\pi}}e^{-\frac{1}{q^2}} + 1 - \mathrm{erf}\,\frac{1}{q} \tag{2.19a}$$

$$C_4(q) \triangleq \frac{3}{4}q^4\,\mathrm{erf}\,\frac{1}{q} - \frac{q}{\sqrt{\pi}}e^{-\frac{1}{q^2}}\left(1 + \frac{3}{2}q^2\right) + 1 - \mathrm{erf}\,\frac{1}{q}\ . \tag{2.19b}$$

Suppose $D(\cdot)$ is three times differentiable at v_*. Then there exists a constant a^* such that for any $0 < a < a^*$ there exist constants $r > 0$, $c > 0$, $\gamma > 0$ and a function $T(\epsilon)\colon (0, \epsilon_0) \to \mathbb{N}$ with the property $\lim_{\epsilon\to 0} T(\epsilon) = \infty$ such that for any initial condition $|\Delta^{\epsilon,a}(0)| < r$, and any $\delta > 0$,

$$\liminf_{\epsilon\to 0}\left\{t \geq 0 : |\Delta^{\epsilon,a}(t)| > c|\Delta^{\epsilon,a}(0)|e^{-\gamma t} + O(a^3) + \delta\right\} = \infty,\ \textit{a.s.} \tag{2.20}$$

and

$$\lim_{\epsilon\to 0} P\left\{|\Delta^{\epsilon,a}(t)| \leq c|\Delta^{\epsilon,a}(0)|e^{-\gamma t} + O(a^3) + \delta, \forall t \in [0, T(\epsilon)]\right\} = 1, \tag{2.21}$$

where $\Delta^{\epsilon,a}(t) \triangleq \begin{pmatrix} v(t) \\ \sigma(t) \\ \hat{v}_*(t) \end{pmatrix} - \begin{pmatrix} v_* - \frac{1}{6}\frac{D'''(v_*)}{D''(v_*)}\frac{C_4}{C_2}a^2 \\ \frac{D(v_*)}{bk_i} + \frac{D''(v_*)}{2}\frac{C_2}{bk_i}a^2 \\ v_* - \frac{1}{6}\frac{D'''(v_*)}{D''(v_*)}\frac{C_4}{C_2}a^2 \end{pmatrix}$.

Theorem 1 roughly states that choosing the gain K_{ES} as a small positive number causes the average airspeed to converge (both almost surely and in probability) to the minimum drag speed, with a small bias. The conditions for this

are that the turbulence amplitude is small and the initial state of the aircraft is sufficiently close to the final average equilibrium. The remainder of this section is dedicated to the proof of Theorem 1. These equations are transformed into error variables that are expected to converge to near zero. Stochastic averaging is used on this error system to find the average system. Then the equilibrium of the average system is found and the stability of the equilibrium is tested. Throughout the analysis, drag is treated as a general convex map. No assumptions are made about the exact nature of the nonlinearity.

2.5.1 Error Variables

Define the error variables

$$v^e = v - v_* \tag{2.22a}$$

$$\sigma^e = \sigma - \frac{D(v_*)}{bk_i} \tag{2.22b}$$

$$\hat{v}_*^e = \hat{v}_* - v \ . \tag{2.22c}$$

The fraction $D(v_*)/bk_i$ is the equilibrium value of the integrator when the aircraft is flying at the minimum drag speed with no disturbances. Also define

$$\chi(t) = \eta(\epsilon t) \tag{2.23a}$$

$$B(t) = \frac{1}{\sqrt{\epsilon}} W(\epsilon t) \ . \tag{2.23b}$$

Then the error system is

$$
\begin{aligned}
m\frac{\mathrm{d}v^e}{\mathrm{d}t} =& -D\big(v^e + v_* + a\,\mathrm{sat}\,\chi(t/\epsilon)\big) \\
&+ b\left[k_p\left(\hat{v}_*^e - a\,\mathrm{sat}\,\chi(t/\epsilon)\right) + k_i\left(\sigma^e + \frac{D(v_*)}{bk_i}\right)\right] && \text{(2.24a)}\\
\frac{\mathrm{d}\sigma^e}{\mathrm{d}t} =& \hat{v}_*^e - a\,\mathrm{sat}\,\chi(t/\epsilon) && \text{(2.24b)}\\
\frac{\mathrm{d}\hat{v}_*^e}{\mathrm{d}t} =& \frac{\mathrm{d}\hat{v}_*}{\mathrm{d}t} - \frac{\mathrm{d}v}{\mathrm{d}t} \\
=& k_{ES}\left[\hat{v}_*^e - a\,\mathrm{sat}\,\chi(t/\epsilon)\right] D\big(v^e + v_* + a\,\mathrm{sat}\,\chi(t/\epsilon)\big) \\
&- \frac{1}{m}\Bigg\{ -D\big(v^e + v_* + a\,\mathrm{sat}\,\chi(t/\epsilon)\big) \\
&+ b\left[k_p\left(\hat{v}_*^e - a\,\mathrm{sat}\,\chi(t/\epsilon)\right) + k_i\left(\sigma^e + \frac{D(v_*)}{bk_i}\right)\right]\Bigg\} && \text{(2.24c)}\\
\mathrm{d}\chi(t) =& -\chi(t)\mathrm{d}t + q\,\mathrm{d}B(t)\ . && \text{(2.24d)}
\end{aligned}
$$

2.5.2 Stochastic Averaging

Using stochastic averaging [3], the average system is then

$$
\begin{aligned}
m\frac{\mathrm{d}v^{e,a}}{\mathrm{d}t} =& \int_{-\infty}^{\infty} -D(v^{e,a} + v_* + a\,\mathrm{sat}\,\eta)\mu(\mathrm{d}\eta) \\
&+ b\left[k_p\left(\hat{v}_*^{e,a} - \int_{-\infty}^{\infty} a\,\mathrm{sat}\,\eta\mu(\mathrm{d}\eta)\right) + k_i\left(\sigma^{e,a} + \frac{D(v_*)}{bk_i}\right)\right] && \text{(2.25a)}\\
\frac{\mathrm{d}\sigma^{e,a}}{\mathrm{d}t} =& \hat{v}_*^{e,a} - \int_{-\infty}^{\infty} a\,\mathrm{sat}\,\eta\mu(\mathrm{d}\eta) && \text{(2.25b)}\\
\frac{\mathrm{d}\hat{v}_*^{e,a}}{\mathrm{d}t} =& \int_{-\infty}^{\infty} k_{ES}\left[\hat{v}_*^{e,a} - a\,\mathrm{sat}\,\eta\right] D(v^{e,a} + v_* + a\,\mathrm{sat}\,\eta)\mu(\mathrm{d}\eta) \\
&- \frac{1}{m}\Bigg\{\int_{-\infty}^{\infty} -D(v^{e,a} + v_* + a\,\mathrm{sat}\,\eta)\mu(\mathrm{d}\eta) \\
&+ b\left[k_p\left(\hat{v}_*^{e,a} - \int_{-\infty}^{\infty} a\,\mathrm{sat}\,\eta\mu(\mathrm{d}\eta)\right) + k_i\left(\sigma^{e,a} + \frac{D(v_*)}{bk_i}\right)\right]\Bigg\} && \text{(2.25c)}
\end{aligned}
$$

where the invariant distribution of η is given by

$$
\mu(\mathrm{d}\eta) = \frac{1}{\sqrt{\pi}q} e^{-\frac{\eta^2}{q^2}}\mathrm{d}\eta\ . \qquad \text{(2.26)}
$$

To simplify these equations, a function $\bar{D}(\cdot)$ is introduced. This function is the same as $D(\cdot)$, but recentered around the minimum drag point,

$$\bar{D}\left(v^{e,a} + a\,\mathrm{sat}\,\eta\right) \equiv D\left(v^{e,a} + v_* + a\,\mathrm{sat}\,\eta\right) - D\left(v_*\right) \ . \tag{2.27}$$

This new drag function is zero when its argument is zero,

$$\bar{D}(0) = 0 \ . \tag{2.28}$$

The average system (2.25) is simplified using $\bar{D}$ and noting that

$$\int_{-\infty}^{\infty} a\,\mathrm{sat}\,\eta\mu(\mathrm{d}\eta) = 0 \ . \tag{2.29}$$

This can be seen since sat is an odd function and μ is an even function, making the integrand odd; the integral from $-\infty$ to 0 cancels the integral from 0 to ∞. The average system becomes the following:

$$m\frac{\mathrm{d}v^{e,a}}{\mathrm{d}t} = -\int_{-\infty}^{\infty} \bar{D}\left(v^{e,a} + a\,\mathrm{sat}\,\eta\right)\mu(\mathrm{d}\eta) + b\left[k_p\hat{v}_*^{e,a} + k_i\sigma^{e,a}\right] \tag{2.30a}$$

$$\frac{\mathrm{d}\sigma^{e,a}}{\mathrm{d}t} = \hat{v}_*^{e,a} \tag{2.30b}$$

$$\begin{aligned}\frac{\mathrm{d}\hat{v}_*^{e,a}}{\mathrm{d}t} = &\int_{-\infty}^{\infty} k_{ES}\left[\hat{v}_*^{e,a} - a\,\mathrm{sat}\,\eta\right]\left[\bar{D}\left(v^{e,a} + a\,\mathrm{sat}\,\eta\right) + D(v_*)\right]\mu(\mathrm{d}\eta) \\ &- \frac{1}{m}\left\{-\int_{-\infty}^{\infty} \bar{D}\left(v^{e,a} + a\,\mathrm{sat}\,\eta\right)\mu(\mathrm{d}\eta) + b\left[k_p\hat{v}_*^{e,a} + k_i\sigma^{e,a}\right]\right\} \ .\end{aligned} \tag{2.30c}$$

2.5.3 Equilibrium of the Average System

To find the equilibrium of the average system, first observe from (2.30b) that the equilibrium value of $\hat{v}_*^{e,a}$ is zero, that is,

$$\hat{v}_{*eq}^{e,a} = 0 \ . \tag{2.31}$$

Next, from (2.30c) it is seen that at equilibrium

$$\int_{-\infty}^{\infty} k_{ES}\left[\hat{v}_{*eq}^{e,a} - a\,\mathrm{sat}\,\eta\right]\left[\bar{D}\left(v_{eq}^{e,a} + a\,\mathrm{sat}\,\eta\right) + D(v_*)\right]\mu(\mathrm{d}\eta) - \left(\frac{\mathrm{d}v^{e,a}}{\mathrm{d}t}\right)_{eq} = 0 \ . \tag{2.32}$$

Here it has been noted that the second term in (2.30c) is just $(\mathrm{d}v^{e,a}/\mathrm{d}t)_{eq}$, which must be zero at equilibrium. After simplification, which employs (2.31) and (2.29), the expression (2.32) reduces to

$$\int_{-\infty}^{\infty} \operatorname{sat}\eta \left[\bar{D}\left(v_{eq}^{e,a} + a \operatorname{sat}\eta\right)\right] \mu(\mathrm{d}\eta) = 0 \ . \tag{2.33}$$

To solve this equation for $v_{eq}^{e,a}$, the process is similar to the proof of stability for a general nonlinear dynamic system presented in [3]. Two expansions are used: one for $v_{eq}^{e,a}$ in a and one for $\bar{D}$ in $v_{eq}^{e,a}$. Take $v_{eq}^{e,a}$ in the form

$$v_{eq}^{e,a} = n_0 + n_1 a + n_2 a^2 + n_3 a^3 + O(a^4) \ . \tag{2.34}$$

Also use an expansion of the drag function $\bar{D}$ in terms of powers of its argument. Center the expansion around n_0.

$$\bar{D}(v) = \bar{D}(n_0) + \bar{D}'(n_0)(v-n_0) + \frac{\bar{D}''(n_0)}{2!}(v-n_0)^2 + \frac{\bar{D}'''(n_0)}{3!}(v-n_0)^3 + O\left((v-n_0)^4\right) \tag{2.35}$$

Using these expansions for $v_{eq}^{e,a}$ and $\bar{D}$, the condition for equilibrium in (2.33) becomes

$$
\begin{aligned}
&\int_{-\infty}^{\infty} \operatorname{sat}\eta \left[\bar{D}\left(v_{eq}^{e,a} + a\operatorname{sat}\eta\right)\right]\mu(\mathrm{d}\eta) \\
&= \int_{-\infty}^{\infty} \operatorname{sat}\eta \left[\bar{D}\left(n_0 + n_1 a + n_2 a^2 + n_3 a^3 + O(a^4) + a\operatorname{sat}\eta\right)\right]\mu(\mathrm{d}\eta) \\
&= \int_{-\infty}^{\infty} \operatorname{sat}\eta \Bigg[\bar{D}(n_0) \\
&\quad + \bar{D}'(n_0)\left(n_1 a + n_2 a^2 + n_3 a^3 + O(a^4) + a\operatorname{sat}\eta\right) \\
&\quad + \frac{\bar{D}''(n_0)}{2!}\left(n_1 a + n_2 a^2 + n_3 a^3 + O(a^4) + a\operatorname{sat}\eta\right)^2 \\
&\quad + \frac{\bar{D}'''(n_0)}{3!}\left(n_1 a + n_2 a^2 + n_3 a^3 + O(a^4) + a\operatorname{sat}\eta\right)^3 \\
&\quad + O\left(\left(n_1 a + n_2 a^2 + n_3 a^3 + O(a^4) + a\operatorname{sat}\eta\right)^4\right)\Bigg]\mu(\mathrm{d}\eta) \\
&= \int_{-\infty}^{\infty} \operatorname{sat}\eta \Bigg[\bar{D}(n_0) \\
&\quad + \bar{D}'(n_0)\left((n_3)\,a^3 + (n_2)\,a^2 + (n_1 + \operatorname{sat}\eta)\,a\right) \\
&\quad + \frac{\bar{D}''(n_0)}{2!}\Big(\left(2n_2\operatorname{sat}\eta + 2n_1 n_2\right)a^3 \\
&\quad + \left(n_1^2 + \operatorname{sat}^2\eta + 2n_1\operatorname{sat}\eta\right)a^2\Big) \\
&\quad + \frac{\bar{D}'''(n_0)}{3!}\left(n_1^3 + 3n_1^2\operatorname{sat}\eta + 3n_1\operatorname{sat}^2\eta + \operatorname{sat}^3\eta\right)a^3\Bigg]\mu(\mathrm{d}\eta) + O(a^4) \\
&= \bar{D}'(n_0)\left((C_2)\,a\right) \\
&\quad + \frac{\bar{D}''(n_0)}{2!}\left((2n_2C_2)a^3 + (2n_1C_2)a^2\right) \\
&\quad + \frac{\bar{D}'''(n_0)}{3!}\left(3n_1^2C_2 + C_4\right)a^3 + O(a^4) = 0\ . \qquad (2.36)
\end{aligned}
$$

Here the following integrals have been used:

$$\int_{-\infty}^{\infty} \operatorname{sat}^{2k+1}\eta\mu(\mathrm{d}\eta) = 0, \text{ where } k = 0, 1, 2, \ldots \qquad (2.37a)$$

$$\int_{-\infty}^{\infty} \operatorname{sat}^2\eta\mu(\mathrm{d}\eta) = \frac{q^2}{2}\operatorname{erf}\frac{1}{q} - \frac{q}{\sqrt{\pi}}e^{-\frac{1}{q^2}} + 1 - \operatorname{erf}\frac{1}{q} \triangleq C_2(q) \qquad (2.37b)$$

$$\int_{-\infty}^{\infty} \operatorname{sat}^4\eta\mu(\mathrm{d}\eta) = \frac{3}{4}q^4\operatorname{erf}\frac{1}{q} - \frac{q}{\sqrt{\pi}}e^{-\frac{1}{q^2}}\left(1 + \frac{3}{2}q^2\right) + 1 - \operatorname{erf}\frac{1}{q} \triangleq C_4(q)\ . \qquad (2.37c)$$

To help understand the expressions for C_2 and C_4, note that C_2 and C_4 can be approximated by

$$C_2(q) \approx \frac{q^2}{2} \tag{2.38a}$$

$$C_4(q) \approx \frac{3}{4}q^4 \tag{2.38b}$$

for small q. For q smaller than 0.5, the approximation for C_2 is accurate to within one percent and the approximation for C_4 is accurate to within three percent. Both C_2 and C_4 are zero when q is zero, and monotonically approach 1 as q grows without bound.

Because the expression in (2.36) is a polynomial in a, and the polynomial is equal to zero, each of the coefficients of a must be zero. This gives us the following system of equations:

$$a^1 : \bar{D}'(n_0)C_2 = 0 \tag{2.39a}$$

$$a^2 : \bar{D}''(n_0)n_1C_2 = 0 \tag{2.39b}$$

$$a^3 : \bar{D}''(n_0)n_2C_2 + \frac{\bar{D}'''(n_0)}{3!}\left(3n_1^2C_2 + C_4\right) = 0\ . \tag{2.39c}$$

Since $\bar{D}$ is assumed convex, its first derivative can only be zero when evaluated at a minimum point. Noting this, and that $\bar{D}$ has been defined with its minimum at zero, the solution to this set of equations is

$$n_0 = 0 \tag{2.40a}$$

$$n_1 = 0 \tag{2.40b}$$

$$n_2 = -\frac{1}{6}\frac{\bar{D}'''(0)}{\bar{D}''(0)}\frac{C_4}{C_2}\ , \tag{2.40c}$$

so an $O(a^3)$ expression for $v_{eq}^{e,a}$ is

$$v_{eq}^{e,a} = -\frac{1}{6}\frac{\bar{D}'''(0)}{\bar{D}''(0)}\frac{C_4(q)}{C_2(q)}a^2 + O(a^3)\ . \tag{2.41}$$

Recalling (2.38), it is noted that, for small q, the following is obtained: $v_{eq}^{e,a} = -\frac{1}{4}\frac{\bar{D}'''(0)}{\bar{D}''(0)}q^2a^2$.

Next, using the expression (2.41) for $v_{eq}^{e,a}$, the equation (2.30a) is set equal to zero and solved for $\sigma_{eq}^{e,a}$. This time a lower order expansion for $\bar{D}$ is used.

$$\bar{D}(v) = \bar{D}(0) + \bar{D}'(0)v + \frac{\bar{D}''(0)}{2!}v^2 + O(v^3) \tag{2.42}$$

The function $\bar{D}$ has been defined so that it has a minimum at the origin, so the first two terms of the expansion are zero and the expression is simplified to

$$\bar{D}(v) = \frac{\bar{D}''(0)}{2!}v^2 + O(v^3) \ . \tag{2.43}$$

Using these expressions for $v_{eq}^{e,a}$ and $\bar{D}$, the condition for equilibrium in (2.30a) becomes

$$\begin{aligned}
&\int_{-\infty}^{\infty} -\bar{D}\left(v_{eq}^{e,a} + a\,\mathrm{sat}\,\eta\right)\mu(\mathrm{d}\eta) + b\left[k_p\hat{v}_{*eq}^{e,a} + k_i\sigma_{eq}^{e,a}\right] \\
&= \int_{-\infty}^{\infty} -\bar{D}\left(n_2a^2 + O(a^3) + a\,\mathrm{sat}\,\eta\right)\mu(\mathrm{d}\eta) + bk_i\sigma_{eq}^{e,a} \\
&= \int_{-\infty}^{\infty} -\frac{\bar{D}''(0)}{2!}\left(n_2a^2 + O(a^3) + a\,\mathrm{sat}\,\eta\right)^2 + O\left(\left(n_2a^2 + O(a^3) + a\,\mathrm{sat}\,\eta\right)^3\right)\mu(\mathrm{d}\eta) \\
&\quad + bk_i\sigma_{eq}^{e,a} \\
&= \int_{-\infty}^{\infty} -\frac{\bar{D}''(0)}{2!}\left(\mathrm{sat}^2\,\eta\right)a^2\mu(\mathrm{d}\eta) + O(a^3) + bk_i\sigma_{eq}^{e,a} \\
&= -\frac{\bar{D}''(0)}{2!}(C_2)a^2 + O(a^3) + bk_i\sigma_{eq}^{e,a} = 0 \ ,
\end{aligned} \tag{2.44}$$

which gives

$$\sigma_{eq}^{e,a} = \frac{\bar{D}''(0)}{2}\frac{C_2}{bk_i}a^2 + O(a^3) \ . \tag{2.45}$$

So an equilibrium of the average system in terms of the error variables has been found. Collecting the expressions in (2.31), (2.41), and (2.45), the equilibrium is expressed as the following:

$$v_{eq}^{e,a} = -\frac{1}{6}\frac{\bar{D}'''(0)}{\bar{D}''(0)}\frac{C_4}{C_2}a^2 + O(a^3) \tag{2.46a}$$

$$\sigma_{eq}^{e,a} = \frac{\bar{D}''(0)}{2}\frac{C_2}{bk_i}a^2 + O(a^3) \tag{2.46b}$$

$$\hat{v}_{*eq}^{e,a} = 0 \ . \tag{2.46c}$$

Converting back to the original variables, the equilibrium of the average system is the following:

$$v_{eq}^{a} = v_* - \frac{1}{6}\frac{D'''(v_*)}{D''(v_*)}\frac{C_4}{C_2}a^2 + O(a^3) \tag{2.47a}$$

$$\sigma_{eq}^{a} = \frac{D(v_*)}{bk_i} + \frac{D''(v_*)}{2}\frac{C_2}{bk_i}a^2 + O(a^3) \tag{2.47b}$$

$$\hat{v}_{*eq}^{a} = v_{eq}^{a} \ . \tag{2.47c}$$

For small disturbance magnitudes (i.e. small a) the average speed of the system has an equilibrium point at the minimum drag speed, v_*. The deviation from the minimum drag speed is proportional to the third derivative of the drag curve at the minimum drag speed and decreases with a^2. If the drag curve is asymmetric, the speed bias is to the flatter side of the drag curve relative to the minimum-drag point.

2.5.4 Stability of the Equilibrium

To determine the stability of the equilibrium, the average system (2.30) is linearized around the equilibrium point and the linearized system is tested for stability.

The Jacobian of the average system (2.30) at the equilibrium point in terms of the error variables $(v^{e,a}, \sigma^{e,a}, \hat{v}_*^{e,a})$ is

$$J = \begin{pmatrix} J_{1,1} & \frac{bk_i}{m} & \frac{bk_p}{m} \\ 0 & 0 & 1 \\ J_{3,1} & -\frac{bk_i}{m} & J_{3,3} \end{pmatrix} \ , \tag{2.48a}$$

where $J_{1,1}$, $J_{3,1}$, and $J_{3,3}$ are given by

$$J_{1,1} = \frac{1}{m}\int_{-\infty}^{\infty} -\bar{D}'\left(v_{eq}^{e,a} + a\,\mathrm{sat}\,\eta\right)\mu(\mathrm{d}\eta) \tag{2.48b}$$

$$\begin{aligned} J_{3,1} = &\int_{-\infty}^{\infty} k_{ES}\left[\hat{v}_{*eq}^{e,a} - a\,\mathrm{sat}\,\eta\right]\left[\bar{D}'\left(v_{eq}^{e,a} + a\,\mathrm{sat}\,\eta\right)\right]\mu(\mathrm{d}\eta) \\ &- \frac{1}{m}\int_{-\infty}^{\infty} -\bar{D}'\left(v_{eq}^{e,a} + a\,\mathrm{sat}\,\eta\right)\mu(\mathrm{d}\eta) \end{aligned} \tag{2.48c}$$

$$J_{3,3} = \int_{-\infty}^{\infty} k_{ES}\left[\bar{D}\left(v_{eq}^{e,a} + a\,\mathrm{sat}\,\eta\right) + D(v_*)\right]\mu(\mathrm{d}\eta) - \frac{bk_p}{m} \ . \tag{2.48d}$$

The characteristic equation of the system is given by $\det(sI - J) = 0$, or

$$\begin{vmatrix} s - J_{1,1} & -\frac{bk_i}{m} & -\frac{bk_p}{m} \\ 0 & s & -1 \\ -J_{3,1} & \frac{bk_i}{m} & s - J_{3,3} \end{vmatrix} = 0 \ . \tag{2.49}$$

Writing this as a polynomial, the characteristic equation is as follows.

$$s^3 - (J_{1,1} + J_{3,3})\, s^2 + \left(J_{1,1}J_{3,3} - \frac{bk_p}{m} J_{3,1} + \frac{bk_i}{m} \right) s - \frac{bk_i}{m} (J_{1,1} + J_{3,1}) = 0 \tag{2.50}$$

By applying Routh's criterion, it is seen that the system is stable if each of the coefficients in the characteristic polynomial are positive and the product of the s^2 and s^1 coefficients is greater than the product of the s^3 and s^0 coefficients. To test this expressions for $J_{1,1}$, $J_{3,1}$, and $J_{3,3}$ are required. Expressions accurate to $O(a^3)$ are found for each.

First, $J_{1,1}$ is found. Using the expressions $v_{eq}^{e,a} = n_2 a^2 + O(a^3)$ and $\bar{D}'(v) = \bar{D}''(0)v + \frac{\bar{D}'''(0)}{2!}v^2 + O(v^3)$ the following is obtained:

$$\begin{aligned} J_{1,1} &= \frac{1}{m} \int_{-\infty}^{\infty} -\bar{D}' \left(v_{eq}^{e,a} + a \operatorname{sat} \eta \right) \mu(\mathrm{d}\eta) \\ &= -\frac{1}{m} \int_{-\infty}^{\infty} \bar{D}' \left(n_2 a^2 + O(a^3) + a \operatorname{sat} \eta \right) \mu(\mathrm{d}\eta) \\ &= -\frac{1}{m} \int_{-\infty}^{\infty} \bar{D}''(0) \left(n_2 a^2 + O(a^3) + a \operatorname{sat} \eta \right) \\ &\quad + \frac{\bar{D}'''(0)}{2!} \left(n_2 a^2 + O(a^3) + a \operatorname{sat} \eta \right)^2 \\ &\quad + O\left(\left(n_2 a^2 + O(a^3) + a \operatorname{sat} \eta \right)^3 \right) \mu(\mathrm{d}\eta) \\ &= -\frac{1}{m} \int_{-\infty}^{\infty} \bar{D}''(0) \left(n_2 a^2 + a \operatorname{sat} \eta \right) \\ &\quad + \frac{\bar{D}'''(0)}{2!} \left(a^2 \operatorname{sat}^2 \eta \right) \mu(\mathrm{d}\eta) + O(a^3) \\ &= -\frac{1}{m} \left[\bar{D}''(0) n_2 + \frac{\bar{D}'''(0)}{2!} C_2 \right] a^2 + O(a^3) \ . \end{aligned} \tag{2.51}$$

Next, using the same expressions for $v_{eq}^{e,a}$ and $\bar{D}'(v) = \bar{D}''(0)v + O(v^2)$ the expression for $J_{3,1}$ is found. Note that the second term in the original expression for $J_{3,1}$ is

the negative of $J_{1,1}$.

$$\begin{aligned}
J_{3,1} = & \int_{-\infty}^{\infty} k_{ES} \left[\hat{v}_{*eq}^{e,a} - a \operatorname{sat} \eta\right] \left[\bar{D}' \left(v_{eq}^{e,a} + a \operatorname{sat} \eta\right)\right] \mu(\mathrm{d}\eta) \\
& - \frac{1}{m} \int_{-\infty}^{\infty} -\bar{D}' \left(v_{eq}^{e,a} + a \operatorname{sat} \eta\right) \mu(\mathrm{d}\eta) \\
= & \int_{-\infty}^{\infty} k_{ES} \left[0 - a \operatorname{sat} \eta\right] \left[\bar{D}' \left(v_{eq}^{e,a} + a \operatorname{sat} \eta\right)\right] \mu(\mathrm{d}\eta) \\
& - J_{1,1} \\
= & - \int_{-\infty}^{\infty} k_{ES} a \operatorname{sat} \eta \\
& \times \left[\bar{D}''(0) \left(n_2 a^2 + O(a^3) + a \operatorname{sat} \eta\right) + O\left(\left(n_2 a^2 + O(a^3) + a \operatorname{sat} \eta\right)^2\right)\right] \mu(\mathrm{d}\eta) \\
& - J_{1,1} \\
= & - \int_{-\infty}^{\infty} k_{ES} a \operatorname{sat} \eta \left[\bar{D}''(0) a \operatorname{sat} \eta\right] \mu(\mathrm{d}\eta) \\
& + O(a^3) - J_{1,1} \\
= & - k_{ES} \bar{D}''(0) C_2 a^2 + O(a^3) - J_{1,1} \\
= & \left[- k_{ES} \bar{D}''(0) C_2 + \frac{1}{m} \left(\bar{D}''(0) n_2 + \frac{\bar{D}'''(0)}{2!} C_2\right)\right] a^2 + O(a^3)
\end{aligned} \tag{2.52}$$

Finally, an expression for $J_{3,3}$ is found. Here the approximations $v_{eq}^{e,a} = 0 + O(a^2)$

and $\bar{D}(v) = \frac{\bar{D}''(0)}{2!}v^2 + O(v^3)$ are used. Then $J_{3,3}$ can be expressed as

$$\begin{aligned}
J_{3,3} &= \int_{-\infty}^{\infty} k_{ES}\left[\bar{D}\left(v_{eq}^{e,a} + a\,\mathrm{sat}\,\eta\right) + D(v_*)\right]\mu(\mathrm{d}\eta) - \frac{bk_p}{m} \\
&= \int_{-\infty}^{\infty} k_{ES}\left[\bar{D}\left(0 + O(a^2) + a\,\mathrm{sat}\,\eta\right) + D(v_*)\right]\mu(\mathrm{d}\eta) - \frac{bk_p}{m} \\
&= \int_{-\infty}^{\infty} k_{ES}\left[\frac{\bar{D}''(0)}{2!}\left(O(a^2) + a\,\mathrm{sat}\,\eta\right)^2\right. \\
&\quad \left. + O\left(\left(O(a^2) + a\,\mathrm{sat}\,\eta\right)^3\right) + D(v_*)\right]\mu(\mathrm{d}\eta) - \frac{bk_p}{m} \\
&= \int_{-\infty}^{\infty} k_{ES}\left[\frac{\bar{D}''(0)}{2!}\left(a^2\,\mathrm{sat}^2\,\eta\right) + D(v_*)\right]\mu(\mathrm{d}\eta) + O(a^3) - \frac{bk_p}{m} \\
&= k_{ES}\left[\frac{\bar{D}''(0)}{2!}\left(a^2 C_2\right) + D(v_*)\right] + O(a^3) - \frac{bk_p}{m} \\
&= \left[k_{ES}D(v_*) - \frac{bk_p}{m}\right] + \left[k_{ES}\frac{\bar{D}''(0)}{2!}C_2\right]a^2 + O(a^3)\ . \qquad (2.53)
\end{aligned}$$

Now, using these expressions for the components of the Jacobian of the system, it is possible to calculate the coefficients in the characteristic equation and test for stability.

$$\begin{aligned}
s^2: & \\
& -\left(J_{1,1} + J_{3,3}\right) \\
=\ & -J_{1,1} - J_{3,3} \\
=\ & -\left(-\frac{1}{m}\left[\bar{D}''(0)n_2 + \frac{\bar{D}'''(0)}{2!}C_2\right]a^2 + O(a^3)\right) \\
& -\left(\left[k_{ES}D(v_*) - \frac{bk_p}{m}\right] + \left[k_{ES}\frac{\bar{D}''(0)}{2!}C_2\right]a^2 + O(a^3)\right) \\
=\ & \left[\frac{bk_p}{m} - k_{ES}D(v_*)\right] \\
& + \left[\frac{1}{m}\left(\bar{D}''(0)n_2 + \frac{\bar{D}'''(0)}{2!}C_2\right) - k_{ES}\frac{\bar{D}''(0)}{2!}C_2\right]a^2 + O(a^3) \qquad (2.54)
\end{aligned}$$

s^1 :

$$
\begin{aligned}
& J_{1,1}J_{3,3} - \frac{bk_p}{m}J_{3,1} + \frac{bk_i}{m} \\
= & \left(-\frac{1}{m}\left[\bar{D}''(0)n_2 + \frac{\bar{D}'''(0)}{2!}C_2\right]a^2 + O(a^3)\right) \\
& \times \left(\left[k_{ES}D(v_*) - \frac{bk_p}{m}\right] + \left[k_{ES}\frac{\bar{D}''(0)}{2!}C_2\right]a^2 + O(a^3)\right) \\
& - \frac{bk_p}{m}\left\{\left[-k_{ES}\bar{D}''(0)C_2 + \frac{1}{m}\left(\bar{D}''(0)n_2 + \frac{\bar{D}'''(0)}{2!}C_2\right)\right]a^2 + O(a^3)\right\} + \frac{bk_i}{m} \\
= & \left(-\frac{1}{m}\left[\bar{D}''(0)n_2 + \frac{\bar{D}'''(0)}{2!}C_2\right]a^2\right)\left(\left[k_{ES}D(v_*) - \frac{bk_p}{m}\right]\right) \\
& - \frac{bk_p}{m}\left\{\left[-k_{ES}\bar{D}''(0)C_2 + \frac{1}{m}\left(\bar{D}''(0)n_2 + \frac{\bar{D}'''(0)}{2!}C_2\right)\right]a^2\right\} + \frac{bk_i}{m} + O(a^3) \\
= & -\frac{1}{m}\left(k_{ES}D(v_*) - \frac{bk_p}{m}\right)\left(\bar{D}''(0)n_2 + \frac{\bar{D}'''(0)}{2!}C_2\right)a^2 \\
& - \frac{bk_p}{m}\left[-k_{ES}\bar{D}''(0)C_2 + \frac{1}{m}\left(\bar{D}''(0)n_2 + \frac{\bar{D}'''(0)}{2!}C_2\right)\right]a^2 + \frac{bk_i}{m} + O(a^3) \\
= & -\frac{1}{m}k_{ES}D(v_*)\left(\bar{D}''(0)n_2 + \frac{\bar{D}'''(0)}{2!}C_2\right)a^2 - \frac{bk_p}{m}\left[-k_{ES}\bar{D}''(0)C_2\right]a^2 + \frac{bk_i}{m} \\
& + O(a^3) \\
= & \frac{bk_i}{m} + \left[-\frac{1}{m}k_{ES}D(v_*)\left(\bar{D}''(0)n_2 + \frac{\bar{D}'''(0)}{2!}C_2\right) - \frac{bk_p}{m}\left[-k_{ES}\bar{D}''(0)C_2\right]\right]a^2 \\
& + O(a^3)
\end{aligned}
\tag{2.55}
$$

s^0 :

$$
\begin{aligned}
& -\frac{bk_i}{m}\left(J_{1,1} + J_{3,1}\right) \\
= & -\frac{bk_i}{m}\left(-\frac{1}{m}\left[\bar{D}''(0)n_2 + \frac{\bar{D}'''(0)}{2!}C_2\right]a^2 + O(a^3)\right) \\
& - \frac{bk_i}{m}\left\{\left[-k_{ES}\bar{D}''(0)C_2 + \frac{1}{m}\left(\bar{D}''(0)n_2 + \frac{\bar{D}'''(0)}{2!}C_2\right)\right]a^2 + O(a^3)\right\} \\
= & \frac{bk_i}{m}\left[k_{ES}\bar{D}''(0)C_2\right]a^2 + O(a^3)
\end{aligned}
\tag{2.56}
$$

So the characteristic equation of the average system can be written as

$$\begin{aligned}
&s^3 \\
&+\left\{\left[\frac{bk_p}{m}-k_{ES}D(v_*)\right]\right. \\
&\left.+\left[\frac{1}{m}\left(\bar{D}''(0)n_2+\frac{\bar{D}'''(0)}{2!}C_2\right)-k_{ES}\frac{\bar{D}''(0)}{2!}C_2\right]a^2+O(a^3)\right\}s^2 \\
&+\left\{\frac{bk_i}{m}+\left[-\frac{1}{m}k_{ES}D(v_*)\left(\bar{D}''(0)n_2+\frac{\bar{D}'''(0)}{2!}C_2\right)\right.\right. \\
&\left.\left.-\frac{bk_p}{m}\left[-k_{ES}\bar{D}''(0)C_2\right]\right]a^2+O(a^3)\right\}s \\
&+\left\{\frac{bk_i}{m}\left[k_{ES}\bar{D}''(0)C_2\right]a^2+O(a^3)\right\}=0
\end{aligned} \tag{2.57}$$

or, more simply, as

$$\begin{aligned}
s^3+\left\{\left[\frac{bk_p}{m}-k_{ES}D(v_*)\right]+O(a^2)\right\}s^2+\left\{\frac{bk_i}{m}+O(a^2)\right\}s \\
+\left\{\frac{bk_i}{m}\left[k_{ES}\bar{D}''(0)C_2\right]a^2+O(a^3)\right\}=0\ .
\end{aligned} \tag{2.58}$$

The first step in checking for stability is to ensure that all of the coefficients of this polynomial are positive. Since all of the constants in this polynomial are assumed positive, for small a the coefficients are all positive if

$$0<k_{ES}<\frac{bk_p}{mD(v_*)}\ . \tag{2.59}$$

It must also be ensured that the product of the s^2 and s^1 coefficients is greater than the product of the s^3 and s^0 coefficients.

$$\begin{aligned}
\left\{\left[\frac{bk_p}{m}-k_{ES}D(v_*)\right]+O(a^2)\right\}\left\{\frac{bk_i}{m}+O(a^2)\right\} \\
>\left\{\frac{bk_i}{m}\left[k_{ES}\bar{D}''(0)C_2\right]a^2+O(a^3)\right\}
\end{aligned} \tag{2.60}$$

By making an $O(a^2)$ approximation, this reduces to

$$\frac{bk_i}{m}\left(\frac{bk_p}{m}-k_{ES}D(v_*)\right)>O(a^2)\ , \tag{2.61}$$

which is true for small a if (2.59) is satisfied. So, by Routh's criterion, the linearized average system is stable for small a if k_{ES} is chosen small enough to satisfy (2.59).

The stability of the linearized average system implies stability of the nonlinear perturbed system. Because the linearized average system is stable, the nonlinear average system (2.30) is locally exponentially stable (Corollary 4.3 in [25]). From the stochastic averaging results in [3], exponential stability of the average system implies that the system is weakly exponentially stable under the random perturbation. This result is formalized in Theorem 1. The stability analysis concludes that turbulence-based extremum seeking stabilizes the aircraft to the the speed for optimal endurance.

2.6 Simulations

A simulation run using Simulink is presented here. The simulation follows (2.18) closely, with the addition of a high pass filter and a low pass filter. Although not necessary for stability, the use of a high pass filter has been shown to improve the rate of convergence in other extremum-seeking applications [3]. Here, the high pass filter is applied to the drag signal in the extremum-seeking loop. A low pass filter is also added to smooth the controller. The filters are shown in Fig. 2.4. The parameters used in simulation are listed in Table 2.1. A plot of the simulation results is shown in Fig. 2.5.

For a direct comparison with the above analysis, a simulation without the high pass and low pass filters is also presented. The simulation parameters are the same as in Table 2.1, except that the filter time constants are not applicable and k_{ES} must be chosen much smaller. The stability limit for k_{ES} can be calculated using Theorem 1 and the simulation parameters in Table 2.1. For the simulation k_{ES} was chosen to be one-eighth of its stability limit. Numerical values for the stability limit of k_{ES} and k_{ES} itself are shown in Table 2.2. Also shown in Table 2.2 are the predicted equilibrium point and Jacobian matrix of the average system, corresponding to (2.47) and (2.48), respectively. The Jacobian elements $J_{1,1}$ $J_{3,1}$ and $J_{3,3}$ are calculated using the $O(a^3)$ approximations given in (2.51) (2.52) and (2.53).

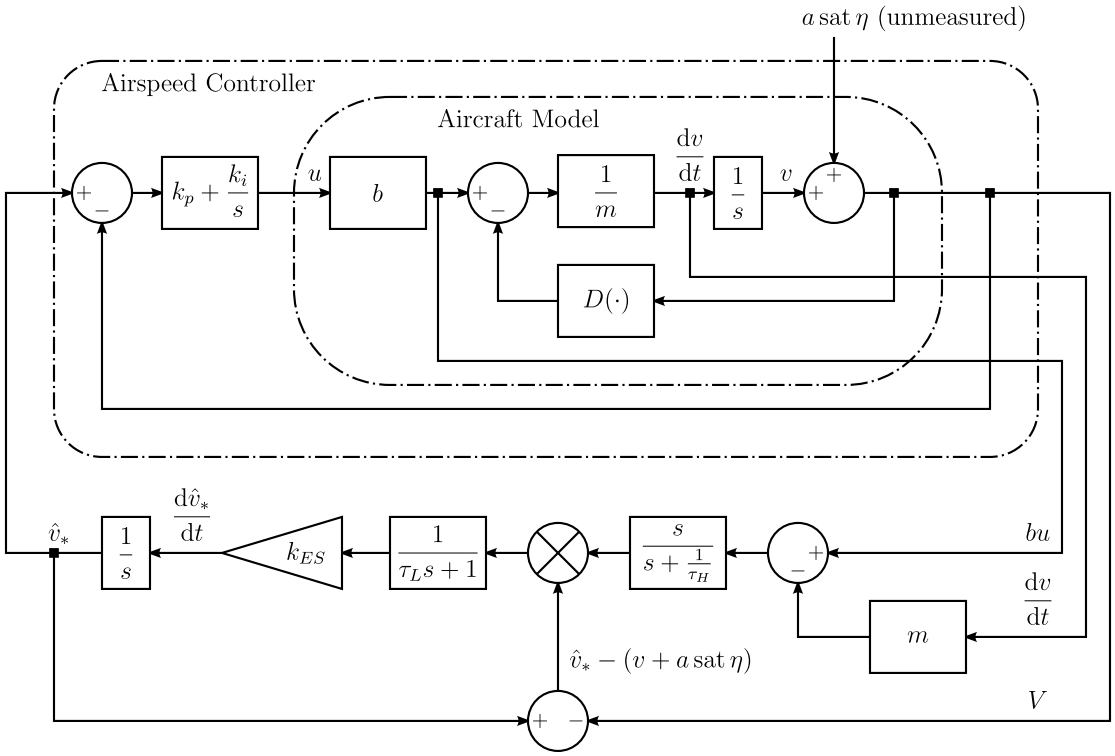

Figure 2.4: Block diagram of the control system as simulated, including added filters.

Table 2.1: Simulation parameters

Parameter	Value	Units
σ_u	3	ft/s
L_u	1750	ft
U_0	142	ft/s
a	149	ft/s
q	0.0285	$s^{-1/2}$
ϵ	12.30	s
mg	14300	lb
m	444	slugs
b	100	lbf/deg
k_p	2.22	deg/(ft/s)
k_i	0.0111	deg/[(ft/s) $\cdot$ s]
k_{ES}	1	[(ft/s)/s]/[(ft/s) $\cdot$ lbf]
τ_H	2	s
τ_L	5	s
$D(V)$	$(5.17 \times 10^6)V^2 + (0.0126)/V^2$	lbf (As in Fig. 2.2)
v_*	142.2	ft/s

Table 2.2: Parameters for simulation without filters

Parameter	Value	Units
$bk_p/mD(v_*)$	9.790×10^{-4}	[(ft/s)/s]/[(ft/s) $\cdot$ lbf]
k_{ES}	1.224×10^{-4}	[(ft/s)/s]/[(ft/s) $\cdot$ lbf]
v_{eq}^a	142.3	ft/s
σ_{eq}^a	460.4	(ft/s) $\cdot$ s
$\hat{v}_{*eq}^a$	142.3	ft/s
$J_{1,1}$	-2.640×10^{-21}	s^{-1}
$J_{1,2}$	0.0025	s^{-2}
$J_{1,3}$	0.5	s^{-1}
$J_{2,1}$	0	None
$J_{2,2}$	0	s^{-1}
$J_{2,3}$	1	None
$J_{3,1}$	-1.112×10^{-4}	s^{-1}
$J_{3,2}$	-0.0025	s^{-2}
$J_{3,3}$	-0.4374	s^{-1}

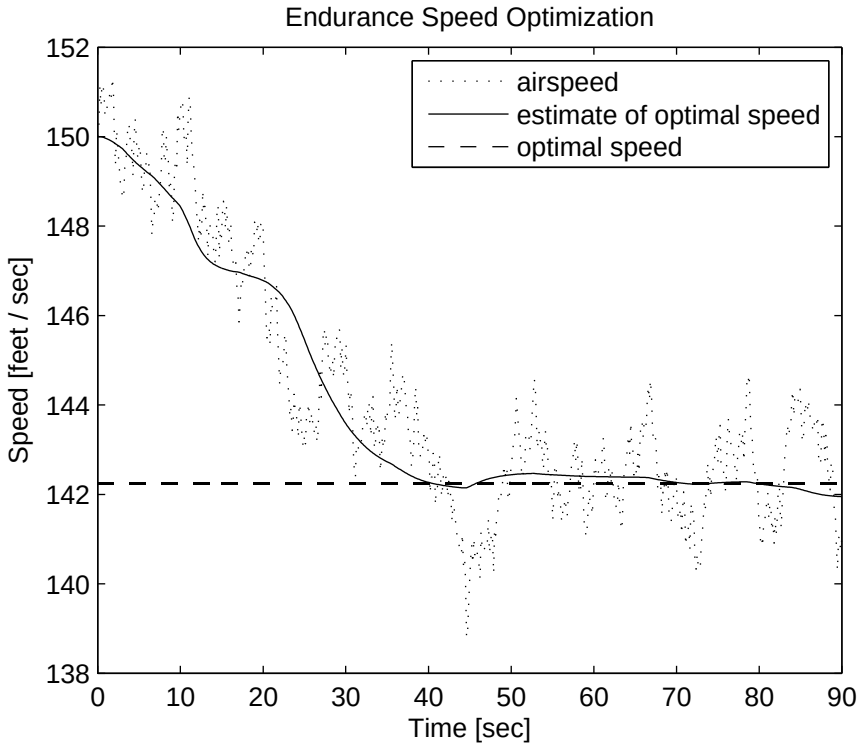

Figure 2.5: Simulation results of endurance speed optimization.

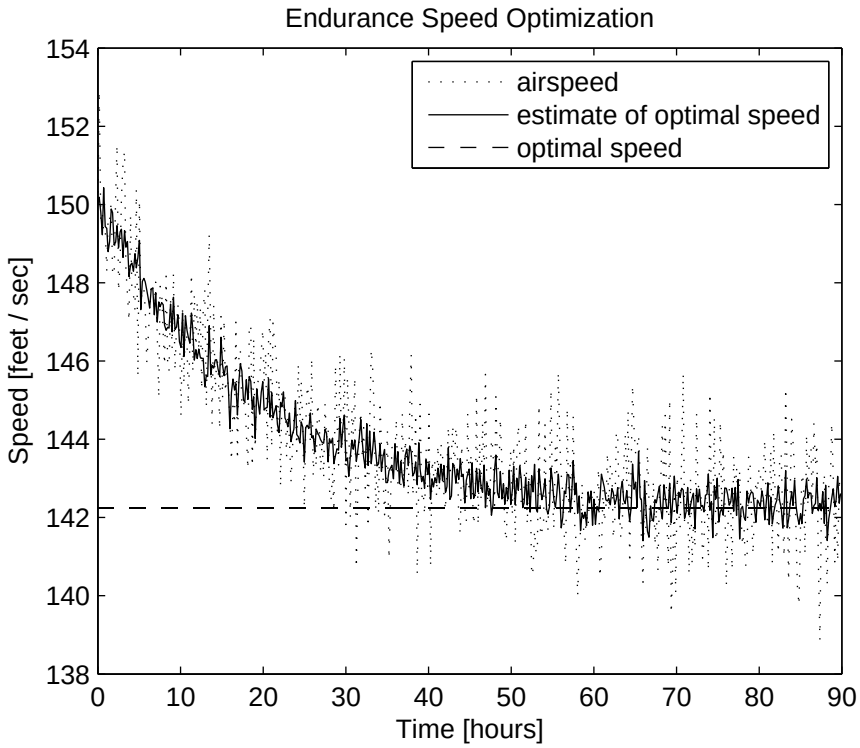

Figure 2.6: Simulation results without added filters. By comparison with Fig. 2.5 it is clear that convergence can be sped up by several orders of magnitude by the addition of the filters.

2.7 Discussion

The turbulence-based extremum-seeking algorithm successfully stabilizes the aircraft model to the airspeed for optimal endurance, with an average bias proportional to the third derivative of the drag curve and the square of turbulence intensity. The extremum-seeking controller does this without adding a perturbation to the set-point of the system. Simulations conducted using a quadratic drag polar show little bias from the true minimum. The drag curve used in simulation is the same shown in Fig. 2.2. Note that while a quadratic drag polar is used, the drag curve is a non-polynomial function of airspeed and contains higher order terms sufficient to investigate the bias of the estimated minimum drag speed predicted by Theorem 1.

The simulation demonstrates performance in turbulence with a root-mean-square amplitude of 3 ft/sec, which represents light to moderate turbulence at most altitudes. This raises the question of how the controller will perform in other turbulence intensities. As shown in analysis, the steady-state bias improves as the turbulence intensity decreases. This is limited only by the fidelity of the accelerometer reading and the accuracy of the thrust and weight estimates. However, for any given k_{ES} the rate of convergence to the minimum drag speed also decreases with the turbulence intensity. Because encounters with turbulence are typically fairly short, on the order of minutes, it is desirable to increase the rate of convergence as much as possible. This can be accomplished by increasing k_{ES}. Care should be taken, though, not to increase k_{ES} too much. The analytical stability result from Theorem 1 is stated in terms of the limiting case as a tends to zero. It is expected that the upper stability bound on k_{ES} will decrease as a increases, implying that k_{ES} should be chosen conservatively to prevent the system from becoming unstable in severe turbulence.

The issue of rate of convergence also demonstrates the necessity of using the high pass and low pass filters. The filters improve the rate of convergence by orders of magnitude. Indeed without them, the control design is not practical. The analysis above considers the simpler control design for improved clarity in the analysis. Omitting the filters keeps the basic style of analysis and functionality of

the controller from being lost in the details.

A limitation of this work is that vertical gusts have been ignored. The results in [26], which show the potential robustness of extremum-seeking control to stochastic disturbances, suggest that vertical gusts may be handled well by this control scheme. Including vertical gusts in future analysis and simulations would increase confidence that the turbulence-based extremum-seeking controller will function as desired in real turbulence. A related limitation is that longitudinal aircraft dynamics are not modeled in simulation. This prevents the simulation from testing the validity of neglecting altitude dynamics.

The advantage of a turbulence-based approach, that it operates without using a perturbation signal, is also its disadvantage. Particularly at higher altitudes, an aircraft may not experience turbulence often. Furthermore, the optimal airspeed varies with the weight of the aircraft, and possibly also with other flight parameters. Because of this, the current optimal airspeed may not be the same as the optimal airspeed found during the last encounter with turbulence. To address these issues, an application of turbulence-based extremum seeking would need to provide means of recording optimal speeds found during encounters with turbulence and extrapolating the recorded speeds to the current flight condition.

Another facet of this application that may prove complicated involves the varying curvature of the drag profile with altitude and weight. To achieve rapid convergence to the optimal speed across the flight envelope would require scheduling the extremum-seeking gain. Alternately, an extremum-seeking control law could be developed that was insensitive to the curvature of the drag profile. Such a method is developed in [27] for traditional sinusoidal-perturbation-based extremum seeking. Adapting this method for stochastic extremum-seeking schemes is a subject of current research.

Finally, it is noted that while the assumptions made in this paper apply to a jet aircraft, it may be possible to modify the controller for propeller aircraft. For jet aircraft, flight at the best lift-to-drag ratio results in maximum endurance, but for propeller aircraft maximum endurance is obtained at the minimum power speed. An extremum-seeking controller for propeller aircraft may be created by

substituting an estimate of required power for the estimated drag. This can be accomplished by multiplying the drag estimate in the extremum-seeking controller by the measured airspeed.

2.8 Conclusion

A turbulence-based form of extremum seeking has been developed for optimizing the speed of an aircraft for maximum endurance. The turbulence-based approach allows extremum seeking to be performed without introducing an external perturbation. Assuming longitudinal turbulence in level flight and a general convex drag curve, analysis shows weak exponential stability to the minimum drag speed. Simulations show similar behavior with high-pass and low-pass filters added to the extremum-seeking loop.

2.9 Acknowledgements

Chapter 2 contains material that appears in the Journal of Guidance, Control, and Dynamics (Krieger, J., and Krstic, M., AIAA, November-December 2011). The authors retain the copyright to this material. The dissertation author was the primary investigator and author of this material.

Chapter 3

Newton Method Stochastic Extremum Seeking with Unknown Dither Amplitude

Extremum seeking controllers have traditionally been composed of a gradient estimator and a simple gradient descent adaptation law. Recently, a new form of extremum seeking has been developed that replaces the gradient descent law with a Newton method optimization scheme. This paper presents a Newton-based algorithm suitable for use where the dither signal is stochastic. A novel feature of the controller is that it does not rely on exact a priori knowledge of the variance or other properties of the stochastic perturbation. This allows for the basic design to be readily extended to systems which rely on naturally occurring stochastic disturbances to excite the gradient/Hessian estimator. The controller is first presented, analyzed, and simulated for the scalar optimization case; the work is then extended to the multi-variable case. Stability of the minimum of a static quadratic map is proven analytically for a map of arbitrarily large dimension. Simulations show average convergence in a straight line towards the minimum of a two-dimensional asymmetric quadratic map.

3.1 Nomenclature

a	=	Stochastic disturbance post-saturation scaling factor
C_2, C_4	=	Averaging constants, scalar analysis
$C_{s2}, C_{v2}, C_{M2}, C_{M4}$	=	Averaging constants, multi-dimensional analysis
C_{2i}, C_{4i}	=	Shorthand for $C_2(q_i), C_4(q_i)$
e_i	=	Unit vector along i-th dimension
g	=	Gradient of map
H	=	Hessian of map
J	=	Jacobian of a system
k_{ES}	=	Extremum-seeking gain
k_0, k_1, k_2	=	Estimator gains
N	=	Constant diagonal matrix used in analysis
n	=	Dimensional of multi-dimensional map
Q	=	An integrand in multi-dimensional analysis
q	=	Stochastic disturbance pre-saturation scaling factor
t	=	Time
V_1, V_2	=	Candidate Lyapunov functions
W	=	Standard Brownian motion
y	=	Output of static map
α	=	Net stochastic input to system
δ	=	Practical adaptation law constant
ϵ	=	Stochastic process time constant
η	=	Stochastic process, pre-saturation
θ	=	Input to static map
θ_0	=	Estimate of minimizing map input
μ	=	Constant diagonal matrix used in analysis
$\mu(\mathrm{d}\eta)$	=	Invariant distribution of η
ν	=	Constant vector used in multi-dimensional analysis

Subscripts

0	=	Quantity evaluated at θ_0
d	=	Diagonal elements of a matrix

eq	=	Equilibrium value
od	=	Off-diagonal elements of a matrix
$*$	=	Pertaining to the minimum of the static map

Accents

Bar $\bar{\bullet}$	=	Average system variable
Dot $\dot{\bullet}$	=	Derivative with respect to t
Hat $\hat{\bullet}$	=	Estimate
Prime $\bullet'$	=	Derivative with respect to θ
Tilde $\tilde{\bullet}$	=	Error variable

3.2 Introduction

In most control applications, the system is regulated to a known set-point; but what if the set-point, or even the system itself, is unknown? Extremum seeking is a form of non-model-based control that addresses this question. The extremum-seeking controller seeks the minimum (or maximum) of a measurable system output by adjusting the system input. The input is perturbed by a small dither signal, traditionally a sine wave. In its simplest form, the output of the system is then demodulated with the dither signal to form an estimate of the local slope of the input-output map. A gradient descent is then performed to minimize the system output. (See [1, 5, 2, 28].)

There have been a number of advancements in extremum seeking in recent years (notably for this paper the development of stochastic extremum seeking [3, 29]). Perhaps the most promising development is a change in the method of optimization from gradient descent to an analog of Newton's method [27, 30, 31]. This requires the controller to generate an estimate of the curvature of the input-output map (in addition to its slope), but enables the system to converge to the extremum at a user-assignable rate. In the case of a multi-dimensional map, Newton-based extremum seeking enables the system to converge to the extremum in a straight line. This is in contrast to traditional extremum seeking, in which the

convergence in one dimension may be much slower than convergence in another.

One other recent development is disturbance-based extremum seeking [4]. In some applications, there exist *naturally occurring* additive disturbances that can be used as the dither signal. Doing so can simplify the controller and reduce control energy; however the nature (specifically, the amplitude) of the signal may not be known at design time. The Newton-based algorithms from [27, 30] depend on knowledge of the nature of the dither signal. Because the amplitude of the dither signal directly affects the rate of system convergence, this can negate the benefits of a Newton-based algorithm.

This paper presents a new form of extremum seeking in which the amplitude of the dither signal has minimal affect on the rate of convergence towards the extremum. By this feature, it can be readily extended for use with naturally occurring disturbances whose properties may not be precisely known at design time. This is done by using a slope (gradient) and curvature (Hessian) estimator based on estimation error; the gradient and Hessian are estimated explicitly and are used to produce an estimate of the system output from the system input – the error in this estimate drives the estimator. This style is motivated by the way in which a time-varying Kalman filter might be used to estimate the variables (as in [31]) but the estimator is based on averaging, so it is of much lower order. There may also be an analog in the parameter-estimation-based extremum seeking work in [32, 33], in that the (quadratic) assumed form of the input-output map is made explicit and its coefficients are estimated.

Intuitively, the proposed design is independent of the dither amplitude since the estimation error becomes zero when the gradient and hessian estimates reach the true values. When the estimation error is zero, the gradient and hessian estimates freeze and so remain at their true value; the amplitude of the perturbations is not a factor. In particular, it is not necessary to multiply or divide by the amplitudes (as in [27, 30]) in order to form an accurate gradient or hessian estimate. This makes the method suited for situations in which the amplitude of the stochastic perturbation is unknown.

This paper is organized as follows:

First, using the simplest relevant problem, a static quadratic map in one dimension, the proposed controller is analyzed for stability. Simulations are also presented. Initially unsuccessful, the simulations reveal the need for modifications to the proposed controller. With these modifications in place, the simulations run smoothly.

Next, a formulation for a multi-dimensional controller is presented and analyzed for stability. This formulation is a higher-dimensional equivalent to the controller described above. Simulation results show convergence in a straight line to the minimum of two-dimensional quadratic map.

Finally, a discussion and a brief conclusion are given. The discussion highlights the advantages of the proposed controller as compared to more traditional extremum-seeking methods.

3.3 Newton Method Stochastic Extremum Seeking in One Dimension

3.3.1 Controller

The extremum-seeking controller in [27] consists of two pieces: a gradient estimator and an adaptation law. The estimator relies on the perturbation signal being a sinusoid. Because of this it is not suitable for use in stochastic extremum-seeking. The adaptation law, though, can be used in a stochastic application with no significant change. A top-level diagram of the proposed stochastic Newton method controller is shown in Figure 3.1. The input to the system is a stochastic process η, defined by

$$\epsilon \, \mathrm{d}\eta = -\eta \, \mathrm{d}t + \sqrt{\epsilon} q \, \mathrm{d}W \ , \tag{3.1}$$

where W is white noise ϵ is a time constant and q is a scaling factor. A saturation function

$$\mathrm{sat}(\eta) = \begin{cases} \eta & \text{if } -1 < \eta < 1 \\ 1 & \text{if } \eta \geq 1 \\ -1 & \text{if } \eta \leq -1 \end{cases} \tag{3.2}$$

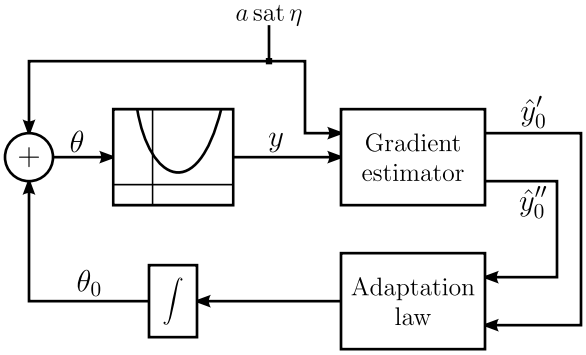

Figure 3.1: Top level structure of a Newton method extremum-seeking controller.

is used to bound η and the result is then scaled by a constant a to give the perturbation quantity: $a \operatorname{sat} \eta$.

The perturbation quantity is added to the current estimate of the minimizing argument of the static map θ_0. This sum is designated θ, which is the current input to the static map. The output of the static map evaluated at θ is denoted by y. In this paper, a hat ($\hat{\bullet}$) indicates an estimate, a prime ($\bullet'$) indicates a derivative with respect to θ, and a subscript 0 ($\bullet_0$) indicates a quantity evaluated at θ_0. So, for example, $\hat{y}_0''$ indicates an estimate of the second derivative of y with respect to θ, evaluated at θ_0.

The gradient estimator uses the perturbation to determine the local slope and curvature of the static map. The proposed gradient estimator is a third order system described by (3.3).

$$\dot{\hat{y}}_0 = k_0 \left(y - \hat{y}\right) \tag{3.3a}$$

$$\dot{\hat{y}}_0' = k_1 \left(a \operatorname{sat} \eta\right) \left(y - \hat{y}\right) \tag{3.3b}$$

$$\dot{\hat{y}}_0'' = k_2 \left(a \operatorname{sat} \eta\right)^2 \left(y - \hat{y}\right) \ , \tag{3.3c}$$

where

$$\hat{y} \triangleq \hat{y}_0 + \hat{y}_0' \left(a \operatorname{sat} \eta\right) + \frac{\hat{y}_0''}{2} \left(a \operatorname{sat} \eta\right)^2 \ , \tag{3.3d}$$

and k_0 k_1 and k_2 are constants.

The adaptation law is essentially

$$\dot{\theta}_0 = -k_{ES} \frac{\hat{y}_0'}{\hat{y}_0''} \ . \tag{3.4}$$

Potential problems with the simpler form occur when the curvature is small or negative, or the local gradient is large. As noted in [27], for practical reasons it may be desirable to use an adaptation law such as

$$\dot{\theta}_0 = -k_{ES}\Delta \ , \tag{3.5a}$$

where

$$\Delta = \begin{cases} \frac{\hat{y}_0'}{\hat{y}_0''} & \text{if } |\hat{y}_0'| < \delta \operatorname{sgn} \hat{y}_0'' \\ \delta \operatorname{sgn} \hat{y}_0' & \text{otherwise.} \end{cases} \tag{3.5b}$$

This formulation ensures that θ_0 will always descend towards a local minimum, and at a rate bounded by $|k_{ES}\delta|$.

3.3.2 Problem Analysis

Here, the simple case of a quadratic static map is analyzed. Under examination is whether the gradient estimator (3.3) and the adaptation law (3.4) cause θ_0 to converge to the minimizing argument of the system

$$y = y_* + \frac{y_*''}{2}\left(\theta - \theta_*\right)^2 \ . \tag{3.6}$$

Here, subscript asterisks ($\bullet_*$) indicate a constant associated with the minimum of the quadratic map: y_* is the minimum value of the map, y_*'' is the curvature of the map at the minimum point, and θ_* is the minimizing argument of the map. [Note: In this problem the curvature of the map is constant, so the asterisk in y_*'' is unnecessary. It is left in for clarity and for compatibility with future work where the notation may be needed.]

In the analysis, difficulties involving (3.4) associated with dividing by zero are ignored, noting that the more practical adaptation law (3.5) can alleviate these difficulties. The latter never divides by zero and behaves like (3.4) near the minimum of the quadratic map, where $\hat{y}_0'$ is small.

In the simplest form, the closed loop system is

$$\dot{\hat{y}}_0 = k_0 \left(y - \hat{y}\right) \tag{3.7a}$$

$$\dot{\hat{y}}'_0 = k_1 \left(a \operatorname{sat} \eta\right) \left(y - \hat{y}\right) \tag{3.7b}$$

$$\dot{\hat{y}}''_0 = k_2 \left(a \operatorname{sat} \eta\right)^2 \left(y - \hat{y}\right) \tag{3.7c}$$

$$\dot{\theta}_0 = -k_{ES} \frac{\hat{y}'_0}{\hat{y}''_0} \tag{3.7d}$$

$$\epsilon \, \mathrm{d}\eta = -\eta \, \mathrm{d}t + \sqrt{\epsilon} q \, \mathrm{d}W \ . \tag{3.7e}$$

Plugging in the expressions for y and $\hat{y}$ from (3.6) and (3.3d), and using $\theta = \theta_0 + a \operatorname{sat} \eta$, the expression $(y - \hat{y})$ is expanded and is grouped by powers of η.

$$\begin{aligned} y - \hat{y} &= \left[y_* + \frac{y''_*}{2} \left(\theta_0 + a \operatorname{sat} \eta - \theta_*\right)^2 \right] - \left[\hat{y}_0 + \hat{y}'_0 \left(a \operatorname{sat} \eta\right) + \frac{\hat{y}''_0}{2} \left(a \operatorname{sat} \eta\right)^2 \right] \\ &= \left[\frac{y''_* - \hat{y}''_0}{2} \right] \left(a \operatorname{sat} \eta\right)^2 + \left[y''_* \left(\theta_0 - \theta_*\right) - \hat{y}'_0 \right] \left(a \operatorname{sat} \eta\right) \\ &\quad + \left[y_* + \frac{y''_*}{2} \left(\theta_0 - \theta_*\right)^2 - \hat{y}_0 \right] \end{aligned} \tag{3.8}$$

From the definition of y in (3.6), note the following:

$$y_* + \frac{y''_*}{2} \left(\theta_0 - \theta_*\right)^2 \triangleq y_0 \tag{3.9a}$$

$$y''_* \left(\theta_0 - \theta_*\right) \triangleq y'_0 \tag{3.9b}$$

$$y''_* \triangleq y''_0 \tag{3.9c}$$

The expression for $(y - \hat{y})$ then simplifies to

$$y - \hat{y} = \left[\frac{y''_0 - \hat{y}''_0}{2} \right] \left(a \operatorname{sat} \eta\right)^2 + \left[y'_0 - \hat{y}'_0 \right] \left(a \operatorname{sat} \eta\right) + \left[y_0 - \hat{y}_0 \right] \ . \tag{3.10}$$

Using this expression, the closed loop system is written

$$\dot{\hat{y}}_0 = k_0 \left(\left[\frac{y_0'' - \hat{y}_0''}{2} \right] (a \operatorname{sat} \eta)^2 + \left[y_0' - \hat{y}_0' \right] (a \operatorname{sat} \eta) + \left[y_0 - \hat{y}_0 \right] \right) \tag{3.11a}$$

$$\dot{\hat{y}}_0' = k_1 \left(\left[\frac{y_0'' - \hat{y}_0''}{2} \right] (a \operatorname{sat} \eta)^3 + \left[y_0' - \hat{y}_0' \right] (a \operatorname{sat} \eta)^2 + \left[y_0 - \hat{y}_0 \right] (a \operatorname{sat} \eta) \right) \tag{3.11b}$$

$$\dot{\hat{y}}_0'' = k_2 \left(\left[\frac{y_0'' - \hat{y}_0''}{2} \right] (a \operatorname{sat} \eta)^4 + \left[y_0' - \hat{y}_0' \right] (a \operatorname{sat} \eta)^3 + \left[y_0 - \hat{y}_0 \right] (a \operatorname{sat} \eta)^2 \right) \tag{3.11c}$$

$$\dot{\theta}_0 = -k_{ES} \frac{\hat{y}_0'}{\hat{y}_0''} \tag{3.11d}$$

$$\epsilon \, \mathrm{d}\eta = -\eta \, \mathrm{d}t + \sqrt{\epsilon} q \, \mathrm{d}W \ . \tag{3.11e}$$

Averaging

Stochastic averaging is used to remove the η dynamics. Briefly, given a system with state variable x and stochastic variable η, with dynamics $\dot{x} = f(x, \eta)$, the stochastic variable can be eliminated from the dynamic equations and a deterministic average system formed by integrating the dynamic equation f over the distribution of a stochastic variable μ:

$$\dot{\bar{x}} = \int f(\bar{x}, \eta) \mu(\mathrm{d}\eta) \tag{3.12}$$

Variables of the average system are denoted by bars ($\bar{\bullet}$). As in [3] and [34], note that the invariant distribution of η is given by

$$\mu(\mathrm{d}\eta) = \frac{1}{\sqrt{\pi} q} e^{-\frac{\eta^2}{q^2}} \mathrm{d}\eta \ , \tag{3.13}$$

and note the values of the following integrals:

$$\int_{-\infty}^{\infty} \operatorname{sat}^{2k+1} \eta \mu(\mathrm{d}\eta) = 0, \text{ where } k = 0, 1, 2, \ldots \tag{3.14a}$$

$$\int_{-\infty}^{\infty} \operatorname{sat}^2 \eta \mu(\mathrm{d}\eta) = \frac{q^2}{2} \operatorname{erf} \frac{1}{q} - \frac{q}{\sqrt{\pi}} e^{-\frac{1}{q^2}} + 1 - \operatorname{erf} \frac{1}{q} \triangleq C_2(q) \tag{3.14b}$$

$$\int_{-\infty}^{\infty} \operatorname{sat}^4 \eta \mu(\mathrm{d}\eta) = \frac{3}{4} q^4 \operatorname{erf} \frac{1}{q} - \frac{q}{\sqrt{\pi}} e^{-\frac{1}{q^2}} \left(1 + \frac{3}{2} q^2 \right) + 1 - \operatorname{erf} \frac{1}{q} \triangleq C_4(q) \ . \tag{3.14c}$$

The average system then follows:[1]

$$\dot{\bar{\hat{y}}}_0 = k_0 \left(\left[\frac{y_0'' - \bar{\hat{y}}_0''}{2} \right] a^2 C_2 + \left[y_0' - \bar{\hat{y}}_0' \right] 0 + \left[y_0 - \bar{\hat{y}}_0 \right] \right) \tag{3.15a}$$

$$\dot{\bar{\hat{y}}}_0' = k_1 \left(\left[\frac{y_0'' - \bar{\hat{y}}_0''}{2} \right] 0 + \left[y_0' - \bar{\hat{y}}_0' \right] a^2 C_2 + \left[y_0 - \bar{\hat{y}}_0 \right] 0 \right) \tag{3.15b}$$

$$\dot{\bar{\hat{y}}}_0'' = k_2 \left(\left[\frac{y_0'' - \bar{\hat{y}}_0''}{2} \right] a^4 C_4 + \left[y_0' - \bar{\hat{y}}_0' \right] 0 + \left[y_0 - \bar{\hat{y}}_0 \right] a^2 C_2 \right) \tag{3.15c}$$

$$\dot{\bar{\theta}}_0 = -k_{ES} \frac{\bar{\hat{y}}_0'}{\bar{\hat{y}}_0''} \ , \tag{3.15d}$$

or simply

$$\dot{\bar{\hat{y}}}_0 = k_0 \left(\left[\frac{y_0'' - \bar{\hat{y}}_0''}{2} \right] a^2 C_2 + \left[y_0 - \bar{\hat{y}}_0 \right] \right) \tag{3.16a}$$

$$\dot{\bar{\hat{y}}}_0' = k_1 \left[y_0' - \bar{\hat{y}}_0' \right] a^2 C_2 \tag{3.16b}$$

$$\dot{\bar{\hat{y}}}_0'' = k_2 \left(\left[\frac{y_0'' - \bar{\hat{y}}_0''}{2} \right] a^4 C_4 + \left[y_0 - \bar{\hat{y}}_0 \right] a^2 C_2 \right) \tag{3.16c}$$

$$\dot{\bar{\theta}}_0 = -k_{ES} \frac{\bar{\hat{y}}_0'}{\bar{\hat{y}}_0''} \ . \tag{3.16d}$$

Equilibrium

The estimator states are in equilibrium when they match the parameters of the quadratic map which they reflect. Moreover, it is an isolated equilibrium so long as (3.16a) and (3.16c) are independent, which is true under the condition that

$$\frac{a^4 C_4}{a^2 C_2} \neq \frac{a^2 C_2}{1} \ , \tag{3.17}$$

or simply that $C_4 \neq C_2^2$. It can be verified that this is true in general, but that they approach equality as q becomes large. Typically q is chosen small to reduce the effect of the saturation function. For $q < 0.5$, the approximations $C_2 \approx q^2/2$ and $C_4 \approx 3q^4/4$ are fairly accurate, so

$$C_4 \approx 3C_2^2 \ . \tag{3.18}$$

[1] A fine point on notation is that in average systems like (3.15) and (3.16), y_0 no longer represents the value of y at θ_0, but rather the value of y at $\bar{\theta}_0$. In order to avoid complicating the notation, and because the meaning can be deduced from context, a new symbol is not introduced to represent this difference.

This confirms the independence of the dynamic equations of the estimator states, and that they have a unique equilibrium. That is,

$$\begin{pmatrix} \bar{\hat{y}}_{0,eq} \\ \bar{\hat{y}}'_{0,eq} \\ \bar{\hat{y}}''_{0,eq} \end{pmatrix} = \begin{pmatrix} y_0 \\ y'_0 \\ y''_0 \end{pmatrix} . \tag{3.19}$$

The adaptation law has an equilibrium when $\bar{\hat{y}}'_0$ is zero. Because $\bar{\hat{y}}'_0$ equals y'_0 at equilibrium and y'_0 is only equal to zero at θ_*, the only equilibrium point of $\bar{\theta}_0$ is at θ_*. That is, the equilibrium of the average system is

$$\begin{pmatrix} \bar{\hat{y}}_{0,eq} \\ \bar{\hat{y}}'_{0,eq} \\ \bar{\hat{y}}''_{0,eq} \\ \bar{\theta}_{0,eq} \end{pmatrix} = \begin{pmatrix} y_* \\ 0 \\ y''_* \\ \theta_* \end{pmatrix} . \tag{3.20}$$

The subscript eq ($\bullet_{eq}$) denotes an equilibrium value. In summary, the average system has one equilibrium and it is located at the minimum of the quadratic map.

Stability

Next, the average system is linearized around the equilibrium point and checked for stability. The Jacobian of the average system (3.16) is

$$J\left(\bar{\hat{y}}_0, \bar{\hat{y}}'_0, \bar{\hat{y}}''_0, \bar{\theta}_0\right) = \begin{bmatrix} -k_0 & 0 & -k_0\frac{a^2C_2}{2} & k_0\left(y'''_0\frac{a^2C_2}{2} + y'_0\right) \\ 0 & -k_1a^2C_2 & 0 & k_1y''_0a^2C_2 \\ -k_2a^2C_2 & 0 & -k_2\frac{a^4C_4}{2} & k_2\left(y'''_0\frac{a^4C_4}{2} + y'_0a^2C_2\right) \\ 0 & -\frac{k_{ES}}{\bar{\hat{y}}''_0} & k_{ES}\frac{\bar{\hat{y}}'_0}{\left(\bar{\hat{y}}''_0\right)^2} & 0 \end{bmatrix} . \tag{3.21}$$

Evaluating the Jacobian at the equilibrium point, and noting that for a quadratic map y'_* and y'''_* are zero, the Jacobian simplifies as follows:

$$J\left(\bar{\hat{y}}_{0,eq}, \bar{\hat{y}}'_{0,eq}, \bar{\hat{y}}''_{0,eq}, \bar{\theta}_{0,eq}\right) = \begin{bmatrix} -k_0 & 0 & -k_0\frac{a^2C_2}{2} & 0 \\ 0 & -k_1a^2C_2 & 0 & k_1y''_*a^2C_2 \\ -k_2a^2C_2 & 0 & -k_2\frac{a^4C_4}{2} & 0 \\ 0 & -\frac{k_{ES}}{y''_*} & 0 & 0 \end{bmatrix} . \tag{3.22}$$

By reordering the variables, the Jacobian becomes block diagonal and the characteristic polynomial is easily found.

$$J\left(\bar{\hat{y}}_{0,eq}, \bar{\hat{y}}''_{0,eq}, \bar{\hat{y}}'_{0,eq}, \bar{\theta}_{0,eq}\right) = \begin{bmatrix} -k_0 & -k_0\frac{a^2C_2}{2} & 0 & 0 \\ -k_2a^2C_2 & -k_2\frac{a^4C_4}{2} & 0 & 0 \\ 0 & 0 & -k_1a^2C_2 & k_1y''_*a^2C_2 \\ 0 & 0 & -\frac{k_{ES}}{y''_*} & 0 \end{bmatrix} . \quad (3.23)$$

$$\begin{aligned} |sI - J| &= \begin{vmatrix} s+k_0 & k_0\frac{a^2C_2}{2} & 0 & 0 \\ k_2a^2C_2 & s+k_2\frac{a^4C_4}{2} & 0 & 0 \\ 0 & 0 & s+k_1a^2C_2 & -k_1y''_*a^2C_2 \\ 0 & 0 & \frac{k_{ES}}{y''_*} & s \end{vmatrix} \\ &= \left[(s+k_0)\left(s+k_2\frac{a^4C_4}{2}\right) - \left(k_0\frac{a^2C_2}{2}\right)\left(k_2a^2C_2\right)\right] \\ &\quad \times \left[\left(s+k_1a^2C_2\right)(s) - \left(-k_1y''_*a^2C_2\right)\left(\frac{k_{ES}}{y''_*}\right)\right] \\ &= \left[s^2 + \left(k_0 + k_2\frac{a^4C_4}{2}\right)s + \left(k_0k_2\frac{a^4\left(C_4 - C_2^2\right)}{2}\right)\right] \\ &\quad \times \left[s^2 + k_1a^2C_2s + k_1k_{ES}a^2C_2\right] \end{aligned} \quad (3.24)$$

By the Routh-Hurwitz criterion, any second order polynomial has roots with negative real parts if it has positive coefficients. Since this fourth-order polynomial factors into two second-order polynomials, it is evident that it is stable if all of the gains are chosen positive, a is non-zero, and C_4 is greater than C_2^2. It is shown below that the latter is true for all $q > 0$.

It is shown that $C_4 - C_2^2 > 0$ by using the integral definitions of C_4 and C_2. This expression is

$$\begin{aligned} C_4 - C_2^2 &= \int_{-\infty}^{\infty} \mathrm{sat}^4\,\eta\mu(\mathrm{d}\eta) - \left(\int_{-\infty}^{\infty} \mathrm{sat}^2\,\eta\mu(\mathrm{d}\eta)\right)^2 \\ &= \int_{\Re} \mathrm{sat}^4\,x\mu(\mathrm{d}x) - \left(\int_{\Re} \mathrm{sat}^2\,x\mu(\mathrm{d}x)\right)\left(\int_{\Re} \mathrm{sat}^2\,y\mu(\mathrm{d}y)\right) , \end{aligned} \quad (3.25)$$

where the dummy variables x and y are introduced as variables of integration.

Since $\int_{\Re} \mu(\mathrm{d}y) = 1$ and combining the right two integrals,

$$\begin{aligned} C_4 - C_2^2 &= \iint_{\Re^2} \mathrm{sat}^4\, x \mu(\mathrm{d}x)\mu(\mathrm{d}y) - \iint_{\Re^2} \mathrm{sat}^2\, x\, \mathrm{sat}^2\, y \mu(\mathrm{d}x)\mu(\mathrm{d}y) \\ &= \iint_{\Re^2} \mathrm{sat}^2\, x \left(\mathrm{sat}^2\, x - \mathrm{sat}^2\, y\right) \mu(\mathrm{d}x)\mu(\mathrm{d}y) \\ &\triangleq \iint_{\Re^2} Q\ . \end{aligned} \tag{3.26}$$

The shorthand Q is used in the following. By symmetry, it is possible to look at only the first quadrant. Further, the integral is broken down into five segments.

$$\begin{aligned} \frac{1}{4}\left(C_4 - C_2^2\right) &= \int_{y=0}^{\infty}\int_{x=0}^{\infty} Q \\ &= \int_{y=1}^{\infty}\int_{x=1}^{\infty} Q \\ &\quad + \int_{y=0}^{1}\int_{x=y}^{1} Q - \int_{x=0}^{1}\int_{y=x}^{1} (-Q) \\ &\quad - \int_{y=0}^{1}\int_{x=1}^{\infty} (-Q) + \int_{x=0}^{1}\int_{y=1}^{\infty} Q \end{aligned} \tag{3.27}$$

Using the definition of the sat function, an expression for Q particular to each integral is given.

$$\begin{aligned} &\frac{1}{4}\left(C_4 - C_2^2\right) \\ &= \int_{y=1}^{\infty}\int_{x=1}^{\infty} 1\,(1-1)\,\mu(\mathrm{d}x)\mu(\mathrm{d}y) \\ &+ \int_{y=0}^{1}\int_{x=y}^{1} x^2\left(x^2 - y^2\right)\mu(\mathrm{d}x)\mu(\mathrm{d}y) - \int_{x=0}^{1}\int_{y=x}^{1} x^2\left(y^2 - x^2\right)\mu(\mathrm{d}y)\mu(\mathrm{d}x) \\ &- \int_{y=0}^{1}\int_{x=1}^{\infty}\left(y^2 - 1\right)\mu(\mathrm{d}x)\mu(\mathrm{d}y) + \int_{x=0}^{1}\int_{y=1}^{\infty} x^2\left(x^2 - 1\right)\mu(\mathrm{d}y)\mu(\mathrm{d}x) \end{aligned} \tag{3.28}$$

The first integral is zero. The third integral can be combined with the second integral by using the change of variables ($x \to y, y \to x$). In a similar fashion, the

fifth integral can be combined with the fourth.

$$\begin{aligned}
&\frac{1}{4}\left(C_4 - C_2^2\right) \\
&= \int_{y=0}^{1}\int_{x=y}^{1} x^2\left(x^2-y^2\right)\mu(\mathrm{d}x)\mu(\mathrm{d}y) - \int_{y=0}^{1}\int_{x=y}^{1} y^2\left(x^2-y^2\right)\mu(\mathrm{d}x)\mu(\mathrm{d}y) \\
&- \int_{y=0}^{1}\int_{x=1}^{\infty}\left(y^2-1\right)\mu(\mathrm{d}x)\mu(\mathrm{d}y) + \int_{y=0}^{1}\int_{x=1}^{\infty} y^2\left(y^2-1\right)\mu(\mathrm{d}x)\mu(\mathrm{d}y) \\
&= \int_{y=0}^{1}\int_{x=y}^{1}\left(x^2-y^2\right)^2\mu(\mathrm{d}x)\mu(\mathrm{d}y) + \int_{y=0}^{1}\int_{x=1}^{\infty} y^2\left(y^2-1\right)^2\mu(\mathrm{d}x)\mu(\mathrm{d}y) \qquad (3.29)
\end{aligned}$$

So for $q > 0$ the integrands are positive. The desired result follows:

$$C_4 > C_2^2 \quad \forall q > 0\ . \qquad (3.30)$$

Therefore, for stability it suffices to choose

$$(k_0, k_1, k_2, k_{ES}, q) > 0 \qquad (3.31)$$

$$a \neq 0\ . \qquad (3.32)$$

3.3.3 Simulations

Initial simulations show some practical difficulties not revealed in the stability analysis. While the equilibrium point is stable, convergence to the equilibrium is characterized by large transients. In particular, the curvature estimate $\hat{y}_0''$ does not stabilize to the true local value of the local curvature until after the minimum is found. This difficulty is overcome by two additions to the controller.

The first addition is a set of simple switches which allow the $\hat{y}_0$ and $\hat{y}_0'$ estimates to converge before the the $\hat{y}_0''$ integrator is switched on. Similarly, a few additional seconds are given to allow the $\hat{y}_0''$ estimator to converge before the $\hat{\theta}_0$ integrator is switched on. This fix eliminates initial transients, but the $\hat{y}_0''$ estimator still tends to diverge from the time the $\hat{\theta}_0$ integrator is switched on to the time the minimum is located.

To solve this problem, a second fix is implemented. The cause of the divergence in the $\hat{y}_0''$ estimator seems to be a lag in the $\hat{y}_0$ estimate that occurs when $\dot{\hat{\theta}}_0 \neq 0$. To remove this lag, an estimate of the rate of change of y with respect

to θ is added to the $\hat{y}_0$ estimator. This is simply the current estimate of the local slope $\hat{y}_0'$ multiplied by the rate of change of the $\hat{\theta}_0$ estimator. A similar estimate is added to the $\hat{y}_0'$ estimator. [The added terms are shown in square brackets below.] These added terms propogate the state in the same way that a continuous-time Kalman filter might in the absence of any estimation error.

$$\dot{\hat{y}}_0 = k_0 (y - \hat{y}) + \left[\hat{y}_0' \dot{\theta}_0\right] \tag{3.33a}$$

$$\dot{\hat{y}}_0' = k_1 (a \operatorname{sat} \eta) (y - \hat{y}) + \left[\hat{y}_0'' \dot{\theta}_0\right] \tag{3.33b}$$

$$\dot{\hat{y}}_0'' = k_2 (a \operatorname{sat} \eta)^2 (y - \hat{y}) \tag{3.33c}$$

$$\dot{\theta}_0 = -k_{ES} \frac{\hat{y}_0'}{\hat{y}_0''} \tag{3.33d}$$

$$\epsilon \, \mathrm{d}\eta = -\eta \, \mathrm{d}t + \sqrt{\epsilon} q \, \mathrm{d}W \ . \tag{3.33e}$$

Using this form of the estimator, the simulations are successful. A forth-order static map shown in Figure 3.2 was used for the simulations. The stochastic disturbance $a \operatorname{sat} \eta$ is shown in Figure 3.3. The simulation results are shown in Figure 3.4.

3.4 Newton Method Stochastic Extremum Seeking in Multiple Dimensions

In this section the controller is extended to multiple dimensions. The analysis here parallels the one-dimensional case to the extent possible.

3.4.1 Controller

Let $\hat{g}_0$ denote the estimate of the gradient at θ_0 and $\hat{H}_0$ the estimate of the Hessian at θ_0. Let α represent the stochastic inputs to the system, where the i-th component of α is defined as

$$\alpha_i = a_i \operatorname{sat} \eta_i \ . \tag{3.34}$$

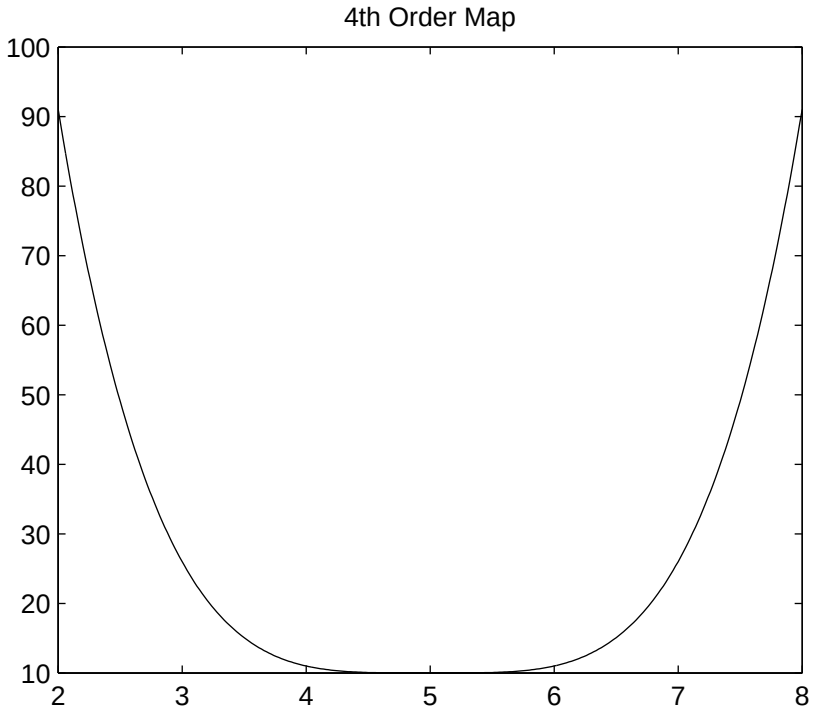

Figure 3.2: Forth-order static map used in simulation.

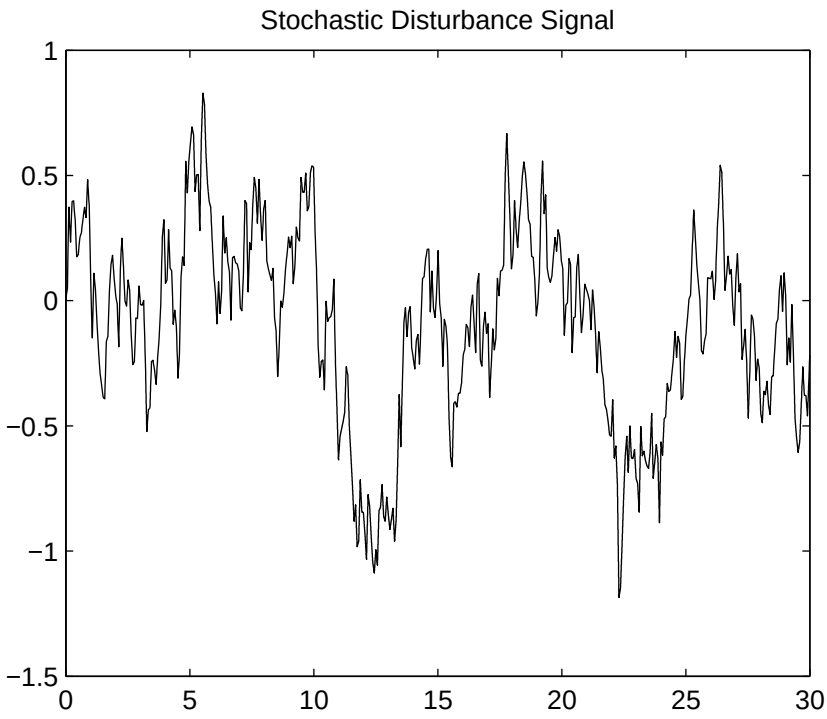

Figure 3.3: Stochastic noise signal $a \operatorname{sat} \eta$ used in simulation.

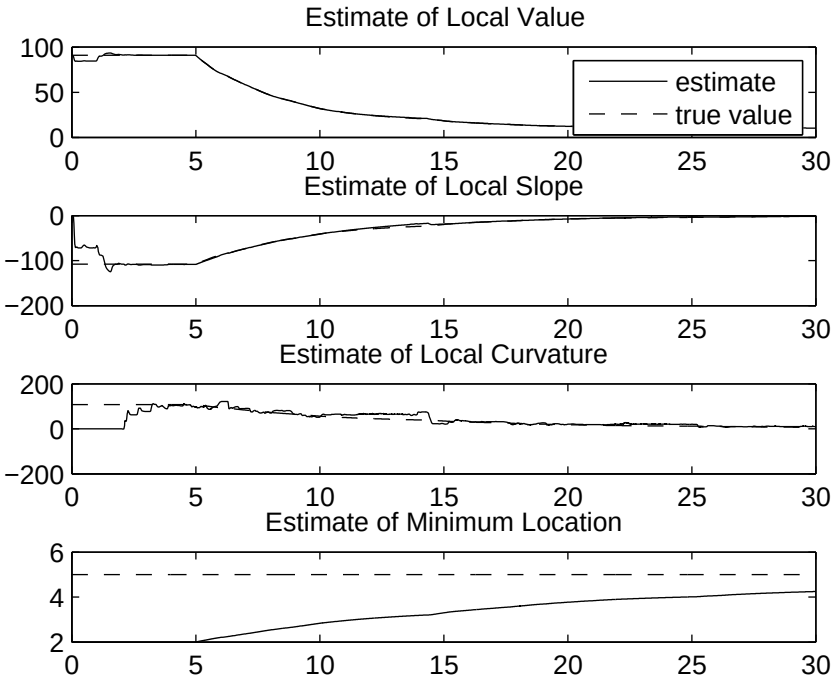

Figure 3.4: Simulation showing convergence to the minimum of a map.

Then the controller (3.33) can be extended to multiple dimensions as follows:

$$\dot{\hat{y}}_0 = k_0 \left(y - \hat{y}\right) + \left[\hat{g}_0^{\mathrm{T}} \dot{\theta}_0\right] \tag{3.35a}$$

$$\dot{\hat{g}}_0 = k_1 \alpha \left(y - \hat{y}\right) + \left[\hat{H}_0 \dot{\theta}_0\right] \tag{3.35b}$$

$$\dot{\hat{H}}_0 = k_2 \alpha \alpha^{\mathrm{T}} \left(y - \hat{y}\right) \tag{3.35c}$$

$$\dot{\theta}_0 = -k_{ES} \hat{H}_0^{-1} \hat{g}_0 \tag{3.35d}$$

$$\epsilon_i \, \mathrm{d}\eta_i = -\eta_i \, \mathrm{d}t + \sqrt{\epsilon_i} q_i \, \mathrm{d}W_i \ , \tag{3.35e}$$

where

$$\hat{y} \triangleq \hat{y}_0 + \alpha^{\mathrm{T}} \hat{g}_0 + \frac{1}{2} \alpha^{\mathrm{T}} \hat{H}_0 \alpha \ . \tag{3.35f}$$

The multi-dimensional method is susceptible to the case of negative curvature, just as the scalar case. If $\hat{H}_0$ has a negative eigenvalue the controller will actually seek a maximum rather than a minimum. This can be avoided by switching to a gradient descent algorithm when the smallest eigenvalue of $\hat{H}_0$ falls below some threshold. Similar to (3.5), the adaptation law can be modified to

$$\dot{\theta}_0 = -k_{ES} \Delta \ , \tag{3.36a}$$

where

$$\Delta = \begin{cases} \hat{H}_0^{-1} \hat{g}_0 & \text{if } \lambda_{min} > \delta \\ \left(\delta I\right)^{-1} \hat{g}_0 & \text{otherwise.} \end{cases} \tag{3.36b}$$

with λ_{min} representing the minimum eigenvalue of $\hat{H}_0$.

3.4.2 Problem Analysis

The analysis in this section parallels the scalar analysis performed above. A multi-dimensional quadratic map is analyzed.

$$y = y_* + \frac{1}{2} \left(\theta - \theta_*\right)^{\mathrm{T}} H_* \left(\theta - \theta_*\right) \tag{3.37}$$

As in the scalar case, difficulties associated with finding the inverse of the Hessian when it becomes nearly singular are ignored, noting that the more practical adaptation law (3.36) avoids these difficulties and behaves like (3.35d) near a local minimum of sufficient curvature.

For analysis, the simplest possible form of the controller is used:

$$\dot{\hat{y}}_0 = k_0 \left(y - \hat{y}\right) \tag{3.38a}$$

$$\dot{\hat{g}}_0 = k_1 \alpha \left(y - \hat{y}\right) \tag{3.38b}$$

$$\dot{\hat{H}}_0 = k_2 \alpha \alpha^{\mathrm{T}} \left(y - \hat{y}\right) \tag{3.38c}$$

$$\dot{\theta}_0 = -k_{ES} \hat{H}_0^{-1} \hat{g}_0 \tag{3.38d}$$

$$\epsilon_i \, \mathrm{d}\eta_i = -\eta_i \, \mathrm{d}t + \sqrt{\epsilon_i} q_i \, \mathrm{d}W_i \ . \tag{3.38e}$$

Plugging in the expressions for y and $\hat{y}$ from (3.37) and (3.35f), and using $\theta = \theta_0 + \alpha$, the expression $(y - \hat{y})$ is expanded and grouped by power of α.

$$\begin{aligned} y - \hat{y} &= \left[y_* + \frac{1}{2} \left(\theta_0 + \alpha - \theta_*\right)^{\mathrm{T}} H_* \left(\theta_0 + \alpha - \theta_*\right) \right] - \left[\hat{y}_0 + \alpha^{\mathrm{T}} \hat{g}_0 + \frac{1}{2} \alpha^{\mathrm{T}} \hat{H}_0 \alpha \right] \\ &= \alpha^{\mathrm{T}} \left[\frac{1}{2} \left(H_* - \hat{H}_0 \right) \right] \alpha + \alpha^{\mathrm{T}} \left[H_* \left(\theta_0 - \theta_*\right) - \hat{g}_0 \right] \\ &\quad + \left[y_* + \frac{1}{2} \left(\theta_0 - \theta_*\right)^{\mathrm{T}} H_* \left(\theta_0 - \theta_*\right) - \hat{y}_0 \right] \end{aligned} \tag{3.39}$$

From the definition of y in (3.37), note the following:

$$y_* + \frac{1}{2} \left(\theta_0 - \theta_*\right)^{\mathrm{T}} H_* \left(\theta_0 - \theta_*\right) \triangleq y_0 \tag{3.40a}$$

$$H_* \left(\theta_0 - \theta_*\right) \triangleq g_0 \tag{3.40b}$$

$$H_* \triangleq H_0 \tag{3.40c}$$

The expression for $(y - \hat{y})$ then simplifies to

$$y - \hat{y} = \alpha^{\mathrm{T}} \left[\frac{1}{2} \left(H_0 - \hat{H}_0 \right) \right] \alpha + \alpha^{\mathrm{T}} \left[g_0 - \hat{g}_0 \right] + \left[y_0 - \hat{y}_0 \right] \ . \tag{3.41}$$

Using this expression, the closed loop system is written

$$\dot{\hat{y}}_0 = k_0 \left(\alpha^{\mathrm{T}} \left[\frac{1}{2} \left(H_0 - \hat{H}_0 \right) \right] \alpha + \alpha^{\mathrm{T}} \left[g_0 - \hat{g}_0 \right] + \left[y_0 - \hat{y}_0 \right] \right) \tag{3.42a}$$

$$\dot{\hat{g}}_0 = k_1 \left(\alpha\alpha^{\mathrm{T}} \left[\frac{1}{2} \left(H_0 - \hat{H}_0 \right) \right] \alpha + \alpha\alpha^{\mathrm{T}} \left[g_0 - \hat{g}_0 \right] + \alpha \left[y_0 - \hat{y}_0 \right] \right) \tag{3.42b}$$

$$\dot{\hat{H}}_0 = k_2 \left(\alpha\alpha^{\mathrm{T}}\alpha^{\mathrm{T}} \left[\frac{1}{2} \left(H_0 - \hat{H}_0 \right) \right] \alpha + \alpha\alpha^{\mathrm{T}}\alpha^{\mathrm{T}} \left[g_0 - \hat{g}_0 \right] + \alpha\alpha^{\mathrm{T}} \left[y_0 - \hat{y}_0 \right] \right) \tag{3.42c}$$

$$\dot{\theta}_0 = -k_{ES} \hat{H}_0^{-1} \hat{g}_0 \tag{3.42d}$$

$$\epsilon_i \, \mathrm{d}\eta_i = -\eta_i \, \mathrm{d}t + \sqrt{\epsilon_i} q_i \, \mathrm{d}W_i \ . \tag{3.42e}$$

Averaging

Stochastic averaging is used to remove the η dynamics. The average of certain vector and matrix products are needed to do so, so these are developed first. In doing so, the following shorthand notation is used: $C_{2i} \triangleq C_2(q_i)$ and similarly for C_4. Below, the notation s denotes a generic scalar, v a generic vector, and M a generic matrix. Integrals are understood to be multiple integrals over

each of the stochastic variables η_i. The following integrals are needed:

$$\int_{\Re^n} \alpha s \mu(\mathrm{d}\eta) = 0 \tag{3.43a}$$

$$\int_{\Re^n} \alpha\alpha^{\mathrm{T}} s \mu(\mathrm{d}\eta) \triangleq C_{s2}(s)$$

$$\left(C_{s2}(s)\right)_{ij} = \begin{cases} a_i^2 C_{2i} s & i = j \\ 0 & i \neq j \end{cases} \tag{3.43b}$$

$$\int_{\Re^n} \alpha^{\mathrm{T}} v \mu(\mathrm{d}\eta) = 0 \tag{3.43c}$$

$$\int_{\Re^n} \alpha\alpha^{\mathrm{T}} v \mu(\mathrm{d}\eta) \triangleq C_{v2}(v), \quad \left(C_{v2}(v)\right)_i = a_i^2 C_{2i} v_i \tag{3.43d}$$

$$\int_{\Re^n} \alpha\alpha^{\mathrm{T}}\alpha^{\mathrm{T}} v \mu(\mathrm{d}\eta) = 0 \tag{3.43e}$$

$$\int_{\Re^n} \alpha^{\mathrm{T}} M \alpha \mu(\mathrm{d}\eta) \triangleq C_{M2}(M) = \sum_k a_k^2 C_{2k} M_{kk} \tag{3.43f}$$

$$\int_{\Re^n} \alpha\alpha^{\mathrm{T}} M \alpha \mu(\mathrm{d}\eta) = 0 \tag{3.43g}$$

$$\int_{\Re^n} \alpha\alpha^{\mathrm{T}}\alpha^{\mathrm{T}} M \alpha \mu(\mathrm{d}\eta) \triangleq C_{M4}(M)$$

$$\left(C_{M4}(M)\right)_{ij} = \begin{cases} a_i^4 C_{4i} M_{ij} + a_i^2 C_{2i} \sum_{k\neq i} a_k^2 C_{2k} M_{kk} & i = j \\ a_i^2 a_j^2 C_{2i} C_{2j} \left(M_{ij} + M_{ji}\right) & i \neq j \end{cases} \tag{3.43h}$$

Note that $C_{M2}(\cdot)$ is scalar-valued, $C_{v2}(\cdot)$ is vector-valued, and $C_{M4}(\cdot)$ and $C_{s2}(\cdot)$ are matrix-valued functions. Also note that all are linear functions of their arguments.

The average system is written[2]

$$\dot{\bar{\hat{y}}}_0 = k_0 \left[\frac{1}{2} C_{M2}\left(H_0 - \bar{\hat{H}}_0\right) + \left(y_0 - \bar{\hat{y}}_0\right)\right] \tag{3.44a}$$

$$\dot{\bar{\hat{g}}}_0 = k_1 \left[C_{v2}\left(g_0 - \bar{\hat{g}}_0\right)\right] \tag{3.44b}$$

$$\dot{\bar{\hat{H}}}_0 = k_2 \left[\frac{1}{2} C_{M4}\left(H_0 - \bar{\hat{H}}_0\right) + C_{s2}\left(y_0 - \bar{\hat{y}}_0\right)\right] \tag{3.44c}$$

$$\dot{\bar{\theta}}_0 = -k_{ES} \bar{\hat{H}}_0^{-1} \bar{\hat{g}}_0 \ . \tag{3.44d}$$

[2]The reader is reminded that $C_{M2}(\cdot)$, $C_{v2}(\cdot)$, $C_{M4}(\cdot)$, and $C_{s2}(\cdot)$ are functions: the quantities following them in parentheses are their arguments, not terms they multiply.

Equilibrium

The estimator states are in equilibrium when they match the parameters of the quadratic map which they reflect.

$$\begin{pmatrix} \bar{\hat{y}}_{0,eq} \\ \bar{\hat{g}}_{0,eq} \\ \bar{\hat{H}}_{0,eq} \end{pmatrix} = \begin{pmatrix} y_0 \\ g_0 \\ H_0 \end{pmatrix} \tag{3.45}$$

To show that this is an isolated equilibrium, first observe that $(C_{v2}(\cdot))_i$ is function of only the i-th element of its argument. From (3.44b) it is evident that at equilibrium every element of $\bar{\hat{g}}_0$ must equal the corresponding element of g_0. The $\dot{\bar{\hat{y}}}_0$ and $\dot{\bar{\hat{H}}}_0$ equations, however, are coupled so showing their elements to have an isolated equilibrium is less straightforward.

Observe that (3.45) is an isolated equilibrium so long as the scalar equation (3.44a) is independent of at least one of the scalar equations represented by the matrix equation (3.44c) at every point other than (3.45). This is true if the condition

$$\exists(i,j) \text{ such that } \frac{(C_{M4}(M))_{ij}}{C_{M2}(M)} \neq \frac{(C_{s2}(s))_{ij}}{s} \tag{3.46}$$

holds for all $(M, s) \neq 0$.

For the off-diagonal ($i \neq j$) case the condition (3.46) expands to

$$\frac{a_i^2 a_j^2 C_{2i} C_{2j} \left(M_{ij} + M_{ji}\right)}{\sum_k a_k^2 C_{2k} M_{kk}} \neq \frac{0}{s} \ . \tag{3.47}$$

This is satisfied for all symmetric matrices with a non-zero (i, j) element. Since the Hessian being estimated is symmetric, this means that (3.46) is satisfied for all non-diagonal M.

For the diagonal ($i = j$) entries, (3.46) expands to

$$\frac{a_i^4 C_{4i} M_{ii} + a_i^2 C_{2i} \sum_{k \neq i} a_k^2 C_{2k} M_{kk}}{\sum_k a_k^2 C_{2k} M_{kk}} \neq \frac{a_i^2 C_{2i} s}{s} \ . \tag{3.48}$$

The factors of s cancel, as do most of terms in the summations, and the equation simplifies to

$$a_i^2 \left(C_{4i} - C_{2i}^2\right) M_{ii} \neq 0 \ . \tag{3.49}$$

Since $C_4 > C_2^2$, this means that (3.46) is satisfied for any M with a non-zero diagonal element. Therefore, since (3.46) is satisfied for all non-diagonal M and all M with a non-zero diagonal element, it is satisfied for all $M \neq 0$. The condition $s \neq 0$ is implicit in the divided by s. So (3.46) is satisfied for all $(M, s) \neq 0$ and the estimator equilibrium in (3.45) is indeed isolated.

The adaptation law has an equilibrium when $\bar{\hat{g}}_0$ is zero. Because $\bar{\hat{g}}_0$ equals g_0 at equilibrium and g_0 is only equal to zero at θ_*, the only equilibrium point of $\bar{\theta}_0$ is at θ_*. That is, the equilibrium of the average system is

$$\begin{pmatrix} \bar{\hat{y}}_{0,eq} \\ \bar{\hat{g}}_{0,eq} \\ \bar{\hat{H}}_{0,eq} \\ \bar{\theta}_{0,eq} \end{pmatrix} = \begin{pmatrix} y_* \\ 0 \\ H_* \\ \theta_* \end{pmatrix} . \tag{3.50}$$

In summary, the average system has one equilibrium and it is located at the minimum of the quadratic map.

Stability

To test stability, expand the vector and matrix differential equations and stack the resulting scalar equations together. Because of their similarity, all of the diagonal elements of $\bar{\hat{H}}_0$ are stacked together and all of the off-diagonal elements are stacked together. Also, because $\bar{\hat{H}}_0$ is symmetric, the elements below the main diagonal are discarded. Let the dimension of the map be n. The complete expanded system is then

$$\dot{\bar{\hat{y}}}_0 = k_0 \left[\frac{1}{2} \sum_k a_k^2 C_{2k} \left(H_0 - \bar{\hat{H}}_0 \right)_{kk} + \left(y_0 - \bar{\hat{y}}_0 \right) \right] \tag{3.51a}$$

$$\left(\dot{\bar{\hat{g}}}_0 \right)_1 = k_1 \left[a_1^2 C_{21} \left(g_0 - \bar{\hat{g}}_0 \right)_1 \right] \tag{3.51b}$$

$$\vdots \quad = \quad \vdots$$

$$\left(\dot{\bar{\hat{g}}}_0 \right)_n = k_1 \left[a_n^2 C_{2n} \left(g_0 - \bar{\hat{g}}_0 \right)_n \right] \tag{3.51c}$$

$$\left(\dot{\bar{\hat{H}}}_0\right)_{11} = k_2\left[\frac{1}{2}\left(a_1^4 C_{41}\left(H_0 - \bar{\hat{H}}_0\right)_{11} + a_1^2 C_{21}\sum_{k\neq 1} a_k^2 C_{2k}\left(H_0 - \bar{\hat{H}}_0\right)_{kk}\right) + a_1^2 C_{21}\left(y_0 - \bar{\hat{y}}_0\right)\right] \tag{3.51d}$$

$$\vdots \quad = \quad \vdots$$

$$\left(\dot{\bar{\hat{H}}}_0\right)_{nn} = k_2\left[\frac{1}{2}\left(a_n^4 C_{4n}\left(H_0 - \bar{\hat{H}}_0\right)_{nn} + a_n^2 C_{2n}\sum_{k\neq n} a_k^2 C_{2k}\left(H_0 - \bar{\hat{H}}_0\right)_{kk}\right) + a_n^2 C_{2n}\left(y_0 - \bar{\hat{y}}_0\right)\right] \tag{3.51e}$$

$$\left(\dot{\bar{\hat{H}}}_0\right)_{12} = k_2\left[a_1^2 a_2^2 C_{21} C_{22}\left(H_0 - \bar{\hat{H}}_0\right)_{12}\right] \tag{3.51f}$$

$$\vdots \quad = \quad \vdots$$

$$\left(\dot{\bar{\hat{H}}}_0\right)_{(n-1)n} = k_2\left[a_{(n-1)}^2 a_n^2 C_{2(n-1)} C_{2n}\left(H_0 - \bar{\hat{H}}_0\right)_{(n-1)n}\right] \tag{3.51g}$$

$$\left(\dot{\bar{\theta}}_0\right)_1 = -k_{ES}\left(\bar{\hat{H}}_0^{-1}\bar{\hat{g}}_0\right)_1 \tag{3.51h}$$

$$\vdots \quad = \quad \vdots$$

$$\left(\dot{\bar{\theta}}_0\right)_n = -k_{ES}\left(\bar{\hat{H}}_0^{-1}\bar{\hat{g}}_0\right)_n \tag{3.51i}$$

By analogy with the scalar case, the Jacobian evaluated at the equilibrium point is likely to be sparse. The non-zero components of the Jacobian at the equilibrium are as follows:

$$\frac{\partial \dot{\bar{\hat{y}}}_0}{\partial \bar{\hat{y}}_0} = -k_0 \tag{3.52a}$$

$$\frac{\partial \dot{\bar{\hat{y}}}_0}{\partial\left(\bar{\hat{H}}_0\right)_{11}} = -\frac{k_0}{2} a_1^2 C_{21} \tag{3.52b}$$

$$\frac{\partial \dot{\bar{\hat{y}}}_0}{\partial\left(\bar{\hat{H}}_0\right)_{nn}} = -\frac{k_0}{2} a_n^2 C_{2n} \tag{3.52c}$$

$$\frac{\partial\left(\dot{\bar{\hat{g}}}_0\right)_1}{\partial\left(\bar{\hat{g}}_0\right)_1} = -k_1 a_1^2 C_{21} \tag{3.52d}$$

$$\frac{\partial\left(\dot{\bar{\hat{g}}}_0\right)_1}{\partial\left(\bar{\theta}_0\right)_1} = k_1 a_1^2 C_{21}\left(H_*\right)_{11} \tag{3.52e}$$

$$\frac{\partial\left(\dot{\bar{\hat{g}}}_0\right)_1}{\partial\left(\bar{\theta}_0\right)_n} = k_1 a_1^2 C_{21}\left(H_*\right)_{1n} \tag{3.52f}$$

$$\frac{\partial\left(\dot{\bar{\hat{g}}}_0\right)_n}{\partial\left(\bar{\hat{g}}_0\right)_n} = -k_1 a_n^2 C_{2n} \tag{3.52g}$$

$$\frac{\partial\left(\dot{\bar{\hat{g}}}_0\right)_n}{\partial\left(\bar{\theta}_0\right)_1} = k_1 a_n^2 C_{2n}\left(H_*\right)_{n1} \tag{3.52h}$$

$$\frac{\partial\left(\dot{\bar{\hat{g}}}_0\right)_n}{\partial\left(\bar{\theta}_0\right)_n} = k_1 a_n^2 C_{2n}\left(H_*\right)_{nn} \tag{3.52i}$$

$$\frac{\partial\left(\dot{\bar{\hat{H}}}_0\right)_{11}}{\partial\bar{\hat{y}}_0} = -k_2 a_1^2 C_{21} \tag{3.52j}$$

$$\frac{\partial\left(\dot{\bar{\hat{H}}}_0\right)_{11}}{\partial\left(\bar{\hat{H}}_0\right)_{11}} = -\frac{k_2}{2} a_1^4 C_{41} \tag{3.52k}$$

$$\frac{\partial\left(\dot{\bar{\hat{H}}}_0\right)_{11}}{\partial\left(\bar{\hat{H}}_0\right)_{nn}} = -\frac{k_2}{2} a_1^2 a_n^2 C_{21} C_{2n} \tag{3.52l}$$

$$\frac{\partial\left(\dot{\bar{\hat{H}}}_0\right)_{nn}}{\partial\bar{\hat{y}}_0} = -k_2 a_n^2 C_{2n} \tag{3.52m}$$

$$\frac{\partial\left(\dot{\bar{\hat{H}}}_0\right)_{nn}}{\partial\left(\bar{\hat{H}}_0\right)_{11}} = -\frac{k_2}{2} a_n^2 a_1^2 C_{2n} C_{21} \tag{3.52n}$$

$$\frac{\partial\left(\dot{\bar{\hat{H}}}_0\right)_{nn}}{\partial\left(\bar{\hat{H}}_0\right)_{nn}} = -\frac{k_2}{2} a_n^4 C_{4n} \tag{3.52o}$$

$$\frac{\partial\left(\dot{\bar{\hat{H}}}_0\right)_{12}}{\partial\left(\bar{\hat{H}}_0\right)_{12}} = -k_2 a_1^2 a_2^2 C_{21} C_{22} \tag{3.52p}$$

$$\frac{\partial\left(\dot{\bar{\hat{H}}}_0\right)_{(n-1)n}}{\partial\left(\bar{\hat{H}}_0\right)_{(n-1)n}} = -k_2 a_{(n-1)}^2 a_n^2 C_{2(n-1)} C_{2n} \tag{3.52q}$$

$$\frac{\partial\left(\dot{\bar{\hat{\theta}}}_0\right)_1}{\partial\left(\bar{\hat{g}}_0\right)_1} = -k_{ES}\left(H_*^{-1}\right)_{11} \tag{3.52r}$$

$$\frac{\partial\left(\dot{\bar{\hat{\theta}}}_0\right)_1}{\partial\left(\bar{\hat{g}}_0\right)_n} = -k_{ES}\left(H_*^{-1}\right)_{1n} \tag{3.52s}$$

$$\frac{\partial\left(\dot{\bar{\hat{\theta}}}_0\right)_n}{\partial\left(\bar{\hat{g}}_0\right)_1} = -k_{ES}\left(H_*^{-1}\right)_{n1} \tag{3.52t}$$

$$\frac{\partial\left(\dot{\bar{\hat{\theta}}}_0\right)_n}{\partial\left(\bar{\hat{g}}_0\right)_n} = -k_{ES}\left(H_*^{-1}\right)_{nn} \tag{3.52u}$$

Note that by assumption the Hessian is a constant so that H_0 does not change with θ_0. Also, note that calculating some of the partial derivatives involves taking derivatives of the elements of matrix inverse with respect to elements of the original matrix; for instance, $\partial\left(\dot{\bar{\hat{\theta}}}_0\right)_1 / \partial\left(\bar{\hat{H}}_0\right)_{11}$. These can be computed using the matrix inversion lemma [35]. However, the gradient appears as a factor in such partial derivatives, and at the equilibrium point the gradient is zero. Because of this such partial derivatives, when evaluated at the equilibrium point, become zero.

Because of the sparsity structure of the Jacobian, the linearized system decouples into three subsystems: one containing $\bar{\hat{y}}_0$ and the diagonal elements of $\bar{\hat{H}}_0$, one containing $\bar{\hat{g}}$ and $\bar{\theta}_0$, and one containing only the off-diagonal elements of $\bar{\hat{H}}_0$. To find conditions for stability, each of the subsystems are analyzed separately. Unlike the one-dimensional case, the Routh-Hurwitz criterion cannot be used because its calculation involves a recursive formula, which poses problems for general analysis of an n-dimensional case. Instead, a Lyapunov analysis is used.

For this analysis, the following error variables are introduced:

$$\tilde{y} = \bar{\hat{y}}_0 - y_* \tag{3.53a}$$

$$\tilde{H}_d = \begin{pmatrix} \bar{\hat{H}}_{11} - (H_*)_{11} \\ \vdots \\ \bar{\hat{H}}_{nn} - (H_*)_{nn} \end{pmatrix} \tag{3.53b}$$

$$\tilde{g} = \begin{pmatrix} \left(\bar{\hat{g}}_0\right)_1 - 0 \\ \vdots \\ \left(\bar{\hat{g}}_0\right)_n - 0 \end{pmatrix} \tag{3.53c}$$

$$\tilde{\theta} = \begin{pmatrix} \left(\bar{\theta}_0\right)_1 - (\theta_*)_1 \\ \vdots \\ \left(\bar{\theta}_0\right)_n - (\theta_*)_n \end{pmatrix} \tag{3.53d}$$

$$\tilde{H}_{od} = \begin{pmatrix} \left(\bar{\hat{H}}_0\right)_{12} - (H_*)_{12} \\ \vdots \\ \left(\bar{\hat{H}}_0\right)_{(n-1)n} - (H_*)_{(n-1)n} \end{pmatrix} , \tag{3.53e}$$

the constant vector ν

$$\nu_i \triangleq a_i^2 C_{2i} , \tag{3.54a}$$

the constant diagonal matrix N

$$(N)_{ij} \triangleq \begin{cases} a_i^2 C_{2i} & i = j \\ 0 & i \neq j , \end{cases} \tag{3.54b}$$

and the constant diagonal matrix μ

$$(\mu)_{ij} = \begin{cases} a_i^4 \left(C_{4i} - C_{2i}^2\right) & i = j \\ 0 & i \neq j . \end{cases} \tag{3.54c}$$

Then the $(\tilde{y}, \tilde{H}_d)$ and $(\tilde{g}, \tilde{\theta})$ linearized subsystems are

$$\dot{\tilde{y}} = -k_0 \tilde{y} - \frac{k_0}{2} \nu^{\mathrm{T}} \tilde{H}_d \tag{3.55a}$$

$$\dot{\tilde{H}}_d = -k_2 \nu \tilde{y} - \frac{k_2}{2} \left(\nu \nu^{\mathrm{T}} + \mu\right) \tilde{H}_d \tag{3.55b}$$

and

$$\dot{\tilde{g}} = -k_1 N\tilde{g} + k_1 N H_* \tilde{\theta} \tag{3.56a}$$

$$\dot{\tilde{\theta}} = -k_{ES} H_*^{-1} \tilde{g} \ . \tag{3.56b}$$

The $\tilde{H}_{od}$ subsystem is actually a set of decoupled equations. Although $\tilde{H}_{od}$ is a vector, it is derived from the off-diagonal entries of a matrix, so a double-index notation is used to denote its elements. For example, $\left(\tilde{H}_{od}\right)_{12}$ refers to the first element of $\tilde{H}_{od}$ as shown in (3.53e). Then the elements of the $\tilde{H}_{od}$ subsystem are written

$$\left(\dot{\tilde{H}}_{od}\right)_{ij} = -k_2\nu_1\nu_2 \left(\tilde{H}_{od}\right)_{ij} \ . \tag{3.57}$$

The subsystems (3.55) (3.56) and (3.57) are analyzed in turn for stability.

To analyze (3.55) the following candidate Lyapunov function is used:

$$V_1 = \frac{1}{2k_0}\tilde{y}^2 + \frac{1}{4k_2}\tilde{H}_d^{\mathrm{T}}\tilde{H}_d \ , \tag{3.58}$$

This function is positive definite if k_0 and k_2 are greater than zero. Then the time derivative of V_1 is

$$\begin{aligned}
\dot{V}_1 &= \frac{1}{k_0}\tilde{y}\dot{\tilde{y}} + \frac{1}{2k_2}\tilde{H}_d^{\mathrm{T}}\dot{\tilde{H}}_d \\
&= \frac{1}{k_0}\tilde{y}\left(-k_0\tilde{y} - \frac{k_0}{2}\nu^{\mathrm{T}}\tilde{H}_d\right) + \frac{1}{2k_2}\tilde{H}_d^{\mathrm{T}}\left(-k_2\nu\tilde{y} - \frac{k_2}{2}\left(\nu\nu^{\mathrm{T}} + \mu\right)\tilde{H}_d\right) \\
&= -\tilde{y}^2 - \frac{1}{2}\tilde{y}\nu^{\mathrm{T}}\tilde{H}_d - \frac{1}{2}\tilde{H}_d^{\mathrm{T}}\nu\tilde{y} - \frac{1}{4}\tilde{H}_d^{\mathrm{T}}\left(\nu\nu^{\mathrm{T}} + \mu\right)\tilde{H}_d \\
&= -\tilde{y}^2 - \left(\tilde{H}_d^{\mathrm{T}}\nu\right)\tilde{y} - \frac{1}{4}\tilde{H}_d^{\mathrm{T}}\nu\nu^{\mathrm{T}}\tilde{H}_d - \frac{1}{4}\tilde{H}_d^{\mathrm{T}}\mu\tilde{H}_d \\
&= -\left(\tilde{y}^2 + \frac{1}{2}\tilde{H}_d^{\mathrm{T}}\nu\right)^2 - \frac{1}{4}\tilde{H}_d^{\mathrm{T}}\mu\tilde{H}_d \ ,
\end{aligned} \tag{3.59}$$

which is negative definite if μ is positive definite. Since C_4 is greater than C_2^2 when q is positive, μ is positive definite when all q_i are positive. Therefore, (3.55) has a stable equilibrium at the origin if k_0 and k_2 are chosen positive and all q_i are positive.

The analysis (3.56) proceeds in a similar fashion. Define the candidate Lyapunov function

$$V_2 = \frac{1}{2k_1}\tilde{g}^{\mathrm{T}}N^{-1}\tilde{g} + \frac{1}{2k_{ES}}\tilde{\theta}^{\mathrm{T}}H_*H_*\tilde{\theta} \tag{3.60}$$

which is positive definite is k_1 and k_{ES} are greater than zero. The time derivative of V_2 is

$$\begin{aligned}
\dot{V}_2 &= \frac{1}{k_1}\tilde{g}^{\mathrm{T}}N^{-1}\dot{\tilde{g}} + \frac{1}{k_{ES}}\tilde{\theta}^{\mathrm{T}}H_*H_*\dot{\tilde{\theta}} \\
&= \frac{1}{k_1}\tilde{g}^{\mathrm{T}}N^{-1}\left(-k_1N\tilde{g} + k_1NH_*\tilde{\theta}\right) + \frac{1}{k_{ES}}\tilde{\theta}^{\mathrm{T}}H_*H_*\left(-k_{ES}H_*^{-1}\tilde{g}\right) \\
&= \tilde{g}^{\mathrm{T}}N^{-1}\left(-N\tilde{g} + NH_*\tilde{\theta}\right) + \tilde{\theta}^{\mathrm{T}}H_*H_*\left(-H_*^{-1}\tilde{g}\right) \\
&= -\tilde{g}^{\mathrm{T}}N^{-1}N\tilde{g} + \tilde{g}^{\mathrm{T}}N^{-1}NH_*\tilde{\theta} - \tilde{\theta}^{\mathrm{T}}H_*H_*H_*^{-1}\tilde{g} \\
&= -\tilde{g}^{\mathrm{T}}\tilde{g} + \tilde{g}^{\mathrm{T}}H_*\tilde{\theta} - \tilde{\theta}^{\mathrm{T}}H_*\tilde{g} \\
&= -\tilde{g}^{\mathrm{T}}\tilde{g}\ , \qquad (3.61)
\end{aligned}$$

which is negative if $\tilde{g} \neq 0$. Moreover, by inspection of (3.56a), if $\tilde{g}$ is stable at zero $\tilde{\theta}$ must also be zero. Therefore, by LaSalle's invariance principle, (3.56) has a stable equilibrium at the origin if k_1 and k_{ES} are chosen positive.

To analyze (3.57) simply note that each of the decoupled equations are stable first order systems when k_2 is chosen positive.

Having analyzed (3.55) (3.56) and (3.57), the assumptions necessary for stability are here collected. As in the scalar case, it suffices to choose positive parameters and non-zero scaling factors:

$$(k_0, k_1, k_2, k_{ES}) > 0 \qquad (3.62a)$$

$$q_i > 0 \quad \forall i \qquad (3.62b)$$

$$a_i \neq 0 \quad \forall i\ . \qquad (3.62c)$$

Under the conditions (3.62) each of the three independent subsystems (3.55) (3.56) and (3.57) are stable. These subsystems are the components of the linearized average system (3.44) about the point (3.50), implying local exponential stability equilibrium point of the average system. By Theorem 2 in [3] this implies weak exponential stability of the original stochastically perturbed system (3.42).

3.4.3 Simulations

Simulation results using the multi-dimensional controller are shown in Figure 3.5 and Figure 3.6. The simulations use a parabolic map with a minimum at

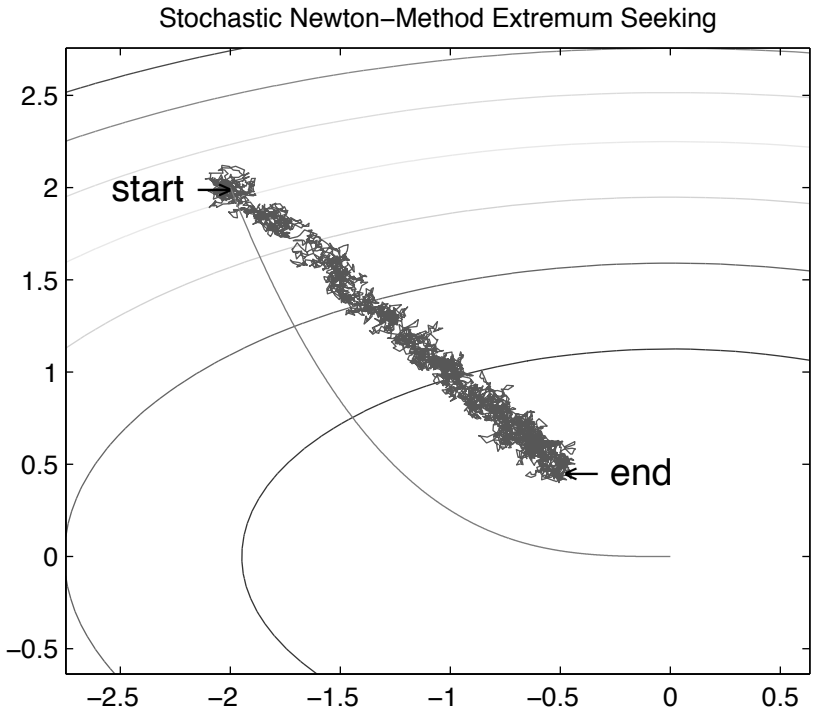

Figure 3.5: Straight line descent of θ towards minimum of map.

the origin. Note the straight line made towards the minimum in Figure 3.5, where the direction of descent is at a clear angle to the gradient. To emphasize this, a theoretical gradient descent from the same starting point is also plotted.

3.5 Discussion

3.5.1 Newton Method Extremum Seeking

The primary motivation for developing a Newton method version of extremum seeking is to allow a straight-line descent towards the minimum of a multi-dimensional map. The common gradient-descent approach can yield fast convergence in one dimension and slow convergence in another. By contrast the Newton method version of extremum seeking converges at a similar rate in all dimensions. This capability is realized and demonstrated through simulation.

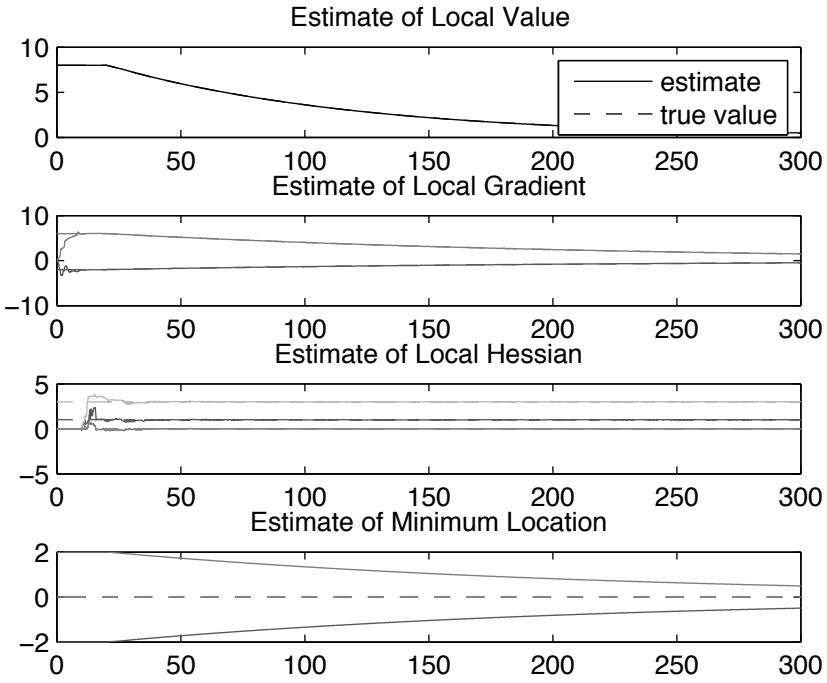

Figure 3.6: Convergence of estimator and adaptation law states.

3.5.2 Extremum Seeking Based on Estimation Error

In a departure from the norm, the presented form of extremum seeking depends on the difference between the measured variable y and its estimate $\hat{y}$. Usually, the dependence is upon y itself. In this respect it aligns with formulations typically seen in optimal linear estimation. This yields certain advantages.

One advantage is the removal of the need for high-pass and low-pass filters. Although not necessary for proofs of stability, in extremum seeking it is often necessary to place a high-pass filter on the measured variable and a low-pass filter on the adaptation law for the sake of performance. As shown by the simulation results, it is not necessary to use additional filters when using a dependence on $(y - \hat{y})$, instead of y alone. The dynamic equation for $\hat{y}_0$, combined with the calculation of $\hat{y}$ effectively removes the steady-state component of y, fulfilling the role of the high-pass filter. The need for a low-pass filter is similarly removed: because the estimator equations are based on the difference between the measured variable and its estimate, when the estimate becomes accurate, the adaptation rate becomes smooth.

A related advantage is that local value, gradient, and Hessian are explicit states. This adds to an intuitive understanding of the estimator. This, in turn, facilitates design and extension of the control system.

3.5.3 Knowledge of the Nature of the Stochastic Signals

The extremum-seeking algorithm requires a measurement of the stochastic signals; however, very little about the nature of the stochastic signals is assumed. They are assumed to be bounded and zero-mean, but the control design does not rely upon knowledge of the amplitude of the signals or any of their higher moments. This is done intentionally with an eye towards possible future applications where such information may not be known. In applications where the perturbation signal is not manually generated, but rather is a naturally occurring disturbance that can only be measured, the amplitude of the signal may not be known ahead of time. It may even change with time. This would prevent implementation of any algorithm that relied upon knowledge of the nature of the stochastic signals.

3.6 Conclusion

The benefits of deterministic Newton method extremum seeking have been transferred to stochastic extremum seeking. Analysis proves weak local exponential stability of the minimum of a static n-dimensional quadratic map. Simulations confirm straight line convergence to the minimum of a two-dimensional quadratic map.

Rather than depending directly upon the measured variable, the extremum-seeking controller depends upon the estimation error of the measured variable. This produces a controller that does not require additional filtering for practical implementation. The controller also has no dependence on the nature of the stochastic perturbations used, allowing it to be used even when such information is unknown.

3.7 Acknowledgements

Chapter 3 contains material that is currently being prepared for submission for publication (Krieger, J., and Krstic, M.). The dissertation author was the primary investigator and author of this material.

Chapter 4

Aircraft Endurance Maximization at Medium Mach Numbers by Extremum Seeking

Aircraft endurance is maximized by optimizing the lift to drag ratio over a two-dimensional space spanned by angle of attack and Mach number, constrained to a one-dimensional curve on which lift equals the weight of the aircraft. The gradient estimator used in the optimization is excited by atmospheric turbulence in the vertical and longitudinal directions. This new form of extremum seeking requires a reformulation of the standard gradient estimator used in extremum seeking to provide gradient estimates that are independent of the amplitude of the dither signal. A new gradient estimator based on an estimation error approach is presented to this end. Through stochastic averaging analysis, the estimator is shown to stabilize the aircraft to the optimal endurance speed, with a bias that is proportional to the square of the turbulence amplitude and thus is small when turbulence is light. The controller is tested in a high fidelity six degree of freedom simulation provided by local industry. Simulation results show maximization of aircraft endurance and even a slight improvement compared to flight at the nominal loiter speed of the aircraft being simulated.

4.1 Nomenclature

A	=	Aspect ratio
a	=	Speed of sound
a_1, a_2	=	Stochastic disturbance post-saturation scaling factors
a_x, a_z	=	Component of acceleration in the x or z body axis directions
C_2, C_4	=	Averaging constants
C_D	=	Coefficient of drag
C_{D0}	=	Zero-lift drag coefficient
C_L	=	Coefficient of Lift
D	=	Drag
e	=	Oswald efficiency number
f	=	Lift to drag ratio
$\hat{f}$	=	The estimator's prediction of f
g	=	Acceleration due to gravity
g_x, g_z	=	Component of g in the x or z body axis directions
J	=	Jacobian of a system
k_{ES}	=	Extremum seeking gain
k_1, k_2, k_3	=	Estimator gains
L	=	Lift
L_u, L_v, L_w	=	Characteristic lengths of turbulence field
		(longitudinal, lateral, vertical)
M	=	Mach number
m	=	Mass of the aircraft
$n_0, n_1, n_2, \ldots$	=	Coefficients of the Taylor expansion of v
q_1, q_2	=	Stochastic disturbance pre-saturation scaling factors
S	=	Reference area
s	=	Laplace variable
s_1	=	Estimator state $\approx f$
s_2	=	Estimator state $\approx f_U$
s_3	=	Estimator state $\approx f_V$
T	=	Thrust

t	=	Time
U_0	=	Nominal airspeed for turbulence model
U	=	Equivalent steady state airspeed
V	=	Airspeed
V_{cmd}	=	Commanded airspeed
V_*	=	Optimal endurance speed
v	=	Zero-wind airspeed (roughly ground speed)
v_{eq}	=	Equilibrium airspeed of the average system
W_1, W_2	=	Instances of standard Brownian motion
α	=	Angle of attack
ϵ_1, ϵ_2	=	Turbulence time constants
η_1, η_2	=	Vertical and longitudinal wind speeds, pre-saturation
λ	=	Thrust angle
$\mu(\mathrm{d}\eta)$	=	Invariant distribution of η
ρ	=	Air density
σ_2, σ_3	=	Control law design parameters
$\sigma_u, \sigma_v, \sigma_w$	=	Root mean square turbulence intensity
		(longitudinal, lateral, and vertical components)
τ	=	Airspeed control time constant
$\Phi_{u_g}, \Phi_{v_g}, \Phi_{w_g}$	=	Turbulence spectra (longitudinal, lateral, vertical)
Ω	=	Spatial frequency
ω	=	Temporal frequency

Subscripts

eq	=	Evalutated at the equilibrium point ($U = V = v_{\text{eq}}$)
U	=	Partial derivative with respect to U
V	=	Partial derivative with respect to V
v	=	Evaluated at an arbitrary airspeed ($U = V = v$)
0	=	Evaluated at the center of the Taylor expansion
		($U = V = n_0$)
$*$	=	Evaluated at the optimal endurance speed ($U = V = V_*$)

4.2 Introduction

This paper is a continuation of the research effort begun in [34], in which the authors present a control algorithm for finding the speed for maximum endurance for a jet aircraft. Flight at the speed for maximum endurance produces the minimum fuel burn rate, allowing the longest duration of flight. The control algorithm in [34] is a novel form of extremum-seeking control in which atmospheric turbulence is used as the dither signal. The present work expands the basic principle developed in [34] by introducing a new algorithm capable of functioning at speeds in which compressibility becomes a factor. The algorithm is tested using a high-fidelity, flight-test validated aircraft simulation program.

Extremum seeking traditionally involves adding a small perturbation, called a dither signal, to the input to a system. The resulting change in the output from the system is then used to determine whether the input should be increased or decreased to drive the output towards its minimum (or maximum) possible value. The dither signal is traditionally chosen to be sinusoidal [1, 5, 6, 36, 33], but can also be chosen to be non-sinusoidal [7] or stochastic [3, 8]. Recently the need for adding a dither signal has been removed by utilizing naturally occurring disturbances in their stead [4]. The general applicability of extremum seeking has encouraged its use for a large variety of applications, including axial flow compressors [11], lean pre-mixed combustion [13, 27, 12], flow control [14, 37], wind turbine energy capture [38], the minimization of drag in formation flight [17], and many other applications in which the process dynamics may not be well known [26, 39, 9, 10, 15, 16, 40, 41, 29, 42, 43, 44].

The authors' previous work [34] introduces a novel variant of extremum seeking intended to optimize the speed of a jet aircraft for optimal endurance. The primary assumptions in [34], which are here removed, are:

1. The pitch and altitude dynamics of the aircraft can be considered quasi-steady.

2. The vertical component of turbulence is negligible.

3. The effect of compressibility is negligible.

The first assumption is removed by optimizing the lift to drag ratio over the (two-dimensional) Mach vs. angle of attack plane, rather than optimizing drag itself over airspeed in one dimension only. Pitch and altitude dynamics can significantly affect the drag of an aircraft, so an algorithm based on an estimate of rate of change of drag with respect to airspeed can only function on a timescale much slower than the aircraft dynamics. Conversely, the lift to drag ratio is very nearly a static map in the Mach vs. angle of attack plane; an approximation of such a map is not significantly restricted by the timescale of the aircraft dynamics.

The second assumption can (and actually must) be removed because the optimization is performed over a two-dimensional map, and as such two independent dither signals are required: the longitudinal and vertical components of atmospheric turbulence. (As explained below and in [24], a standard assumption in turbulence modeling is that the components of turbulence are independent stochastic processes.)

The third assumption is addressed explicitly by letting the lift to drag ratio be a function of Mach number, as already mentioned.

So the removal of the assumptions listed above is achieved by optimizing the lift to drag ratio over a two-dimensional space. Atmospheric turbulence, having independent longitudinal and vertical components, provides excitation over the two-dimensional space. This is used to produce an estimate of the local two-dimensional gradient, that is, to produce an estimate of the slope of the lift to drag ratio with respect to Mach number and an estimate of the slope with respect to angle of attack. In a typical multi-dimensional application, extremum seeking is then used to find the maximizing point in the two-dimensional space; however, the aircraft cannot move freely in two dimensions. Rather, to achieve level flight it must fly at a combination of Mach number and angle of attack that produces lift equal to the weight of the aircraft: a one-dimensional curve in a two-dimensional space.

Optimization over this curve is achieved by calculating the inner product of the gradient estimate with a vector locally tangent to the curve. This inner product gives the slope of the lift to drag ratio along the curve, which indicates

whether a faster or slower airspeed would improve the lift to drag ratio. Here the standard extremum seeking algorithm fails: it produces an estimate of the gradient vector that points in the wrong direction. (An explanation now follows.) The standard multi-dimensional gradient estimator operates by demodulating the output with the two independent dither signals. This produces an estimate of the gradient in which each component is scaled by the variance of its respective dither signal. (This is acceptable because at the maximum of a two dimensional map, the gradient is zero, and the zero vector is zero no matter how its components are scaled.) At the optimal point along the curve of constant lift, the gradient should be perpendicular to the curve, but it should not in general be zero. If the components of the gradient are unequally scaled, the direction of the gradient will be incorrect and the calculated inner product will be incorrect. This causes the optimization to fail. Of course this can be corrected if the relative amplitudes of the dither signals are known, but in an application that uses atmospheric turbulence to provide the dither signals, the relative amplitude of the dither signals is not known.

This difficulty motivates the development of a new form of the gradient estimator, one based on estimation error rather than simple demodulation. A three-state gradient estimator is developed that creates an estimate of the lift to drag ratio based on the measured Mach number and angle of attack. The states represent 1) the lift to drag ratio at the current average Mach number and angle of attack, 2) the slope with angle of attack, and 3) the slope with Mach number. The difference between the estimated and the measured lift to drag ratio is used as feedback for the gradient estimator. As the states converge the estimation error approaches zero. The critical feature of this design is that the equilibrium value of the gradient estimate does not depend on the amplitudes of the dither signals. The gradient estimate can be used to accurately determine the slope along the curve of constant lift. With this estimate of the slope, the optimal endurance speed can be accurately found.

The paper begins with an overview of relevant aerodynamics. An extremum seeking algorithm is then developed that finds the optimal endurance speed. (The

new form of the gradient estimator is developed at this point.) Convergence to the optimal airspeed is then shown through analysis and the algorithm is tested in simulation.

4.3 Aerodynamics

This section presents background aerodynamic information relevant to the following control development. Additional background can be found in [22].

4.3.1 Optimal Endurance

Endurance is the length of time an aircraft can remain airborne. For jet aircraft, endurance in level flight may be optimized by flying at an airspeed that minimizes drag, or equivalently that maximizes the lift to drag ratio. The lift to drag ratio is a function of several variables, the most important, perhaps, being angle of attack. In compressible flows, Mach number also has a significant effect. As a function of angle of attack and Mach number, the optimal lift to drag ratio is found at a point in a two-dimensional space; however, to maintain level flight the aircraft must fly at a combination of Mach number and angle of attack that produces lift equal to the weight of the aircraft. That is, in level flight an aircraft is constrained to a curve of constant lift in a two-dimensional (Mach number, angle of attack) space. The optimal endurance speed corresponds to the point on this curve that produces the highest lift to drag ratio.

The optimal endurance speed generally varies with aircraft weight and altitude. However, under certain common assumptions, it can be shown that optimal endurance occurs at the same coefficient of lift. Assume that the coefficient of lift increases with Mach number as $1/\sqrt{1-M^2}$ according to the Prandtl-Glauert rule. Assume a quadratic drag polar that does not change with Mach number. (Accounting for compressibility effects in this manner is valid for Mach numbers

less than about 0.75 [45].) These two assumptions are expressed as

$$C_L = \frac{C_L|_{M=0}}{\sqrt{1-M^2}} \tag{4.1}$$

$$C_D = C_{D0} + \frac{\left(C_L|_{M=0}\right)^2}{\pi Ae} \tag{4.2}$$

The lift to drag ratio is then

$$f = \frac{L}{D} = \frac{C_L \frac{1}{2}\rho V^2 S}{C_D \frac{1}{2}\rho V^2 S} = \frac{C_L}{C_D} = \frac{C_L}{C_{D0} + \frac{\left(C_L|_{M=0}\right)^2}{\pi Ae}} = \frac{C_L}{C_{D0} + \frac{C_L^2}{\pi Ae}\left(1-M^2\right)} \tag{4.3}$$

Mach number can be expressed in terms of lift and C_L as

$$M = \frac{V}{a} = \frac{1}{a}\sqrt{\frac{L}{C_L \frac{1}{2}\rho S}} = \sqrt{\frac{L}{C_L \frac{1}{2}\rho a^2 S}} \tag{4.4}$$

so the lift to drag ratio can be written as a function of lift and C_L

$$f(C_L, L) = \frac{C_L}{C_{D0} + \frac{C_L^2}{\pi Ae}\left(1 - \frac{L}{C_L \frac{1}{2}\rho a^2 S}\right)} = \frac{C_L}{C_{D0} - \frac{C_L L}{\pi Ae \frac{1}{2}\rho a^2 S} + \frac{C_L^2}{\pi Ae}} \tag{4.5}$$

The lift to drag ratio at any given value of lift is maximized when the partial derivative with respect to C_L is zero. The partial derivative is

$$\frac{\partial f(C_L, L)}{\partial C_L} = \frac{C_{D0} - \frac{C_L^2}{\pi Ae}}{\left(C_{D0} - \frac{C_L L}{\pi Ae \frac{1}{2}\rho a^2 S} + \frac{C_L^2}{\pi Ae}\right)^2} \tag{4.6}$$

Setting this equal to zero and solving for the coefficient of lift gives

$$C_L = \sqrt{C_{D0}\pi Ae} \tag{4.7}$$

This optimal C_L is a constant depending only on the parameters of the quadratic drag polar. It does not vary with density or lift. Under the assumption of a quadratic drag polar and the Prandtl-Glauert rule, the optimal airspeed for a certain flight condition can be related to the optimal airspeed at another altitude or aircraft weight by equating coefficients of lift.

4.3.2 Measurement of Lift and Drag

Although lift and drag are not directly measurable, they can be computed based on other quantities which may be more readily available. They can be calculated based on longitudinal and vertical body axis accelerometer measurements ($(a_x - g_x)$ and $(a_z - g_z)$, respectively) and estimates of aircraft mass (m), engine thrust (T), and the thrust angle (λ). Using a free body diagram like the one shown in Fig. 4.1, lift can be calculated from the measured and estimated variables as

$$L = \sin\alpha\left[-T\cos\lambda + m\left(a_x - g_x\right)\right] + \cos\alpha\left[-T\sin\lambda + m\left(a_z - g_z\right)\right] \tag{4.8}$$

and drag can be calculated as

$$D = -\cos\alpha\left[-T\cos\lambda + m\left(a_x - g_x\right)\right] + \sin\alpha\left[-T\sin\lambda + m\left(a_z - g_z\right)\right] \ . \tag{4.9}$$

Equivalent small angle expressions are

$$L = m\left[\alpha\left(a_x - g_x\right) + \left(a_z - g_z\right)\right] - T\left(\alpha + \lambda\right) \tag{4.10}$$

and

$$D = T - m\left[\left(a_x - g_x\right) - \alpha\left(a_z - g_z\right)\right] \ , \tag{4.11}$$

where angles are in radians.

4.3.3 Turbulence

Atmospheric turbulence is conventionally modeled as filtered gaussian white noise. The longitudinal, lateral and vertical components are modeled independently. The Dryden turbulence model is one commonly used atmospheric turbulence model [24]. It specifies the spectra of the three components as follows:

$$\Phi_{u_g}(\Omega) = \sigma_u^2 \frac{2L_u}{\pi} \frac{1}{1 + (L_u\Omega)^2} \tag{4.12a}$$

$$\Phi_{v_g}(\Omega) = \sigma_v^2 \frac{L_v}{\pi} \frac{1 + 3(L_v\Omega)^2}{\left[1 + (L_v\Omega)^2\right]^2} \tag{4.12b}$$

$$\Phi_{w_g}(\Omega) = \sigma_w^2 \frac{L_w}{\pi} \frac{1 + 3(L_w\Omega)^2}{\left[1 + (L_w\Omega)^2\right]^2} \ . \tag{4.12c}$$

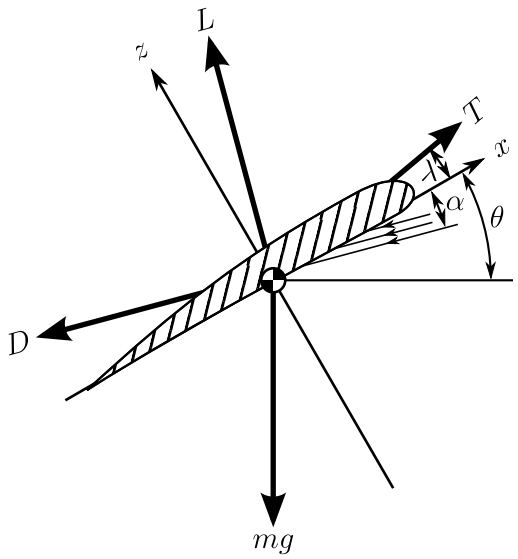

Figure 4.1: Aerodynamic forces and angles.

The spectra are given in terms of spatial frequency, which is converted to temporal frequency ω by multiplying by the speed of the aircraft:

$$\omega = \Omega U_0 \ . \tag{4.13}$$

At medium to high altitudes (above 2,000 feet) the turbulence is assumed to be isotropic. The characteristic lengths and the intensities in each direction are equal to each other. A typical characteristic length is 1,750 feet. Intensities are charted as a function of altitude. Moderate turbulence has a root mean square intensity of about 10 ft/sec at 2,000 feet, decreasing roughly linearly to near zero at 60,000 feet.

Whereas lateral turbulence has little effect on the speed of an aircraft, longitudinal turbulence has a direct effect on airspeed. Longitudinal turbulence with a spectrum matching that given in (4.12a) can be obtained by passing white noise through a filter of the form

$$\sigma_u \sqrt{\frac{2L_u}{U_0}} \frac{1}{\frac{L_u}{U_0} s + 1} \ . \tag{4.14}$$

Vertical turbulence could be simulated by passing white noise through a filter of

the form

$$\sigma_w \sqrt{\frac{L_w}{U_0}} \frac{1 + \sqrt{3}\frac{L_w}{U_0}s}{\left(1 + \frac{L_w}{U_0}s\right)^2} \tag{4.15}$$

but for simplicity this can be approximated as

$$\sigma_w \sqrt{\frac{L_w}{U_0}} \frac{1}{1 + \frac{L_w}{U_0}s} \tag{4.16}$$

4.4 Control Law

The equations required to implement the extremum seeking control law are as follows:

$$\hat{f} \triangleq s_1 + s_2 (U - V_{cmd}) + s_3 (V - V_{cmd}) \tag{4.17a}$$

$$\dot{s}_1 = k_1 \left(f - \hat{f}\right) + (s_2 + s_3) \dot{V}_{cmd} \tag{4.17b}$$

$$\dot{s}_2 = k_2 (U - V_{cmd}) \left(f - \hat{f}\right) + \sigma_2 \dot{V}_{cmd} \tag{4.17c}$$

$$\dot{s}_3 = k_3 (V - V_{cmd}) \left(f - \hat{f}\right) + \sigma_3 \dot{V}_{cmd} \tag{4.17d}$$

$$\dot{V}_{cmd} = k_{ES} (s_2 + s_3) \tag{4.17e}$$

where

$$f \triangleq \frac{L}{D} \approx \frac{m [\alpha (a_x - g_x) + (a_z - g_z)] - T (\alpha + \lambda)}{T - m [(a_x - g_x) - \alpha (a_z - g_z)]} \tag{4.18a}$$

$$U \triangleq V \sqrt{\frac{mg}{L}} \approx V \sqrt{\frac{mg}{m [\alpha (a_x - g_x) + (a_z - g_z)] - T (\alpha + \lambda)}} \tag{4.18b}$$

Details and motivations will be provided over the next several paragraphs.

The control law is a four-state nonlinear controller that provides as its output an airspeed command (V_{cmd}) to an inner-loop airspeed controller (which is assumed to already be in place). The inputs to the control law are the lift to drag ratio (f), airspeed (V), and equivalent steady state airspeed (U). These inputs can be calculated from the following measured or approximated quantities: angle of attack (α), engine thrust (T), aircraft mass (m), longitudinal and vertical body axis accelerometer readings ($(a_x - g_x)$ and $(a_z - g_z)$), thrust angle (λ), acceleration due to gravity (g), and airspeed (V). Small angle approximations of f and U in

terms of these quantities are given in (4.18). The control law design parameters are k_1, k_2, k_3, k_{ES}, σ_2, and σ_3. [Note that σ_2 and σ_3 have no relation to the RMS turbulence intensities σ_u, σ_v, and σ_w.]

Loosely speaking, the control law operates by determining a measurement of the lift to drag ratio, determining if the lift to drag ratio improves with increasing or decreasing airspeed, and adjusting the airspeed command until the highest possible lift to drag ratio is achieved. Conceptually, an estimator, excited by transients in Mach number and angle of attack, then approximates the gradient of the lift to drag ratio. In level flight, a change in Mach number is always accompanied by a change in angle of attack, so it is not possible to independently control both airspeed and angle of attack. The optimal speed is that which provides the maximum lift to drag ratio possible along a curve of constant lift in the angle of attack versus Mach number plane. A gradient ascent is performed to the optimal point.

Seeking to implement such a control law, though, a number of difficulties arise (not the least of which is that the non-linear relationship between angle of attack and airspeed can destabilize the control system.) It is advantageous to reformulate the lift to drag ratio as a function of two variables other than angle of attack and Mach number. As a basis for the function, airspeed V is used in place of Mach number. In place of angle of attack is used equivalent steady state airspeed U, defined as the airspeed required to produce an amount of lift equal to the weight of the aircraft while in flight at the current coefficient of lift and altitude. The estimator approximates the gradient of the lift to drag ratio in the (U, V) plane. When the lift produced by the aircraft is equal to its weight, U is equal to V, so in the (U, V) plane, the curve of constant lift is simply $U = V$. Based on the estimated gradient, the control law performs a gradient ascent along this line towards the speed at which the maximum lift to drag ratio is achieved.

The extremum seeking algorithm is designed to use naturally occurring disturbances such as atmospheric turbulence to provide sufficient excitation to the estimator. The intensity of the turbulence is of course not known or constant; neither are the relative intensities of the vertical component of turbulence (affecting U) and the horizontal component (affecting V). In such a situation, a standard

extremum seeking algorithm (which estimates slope by demodulating the lift to drag ratio with U and V) produces slope estimates that are proportional to the true slope, but the estimates are scaled by the square of the amplitudes of the vertical and horizontal components of turbulence, respectively. If the two slope estimates are scaled differently, the estimated slope along the line of constant lift cannot be determined. Because of this, the control algorithm uses a gradient estimator that is different from those commonly used in extremum seeking.

The gradient estimator is based on an estimate of the lift to drag ratio at the current U and V. The estimate is linear in the three estimator states, with the first state s_1 representing the lift to drag ratio at the commanded airspeed in steady flight, the second state s_2 representing the slope of the lift to drag ratio with U, and the third state s_3 representing the slope with respect to V. The states are updated based on the difference between the measured and estimated lift to drag ratios (f and $\hat{f}$). The slope of the lift to drag ratio along the line of constant lift is the sum of the second and third estimator states (s_2 and s_3) and the airspeed command is changed at a rate proportional to this slope. [The simplicity seen in this calculation of the slope along the line of constant lift is part of the motivation for reformulating f as a function of U and V. Calculating the slope along the curve of constant lift in the angle of attack versus Mach number plane is less than straightforward; the direction of a line tangent to the curve cannot be found without assuming knowledge of the rate of change of C_L with α, and the fundamental goal of extremum seeking is to perform optimization without making assumptions about aerodynamic characteristics of the aircraft.]

Note that several terms not related to estimation error appear in the estimator equations. These terms (the last terms in (4.17b) (4.17c) and (4.17d)) improve transient performance by providing an estimate of how the estimator states are expected to change based on the rate of change of the airspeed command. As is shown in the following analysis, this also has a positive effect on stability of the algorithm. These terms are motivated by the expected change in the estimator states given a change in V_{cmd}. For example, $[(s_2 + s_3)\dot{V}_{cmd}]$ can be thought of as $[(f_U + f_V)\dot{V}_{cmd}]$ or $[(\mathrm{d}f/\mathrm{d}V_{cmd})\dot{V}_{cmd}]$, which is $\dot{f}$. This provides a sort of feedforward

to s_1 (which is the estimate of f) when V_{cmd} changes. The terms in the $\dot{s}_2$ and $\dot{s}_3$ equations are similarly motivated. In this way, the design parameters σ_2 and σ_3 can be thought of as *a priori* estimates of $\mathrm{d}f_U/\mathrm{d}V_{cmd}$ and $\mathrm{d}f_V/\mathrm{d}V_{cmd}$, respectively.

Finally, a note about the order of the controller may be appropriate. The controller estimates a gradient in two dimensions for what is essentially a one-dimensional optimization. It is tempting to reformulate the problem as a one-dimensional optimization in *one* dimension so that the order of the gradient estimator can be reduced. Specifically, the gradient estimator could replace the two states s_2 and s_3 (which estimate f_U and f_V respectively) with one state (say s_{2+3}) which directly estimates the sum $f_U + f_V$. Such a controller could be derived by defining $s_{2+3} \triangleq s_2 + s_3$ and $s_{2-3} \triangleq s_2 - s_3$, rewriting the controller in terms of these new variables, and dropping all terms containing s_{2-3}. This would be possible because the new update law ($\dot{V}_{cmd} = k_{ES}\, s_{2+3}$) would not depend on s_{2-3}. Furthermore, the expectation would be that disturbances accounted for by s_{2-3} in the estimate of the lift to drag ratio $\hat{f}$ would average to zero and could be ignored.

The problem is that disturbances in $(U+V)$ are likely to be strongly correlated with disturbances in $(U-V)$. This is the case even if it is assumed that U is not correlated with V because the amplitudes of the disturbances in U and V are not the same size; in general, disturbances in U are larger than disturbances in V, even in isotropic turbulence (and given two uncorrelated random variables, their sum is correlated with their difference unless their variances are equal). Although not presented in this paper, it can be shown through analysis that this correlation causes a bias in the estimate of the optimal endurance speed. Estimating the gradient in two dimensions, rather than one, removes this source of bias.

4.5 Analysis

For the analysis, assume that measurements of f, U, and V are available and implement the control law given in (4.17). Let f be a static map in two dimensions. Assume that along the curve where lift equals the weight of the aircraft, the map is convex. Assume stochastic perturbations in U and V that are each represented

by filtered white noise. These stochastic perturbations approximate longitudinal and vertical components of turbulence. Under these assumptions, U and V are

$$\epsilon_1 \, \mathrm{d}\eta_1 = -\eta_1 \, \mathrm{d}t + \sqrt{\epsilon_1} q_1 \, \mathrm{d}W_1 \tag{4.19a}$$

$$\Delta U = a_1 \operatorname{sat} \eta_1 \tag{4.19b}$$

$$U = v + \Delta U \tag{4.19c}$$

$$\epsilon_2 \, \mathrm{d}\eta_2 = -\eta_2 \, \mathrm{d}t + \sqrt{\epsilon_2} q_2 \, \mathrm{d}W_2 \tag{4.20a}$$

$$\Delta V = a_2 \operatorname{sat} \eta_2 \tag{4.20b}$$

$$V = v + \Delta V \tag{4.20c}$$

The saturation function is defined as

$$\operatorname{sat}(\eta) = \begin{cases} \eta & \text{if } -1 < \eta < 1 \\ 1 & \text{if } \eta \geq 1 \\ -1 & \text{if } \eta \leq -1 \end{cases} \tag{4.21}$$

It is included primarily for mathematical convenience, but also conveys the fact that real turbulence has a finite amplitude. Approximate the aircraft's control over airspeed using simple first order dynamics:

$$\dot{v} = \frac{1}{\tau} \left(V_{cmd} - V \right) \tag{4.22}$$

This simple aircraft model is used to limit the order of the system being analyzed; other aircraft dynamics are subsumed in the stochastic perturbations to U and V. The time constant involved in the aircraft's control over airspeed is explicitly modeled because the analysis in [34] shows it to have possible implications for stability.

With these models the closed loop system is

$$\dot{v} = \frac{1}{\tau}\left(V_{cmd} - v - a_2 \operatorname{sat}\eta_2\right) \tag{4.23a}$$

$$\begin{aligned}\dot{s}_1 = {} & k_1\left(f - s_1 - s_2\left(v + a_1 \operatorname{sat}\eta_1 - V_{cmd}\right) - s_3\left(v + a_2 \operatorname{sat}\eta_2 - V_{cmd}\right)\right) \\ & + \left(s_2 + s_3\right)\dot{V}_{cmd}\end{aligned} \tag{4.23b}$$

$$\begin{aligned}\dot{s}_2 = {} & k_2\left(v + a_1 \operatorname{sat}\eta_1 - V_{cmd}\right) \\ & \times \left(f - s_1 - s_2\left(v + a_1 \operatorname{sat}\eta_1 - V_{cmd}\right) - s_3\left(v + a_2 \operatorname{sat}\eta_2 - V_{cmd}\right)\right) \\ & + \sigma_2\dot{V}_{cmd}\end{aligned} \tag{4.23c}$$

$$\begin{aligned}\dot{s}_3 = {} & k_3\left(v + a_2 \operatorname{sat}\eta_2 - V_{cmd}\right) \\ & \times \left(f - s_1 - s_2\left(v + a_1 \operatorname{sat}\eta_1 - V_{cmd}\right) - s_3\left(v + a_2 \operatorname{sat}\eta_2 - V_{cmd}\right)\right) \\ & + \sigma_3\dot{V}_{cmd}\end{aligned} \tag{4.23d}$$

$$\dot{V}_{cmd} = k_{ES}\left(s_2 + s_3\right) \tag{4.23e}$$

$$\epsilon_1\,\mathrm{d}\eta_1 = -\eta_1\,\mathrm{d}t + \sqrt{\epsilon_1}q_1\,\mathrm{d}W_1 \tag{4.23f}$$

$$\epsilon_2\,\mathrm{d}\eta_2 = -\eta_2\,\mathrm{d}t + \sqrt{\epsilon_2}q_2\,\mathrm{d}W_2 \tag{4.23g}$$

It is this closed loop system that is considered in the following analysis.

Theorem 2. *Consider system* (4.23) *where* $f = f(U,V) = f(v + a_1 \operatorname{sat}\eta_1, v + a_2 \operatorname{sat}\eta_2)$ *is a two-dimensional map that, along the line* $V = U$*, is convex with a maximum at* (V_*, V_*)*. Assume all constants are positive, with the exception of* σ_2 *and* σ_3*, which are chosen so that* $\sigma_3 < \frac{1}{2}\left(f_{VV*} - f_{UU*}\right)$ *and* $\sigma_2 < \frac{1}{2}\left(f_{UU*} - f_{VV*}\right)$*. Let constants* C_2 *and* C_4 *be defined by*

$$C_2(q_i) \triangleq \frac{q_i^2}{2}\operatorname{erf}\frac{1}{q_i} - \frac{q_i}{\sqrt{\pi}}e^{-\frac{1}{q_i^2}} + 1 - \operatorname{erf}\frac{1}{q_i} \tag{4.24a}$$

$$C_4(q_i) \triangleq \frac{3}{4}q_i^4\operatorname{erf}\frac{1}{q_i} - \frac{q_i}{\sqrt{\pi}}e^{-\frac{1}{q_i^2}}\left(1 + \frac{3}{2}q_i^2\right) + 1 - \operatorname{erf}\frac{1}{q_i}\ . \tag{4.24b}$$

Suppose $f(U,V)$ *is three times differentiable at* (V_*, V_*)*. Then there exists a constant* a^* *such that for any* $0 < (a_1, a_2) < a^*$ *there exist constants* $r > 0$*,* $c > 0$*,* $\gamma > 0$ *and a function* $T(\epsilon_1, \epsilon_2)\colon (0, \epsilon_0)\times(0, \epsilon_0) \to \mathbb{N}$ *with the property* $\lim_{\epsilon_1,\epsilon_2\to 0} T(\epsilon_1, \epsilon_2) =$

∞ *such that for any initial condition* $|\Delta^{\epsilon,a}(0)| < r$*, and any* $\delta > 0$*,*

$$\lim_{\epsilon_1,\epsilon_2\to 0} \inf \big\{ t \geq 0 : |\Delta^{\epsilon,a}(t)| > c|\Delta^{\epsilon,a}(0)|e^{-\gamma t} + O(a_1^4 a_2^{-1}) + O(a_1^3) \\ + O(a_1^2 a_2) + O(a_1 a_2^2) + O(a_2^3) + O(a_1^{-1} a_2^4) + \delta \big\} = \infty, \text{ a.s.} \quad (4.25)$$

and

$$\lim_{\epsilon_1,\epsilon_2\to 0} P\big\{ |\Delta^{\epsilon,a}(t)| \leq c|\Delta^{\epsilon,a}(0)|e^{-\gamma t} + O(a_1^4 a_2^{-1}) + O(a_1^3) + O(a_1^2 a_2) \\ + O(a_1 a_2^2) + O(a_2^3) + O(a_1^{-1} a_2^4) + \delta, \forall t \in [0, T(\epsilon_1, \epsilon_2)] \big\} = 1, \quad (4.26)$$

where $\Delta^{\epsilon,a}(t) \triangleq \begin{pmatrix} v(t) \\ s_1(t) \\ s_2(t) \\ s_3(t) \\ V_{cmd}(t) \end{pmatrix} - \begin{pmatrix} \bar{v} \\ \bar{s}_1 \\ \bar{s}_2 \\ \bar{s}_3 \\ \bar{V}_{cmd} \end{pmatrix}$ *and*

$$\bar{v} = V_* - \frac{f_{UUU*}C_4(q_1) + 3f_{UUV*}\left(C_2(q_1)\right)^2}{6\left(f_{UU*} + 2f_{UV*} + f_{VV*}\right)C_2(q_1)}a_1^2 \tag{4.27a}$$

$$- \frac{3f_{UVV*}\left(C_2(q_2)\right)^2 + f_{VVV*}C_4(q_2)}{6\left(f_{UU*} + 2f_{UV*} + f_{VV*}\right)C_2(q_2)}a_2^2 \tag{4.27b}$$

$$\bar{s}_1 = f_* + \frac{1}{2}\left[f_{UU*}a_1^2C_2(q_1) + f_{VV*}a_2^2C_2(q2)\right] \tag{4.27c}$$

$$\begin{aligned}\bar{s}_2 = {} & f_{U*} - \left(f_{UU*} + f_{UV*}\right) \\ & \times \left[\frac{f_{UUU*}C_4(q_1) + 3f_{UUV*}\left(C_2(q_1)\right)^2}{6\left(f_{UU*} + 2f_{UV*} + f_{VV*}\right)C_2(q_1)}a_1^2\right. \\ & \left. + \frac{3f_{UVV*}\left(C_2(q_2)\right)^2 + f_{VVV*}C_4(q_2)}{6\left(f_{UU*} + 2f_{UV*} + f_{VV*}\right)C_2(q_2)}a_2^2\right] \\ & + \frac{1}{6}f_{UUU*}a_1^2\frac{C_4(q_1)}{C_2(q_1)} + \frac{1}{2}f_{UVV*}a_2^2C_2(q_2)\end{aligned} \tag{4.27d}$$

$$\begin{aligned}\bar{s}_3 = {} & f_{V*} - \left(f_{UV*} + f_{VV*}\right) \\ & \times \left[\frac{f_{UUU*}C_4(q_1) + 3f_{UUV*}\left(C_2(q_1)\right)^2}{6\left(f_{UU*} + 2f_{UV*} + f_{VV*}\right)C_2(q_1)}a_1^2\right. \\ & \left. + \frac{3f_{UVV*}\left(C_2(q_2)\right)^2 + f_{VVV*}C_4(q_2)}{6\left(f_{UU*} + 2f_{UV*} + f_{VV*}\right)C_2(q_2)}a_2^2\right] \\ & + \frac{1}{2}f_{UUV*}a_1^2C_2(q_1) + \frac{1}{6}f_{VVV*}a_2^2\frac{C_4(q_2)}{C_2(q_2)}\end{aligned} \tag{4.27e}$$

$$\bar{V}_{cmd} = V_* - \frac{f_{UUU*}C_4(q_1) + 3f_{UUV*}\left(C_2(q_1)\right)^2}{6\left(f_{UU*} + 2f_{UV*} + f_{VV*}\right)C_2(q_1)}a_1^2 \tag{4.27f}$$

$$- \frac{3f_{UVV*}\left(C_2(q_2)\right)^2 + f_{VVV*}C_4(q_2)}{6\left(f_{UU*} + 2f_{UV*} + f_{VV*}\right)C_2(q_2)}a_2^2 \tag{4.27g}$$

Theorem 2 roughly states that the stochastic system converges on average to the airspeed for optimal endurance, with a bias that is proportional to the square of the turbulence intensity and the third partial derivatives of the lift to drag ratio map. (Mathematically speaking, the system converges both almost

surely and in probability.) The theorem concerns system behavior for small turbulence intensities and for timescales that are long compared to the turbulence time constants.

4.5.1 Proof of Theorem

The average system is formed by performing stochastic averaging over the invariant distributions of η_1 and η_2. The distributions of the stochastic variables are given by

$$\mu(\mathrm{d}\eta) = \frac{1}{\sqrt{\pi}q} e^{-\frac{\eta^2}{q^2}} \mathrm{d}\eta \tag{4.28}$$

where the appropriate subscript is to be appended to η and q. Note that

$$\int_{-\infty}^{\infty} \mu(\mathrm{d}\eta) = 1 \tag{4.29}$$

$$\int_{-\infty}^{\infty} (\mathrm{sat}\,\eta)^k \mu(\mathrm{d}\eta) = 0 \quad \text{for k = 1,3,5,...} \tag{4.30}$$

$$\int_{-\infty}^{\infty} (\mathrm{sat}\,\eta)^2 \mu(\mathrm{d}\eta) = C_2(q) \tag{4.31}$$

$$\int_{-\infty}^{\infty} (\mathrm{sat}\,\eta)^4 \mu(\mathrm{d}\eta) = C_4(q) \tag{4.32}$$

Taking $\dot{v}$ as an example, averaging over both stochastic variables gives

$$\begin{aligned}
\dot{v} &= \int_{-\infty}^{\infty} \int_{-\infty}^{\infty} \frac{1}{\tau} \left(V_{cmd} - v - a_2\,\mathrm{sat}\,\eta_2\right) \mu(\mathrm{d}\eta_1)\mu(\mathrm{d}\eta_2) \\
&= \int_{-\infty}^{\infty} \frac{1}{\tau} \left(V_{cmd} - v - a_2\,\mathrm{sat}\,\eta_2\right) \mu(\mathrm{d}\eta_2) \\
&= \frac{1}{\tau} \left(V_{cmd} - v\right)
\end{aligned} \tag{4.33}$$

After performing similar averaging on all dynamic equations, the average system

is

$$\dot{v} = \frac{1}{\tau}\left(V_{cmd} - v\right) \tag{4.34a}$$

$$\begin{aligned}\dot{s}_1 = k_1 &\left(\int_{-\infty}^{\infty}\int_{-\infty}^{\infty} f\mu(\mathrm{d}\eta_1)\mu(\mathrm{d}\eta_2) - s_1 - s_2\left(v - V_{cmd}\right) - s_3\left(v - V_{cmd}\right)\right) \\ &+ \left(s_2 + s_3\right)\dot{V}_{cmd}\end{aligned} \tag{4.34b}$$

$$\begin{aligned}\dot{s}_2 = {} & k_2\left(v - V_{cmd}\right) \\ & \times \left(\int_{-\infty}^{\infty}\int_{-\infty}^{\infty} f\mu(\mathrm{d}\eta_1)\mu(\mathrm{d}\eta_2) - s_1 - s_2\left(v - V_{cmd}\right) - s_3\left(v - V_{cmd}\right)\right) \\ & + k_2\left(\int_{-\infty}^{\infty}\int_{-\infty}^{\infty} a_1 \operatorname{sat}\eta_1 f\mu(\mathrm{d}\eta_1)\mu(\mathrm{d}\eta_2) - s_2 a_1^2 C_2(q_1)\right) \\ & + \sigma_2\dot{V}_{cmd}\end{aligned} \tag{4.34c}$$

$$\begin{aligned}\dot{s}_3 = {} & k_3\left(v - V_{cmd}\right) \\ & \times \left(\int_{-\infty}^{\infty}\int_{-\infty}^{\infty} f\mu(\mathrm{d}\eta_1)\mu(\mathrm{d}\eta_2) - s_1 - s_2\left(v - V_{cmd}\right) - s_3\left(v - V_{cmd}\right)\right) \\ & + k_3\left(\int_{-\infty}^{\infty}\int_{-\infty}^{\infty} a_2 \operatorname{sat}\eta_2 f\mu(\mathrm{d}\eta_1)\mu(\mathrm{d}\eta_2) - s_3 a_2^2 C_2(q_2)\right) \\ & + \sigma_3\dot{V}_{cmd}\end{aligned} \tag{4.34d}$$

$$\dot{V}_{cmd} = k_{ES}\left(s_2 + s_3\right) \tag{4.34e}$$

At equilibrium, setting the time derivatives to zero and assuming non-zero constants, the system of equations reduces to

$$0 = V_{cmd} - v \tag{4.35a}$$

$$0 = \int_{-\infty}^{\infty}\int_{-\infty}^{\infty} f\mu(\mathrm{d}\eta_1)\mu(\mathrm{d}\eta_2) - s_1 \tag{4.35b}$$

$$0 = \int_{-\infty}^{\infty}\int_{-\infty}^{\infty} a_1 \operatorname{sat}\eta_1 f\mu(\mathrm{d}\eta_1)\mu(\mathrm{d}\eta_2) - s_2 a_1^2 C_2(q_1) \tag{4.35c}$$

$$0 = \int_{-\infty}^{\infty}\int_{-\infty}^{\infty} a_2 \operatorname{sat}\eta_2 f\mu(\mathrm{d}\eta_1)\mu(\mathrm{d}\eta_2) - s_3 a_2^2 C_2(q_2) \tag{4.35d}$$

$$0 = s_2 + s_3 \tag{4.35e}$$

To evaluate the integrals in questions, take a two-dimensional Taylor expansion of

v in a_1 and a_2:

$$\begin{aligned} v = n_0 &+ [n_1 a_1 + n_2 a_2] + \left[n_{11} a_1^2 + n_{12} a_1 a_2 + n_{22} a_2^2\right] \\ &+ \left[n_{111} a_1^3 + n_{112} a_1^2 a_2 + n_{122} a_1 a_2^2 + n_{222} a_2^3\right] \\ &+ O(a_1^4) + O(a_1^3 a_2) + O(a_1^2 a_2^2) + O(a_1 a_2^3) + O(a_2^4) \end{aligned} \tag{4.36}$$

Note that U and V can be expressed in terms of v:

$$U = v + a_1 \operatorname{sat} \eta_1 \tag{4.37a}$$

$$V = v + a_2 \operatorname{sat} \eta_2 \tag{4.37b}$$

Then

$$\begin{aligned} U = n_0 &+ [n_1 a_1 + n_2 a_2] + \left[n_{11} a_1^2 + n_{12} a_1 a_2 + n_{22} a_2^2\right] \\ &+ \left[n_{111} a_1^3 + n_{112} a_1^2 a_2 + n_{122} a_1 a_2^2 + n_{222} a_2^3\right] \\ &+ a_1 \operatorname{sat} \eta_1 + O(a_1^4) + O(a_1^3 a_2) + O(a_1^2 a_2^2) + O(a_1 a_2^3) + O(a_2^4) \end{aligned} \tag{4.38}$$

$$\begin{aligned} V = n_0 &+ [n_1 a_1 + n_2 a_2] + \left[n_{11} a_1^2 + n_{12} a_1 a_2 + n_{22} a_2^2\right] \\ &+ \left[n_{111} a_1^3 + n_{112} a_1^2 a_2 + n_{122} a_1 a_2^2 + n_{222} a_2^3\right] \\ &+ a_2 \operatorname{sat} \eta_2 + O(a_1^4) + O(a_1^3 a_2) + O(a_1^2 a_2^2) + O(a_1 a_2^3) + O(a_2^4) \end{aligned} \tag{4.39}$$

Use these expressions in a two-dimensional Taylor expansion of f, which is a function of U and V. Let the expansion be centered at the point (n_0, n_0). The notation f_0 is used to mean the value of the lift to drag ratio at this point. Similarly, f_{U0} is used to mean the partial derivative of the lift to drag ratio with respect to U at the same point; f_{V0} is the partial derivative with respect to V; f_{UV0} and similar

denote higher partial derivatives. The expansion of f is

$$\begin{aligned} f = f_0 &+ \left[f_{U0}\left(U-n_0\right) + f_{V0}\left(V-n_0\right)\right] \\ &+ \frac{1}{2}\left[f_{UU0}\left(U-n_0\right)^2 + 2f_{UV0}\left(U-n_0\right)\left(V-n_0\right) + f_{VV0}\left(V-n_0\right)^2\right] \\ &+ \frac{1}{3!}\Big[f_{UUU0}\left(U-n_0\right)^3 + 3f_{UUV0}\left(U-n_0\right)^2\left(V-n_0\right) \\ &+ 3f_{UVV0}\left(U-n_0\right)\left(V-n_0\right)^2 + f_{VVV0}\left(V-n_0\right)^3\Big] \\ &+ O\left(\left(U-n_0\right)^4\right) \\ &+ O\left(\left(U-n_0\right)^3\left(V-n_0\right)\right) \\ &+ O\left(\left(U-n_0\right)^2\left(V-n_0\right)^2\right) \\ &+ O\left(\left(U-n_0\right)\left(V-n_0\right)^3\right) \\ &+ O\left(\left(V-n_0\right)^4\right) \end{aligned} \tag{4.40}$$

The expression $(U - n_0)$ simplifies by the cancellation of the n_0 terms to the following:

$$\begin{aligned} U - n_0 = &\left[n_1a_1 + n_2a_2\right] + \left[n_{11}a_1^2 + n_{12}a_1a_2 + n_{22}a_2^2\right] \\ &+ \left[n_{111}a_1^3 + n_{112}a_1^2a_2 + n_{122}a_1a_2^2 + n_{222}a_2^3\right] \\ &+ a_1 \operatorname{sat}\eta_1 + O(a_1^4) + O(a_1^3a_2) + O(a_1^2a_2^2) + O(a_1a_2^3) + O(a_2^4) \end{aligned} \tag{4.41}$$

Note that

$$O\left(U-n_0\right) = O(a_1) + O(a_2) \tag{4.42}$$

Similarly

$$\begin{aligned} V - n_0 = &\left[n_1a_1 + n_2a_2\right] + \left[n_{11}a_1^2 + n_{12}a_1a_2 + n_{22}a_2^2\right] \\ &+ \left[n_{111}a_1^3 + n_{112}a_1^2a_2 + n_{122}a_1a_2^2 + n_{222}a_2^3\right] \\ &+ a_2 \operatorname{sat}\eta_2 + O(a_1^4) + O(a_1^3a_2) + O(a_1^2a_2^2) + O(a_1a_2^3) + O(a_2^4) \end{aligned} \tag{4.43}$$

and

$$O\left(V-n_0\right) = O(a_1) + O(a_2) \tag{4.44}$$

Substituting the Taylor expansions of U and V into the expansion of f and simplifying gives

$$
\begin{aligned}
f &= f_0 \\
&+ \Bigg[f_{U0} \Big([n_1 a_1 + n_2 a_2] + \left[n_{11} a_1^2 + n_{12} a_1 a_2 + n_{22} a_2^2 \right] \\
&+ \left[n_{111} a_1^3 + n_{112} a_1^2 a_2 + n_{122} a_1 a_2^2 + n_{222} a_2^3 \right] + a_1 \operatorname{sat} \eta_1 \Big) \\
&+ f_{V0} \Big([n_1 a_1 + n_2 a_2] + \left[n_{11} a_1^2 + n_{12} a_1 a_2 + n_{22} a_2^2 \right] \\
&+ \left[n_{111} a_1^3 + n_{112} a_1^2 a_2 + n_{122} a_1 a_2^2 + n_{222} a_2^3 \right] + a_2 \operatorname{sat} \eta_2 \Big) \Bigg] \\
&+ \frac{1}{2} \Bigg[f_{UU0} \Big([n_1 a_1 + n_2 a_2] + \left[n_{11} a_1^2 + n_{12} a_1 a_2 + n_{22} a_2^2 \right] + a_1 \operatorname{sat} \eta_1 \Big)^2 \\
&+ 2 f_{UV0} \Big([n_1 a_1 + n_2 a_2] + \left[n_{11} a_1^2 + n_{12} a_1 a_2 + n_{22} a_2^2 \right] + a_1 \operatorname{sat} \eta_1 \Big) \\
&\times \Big([n_1 a_1 + n_2 a_2] + \left[n_{11} a_1^2 + n_{12} a_1 a_2 + n_{22} a_2^2 \right] + a_2 \operatorname{sat} \eta_2 \Big) \\
&+ f_{VV0} \Big([n_1 a_1 + n_2 a_2] + \left[n_{11} a_1^2 + n_{12} a_1 a_2 + n_{22} a_2^2 \right] + a_2 \operatorname{sat} \eta_2) \Big)^2 \Bigg] \\
&+ \frac{1}{3!} \Bigg[f_{UUU0} \Big([n_1 a_1 + n_2 a_2] + a_1 \operatorname{sat} \eta_1 \Big)^3 \\
&+ 3 f_{UUV0} \Big([n_1 a_1 + n_2 a_2] + a_1 \operatorname{sat} \eta_1 \Big)^2 \Big([n_1 a_1 + n_2 a_2] + a_2 \operatorname{sat} \eta_2 \Big) \\
&+ 3 f_{UVV0} \Big([n_1 a_1 + n_2 a_2] + a_1 \operatorname{sat} \eta_1 \Big) \Big([n_1 a_1 + n_2 a_2] + a_2 \operatorname{sat} \eta_2 \Big)^2 \\
&+ f_{VVV0} \Big([n_1 a_1 + n_2 a_2] + a_2 \operatorname{sat} \eta_2 \Big)^3 \Bigg] \\
&+ O(a_1^4) + O(a_1^3 a_2) + O(a_1^2 a_2^2) + O(a_1 a_2^3) + O(a_2^4)
\end{aligned}
\tag{4.45}
$$

The integrals in (4.35) are then

$$
\begin{aligned}
&\int_{-\infty}^{\infty}\int_{-\infty}^{\infty} f\mu(\mathrm{d}\eta_1)\mu(\mathrm{d}\eta_2) = f_0 \\
&+ \Bigg[f_{U0}\Big(\left[n_1a_1 + n_2a_2\right] + \left[n_{11}a_1^2 + n_{12}a_1a_2 + n_{22}a_2^2\right] \\
&+ \left[n_{111}a_1^3 + n_{112}a_1^2a_2 + n_{122}a_1a_2^2 + n_{222}a_2^3\right] \Big) \\
&+ f_{V0}\Big(\left[n_1a_1 + n_2a_2\right] + \left[n_{11}a_1^2 + n_{12}a_1a_2 + n_{22}a_2^2\right] \\
&+ \left[n_{111}a_1^3 + n_{112}a_1^2a_2 + n_{122}a_1a_2^2 + n_{222}a_2^3\right] \Big) \Bigg] \\
&+ \frac{1}{2}\Bigg[f_{UU0}\Big(\left(\left[n_1a_1 + n_2a_2\right] + \left[n_{11}a_1^2 + n_{12}a_1a_2 + n_{22}a_2^2\right]\right)^2 + a_1^2C_2(q_1) \Big) \\
&+ 2f_{UV0}\Big(\left[n_1a_1 + n_2a_2\right] + \left[n_{11}a_1^2 + n_{12}a_1a_2 + n_{22}a_2^2\right] \Big) \\
&\times \Big(\left[n_1a_1 + n_2a_2\right] + \left[n_{11}a_1^2 + n_{12}a_1a_2 + n_{22}a_2^2\right] \Big) \\
&+ f_{VV0}\Big(\left(\left[n_1a_1 + n_2a_2\right] + \left[n_{11}a_1^2 + n_{12}a_1a_2 + n_{22}a_2^2\right]\right)^2 + a_2^2C_2(q_2) \Big) \Bigg] \\
&+ \frac{1}{3!}\Bigg[f_{UUU0}\Big(\left[n_1a_1 + n_2a_2\right]^3 + 3\left[n_1a_1 + n_2a_2\right]a_1^2C_2(q_1) \Big) \\
&+ 3f_{UUV0}\Big(\left[n_1a_1 + n_2a_2\right]^2 + a_1^2C_2(q_1) \Big)\Big(\left[n_1a_1 + n_2a_2\right] \Big) \\
&+ 3f_{UVV0}\Big(\left[n_1a_1 + n_2a_2\right] \Big)\Big(\left[n_1a_1 + n_2a_2\right] + a_2^2C_2(q_2) \Big) \\
&+ f_{VVV0}\Big(\left[n_1a_1 + n_2a_2\right]^3 + 3\left[n_1a_1 + n_2a_2\right]a_2^2C_2(q_2) \Big) \Bigg] \\
&+ O(a_1^4) + O(a_1^3a_2) + O(a_1^2a_2^2) + O(a_1a_2^3) + O(a_2^4)
\end{aligned}
\tag{4.46}
$$

$$
\begin{aligned}
&\int_{-\infty}^{\infty}\int_{-\infty}^{\infty} a_1 \,\mathrm{sat}\,\eta_1 f\mu(\mathrm{d}\eta_1)\mu(\mathrm{d}\eta_2) = \\
&\left[f_{U0}a_1^2C_2(q_1)\right] \\
&+\frac{1}{2}\Bigg[f_{UU0}\Big(2a_1^2C_2(q_1)\left([n_1a_1+n_2a_2]+\left[n_{11}a_1^2+n_{12}a_1a_2+n_{22}a_2^2\right]\right)\Big) \\
&+2f_{UV0}\Big(a_1^2C_2(q_1)\Big)\Big(\left[n_1a_1+n_2a_2\right]+\left[n_{11}a_1^2+n_{12}a_1a_2+n_{22}a_2^2\right]\Big)\Bigg] \\
&+\frac{1}{3!}\Bigg[f_{UUU0}\Big(\left[n_1a_1+n_2a_2\right]^2a_1^2C_2(q_1)+a_1^4C_4(q_1)\Big) \\
&+3f_{UUV0}\Big(2a_1^2C_2(q_1)\left[n_1a_1+n_2a_2\right]\Big)\Big(\left[n_1a_1+n_2a_2\right]\Big) \\
&+3f_{UVV0}\Big(a_1^2C_2(q_1)\Big)\Big(\left[n_1a_1+n_2a_2\right]^2+a_2^2C_2(q_2)\Big)\Bigg] \\
&+O(a_1^5)+O(a_1^4a_2)+O(a_1^3a_2^2)+O(a_1^2a_2^3)+O(a_1a_2^4) \\
&=f_{U0}a_1^2C_2(q_1) \\
&+f_{UU0}a_1^2C_2(q_1)\left([n_1a_1+n_2a_2]+\left[n_{11}a_1^2+n_{12}a_1a_2+n_{22}a_2^2\right]\right) \\
&+f_{UV0}a_1^2C_2(q_1)\left([n_1a_1+n_2a_2]+\left[n_{11}a_1^2+n_{12}a_1a_2+n_{22}a_2^2\right]\right) \\
&+\frac{1}{6}f_{UUU0}\left(\left[n_1a_1+n_2a_2\right]^2a_1^2C_2(q_1)+a_1^4C_4(q_1)\right) \\
&+f_{UUV0}a_1^2C_2(q_1)\left[n_1a_1+n_2a_2\right]^2 \\
&+\frac{1}{2}f_{UVV0}a_1^2C_2(q_1)\left(\left[n_1a_1+n_2a_2\right]^2+a_2^2C_2(q_2)\right) \\
&+O(a_1^5)+O(a_1^4a_2)+O(a_1^3a_2^2)+O(a_1^2a_2^3)+O(a_1a_2^4) \qquad (4.47)
\end{aligned}
$$

$$
\begin{aligned}
&\int_{-\infty}^{\infty}\int_{-\infty}^{\infty} a_2 \,\mathrm{sat}\,\eta_2 f\mu(\mathrm{d}\eta_1)\mu(\mathrm{d}\eta_2) = \\
&\left[f_{V0}a_2^2C_2(q_2)\right] \\
&+\frac{1}{2}\Bigg[2f_{UV0}\Big(a_2^2C_2(q_2)\Big)\Big(\,[n_1a_1+n_2a_2]+\left[n_{11}a_1^2+n_{12}a_1a_2+n_{22}a_2^2\right] \\
&+f_{VV0}\Big(2a_2^2C_2(q_2)\left([n_1a_1+n_2a_2]+\left[n_{11}a_1^2+n_{12}a_1a_2+n_{22}a_2^2\right]\right)\Big)\Big)\Bigg] \\
&+\frac{1}{3!}\Bigg[3f_{UUV0}\Big(a_2^2C_2(q_2)\Big)\Big(\,[n_1a_1+n_2a_2]^2+a_1^2C_2(q_1)\Big) \\
&+3f_{UVV0}\Big(2a_2^2C_2(q_2)\,[n_1a_1+n_2a_2]\,\Big)\Big(\,[n_1a_1+n_2a_2]\,\Big) \\
&+f_{VVV0}\Big(\,[n_1a_1+n_2a_2]^2\,a_2^2C_2(q_2)+a_2^4C_4(q_2)\Big)\Bigg] \\
&+O(a_1^4a_2)+O(a_1^3a_2^2)+O(a_1^2a_2^3)+O(a_1a_2^4)+O(a_2^5) \\
&=f_{V0}a_2^2C_2(q_2) \\
&+f_{UV0}a_2^2C_2(q_2)\left([n_1a_1+n_2a_2]+\left[n_{11}a_1^2+n_{12}a_1a_2+n_{22}a_2^2\right]\right) \\
&+f_{VV0}a_2^2C_2(q_2)\left([n_1a_1+n_2a_2]+\left[n_{11}a_1^2+n_{12}a_1a_2+n_{22}a_2^2\right]\right) \\
&+\frac{1}{2}f_{UUV0}a_2^2C_2(q_2)\Big(\,[n_1a_1+n_2a_2]^2+a_1^2C_2(q_1)\Big) \\
&+f_{UVV0}a_2^2C_2(q_2)\,[n_1a_1+n_2a_2]^2 \\
&+\frac{1}{6}f_{VVV0}\Big(\,[n_1a_1+n_2a_2]^2\,a_2^2C_2(q_2)+a_2^4C_4(q_2)\Big) \\
&+O(a_1^4a_2)+O(a_1^3a_2^2)+O(a_1^2a_2^3)+O(a_1a_2^4)+O(a_2^5)
\end{aligned}
\tag{4.48}
$$

Solving (4.35c) and (4.35d) for s_2 and s_3 gives

$$\begin{aligned}
s_2 = {} & f_{U0} \\
& + f_{UU0}\left([n_1a_1 + n_2a_2] + \left[n_{11}a_1^2 + n_{12}a_1a_2 + n_{22}a_2^2\right]\right) \\
& + f_{UV0}\left([n_1a_1 + n_2a_2] + \left[n_{11}a_1^2 + n_{12}a_1a_2 + n_{22}a_2^2\right]\right) \\
& + \frac{1}{6}f_{UUU0}\left([n_1a_1 + n_2a_2]^2 + a_1^2\frac{C_4(q_1)}{C_2(q_1)}\right) \\
& + f_{UUV0}\left[n_1a_1 + n_2a_2\right]^2 \\
& + \frac{1}{2}f_{UVV0}\left([n_1a_1 + n_2a_2]^2 + a_2^2C_2(q_2)\right) \\
& + O(a_1^3) + O(a_1^2a_2) + O(a_1a_2^2) + O(a_2^3) + O(a_1^{-1}a_2^4)
\end{aligned} \tag{4.49}$$

$$\begin{aligned}
s_3 = {} & f_{V0} \\
& + f_{UV0}\left([n_1a_1 + n_2a_2] + \left[n_{11}a_1^2 + n_{12}a_1a_2 + n_{22}a_2^2\right]\right) \\
& + f_{VV0}\left([n_1a_1 + n_2a_2] + \left[n_{11}a_1^2 + n_{12}a_1a_2 + n_{22}a_2^2\right]\right) \\
& + \frac{1}{2}f_{UUV0}\left([n_1a_1 + n_2a_2]^2 + a_1^2C_2(q_1)\right) \\
& + f_{UVV0}\left[n_1a_1 + n_2a_2\right]^2 \\
& + \frac{1}{6}f_{VVV0}\left([n_1a_1 + n_2a_2]^2 + a_2^2\frac{C_4(q_2)}{C_2(q_2)}\right) \\
& + O(a_1^4a_2^{-1}) + O(a_1^3) + O(a_1^2a_2) + O(a_1a_2^2) + O(a_2^3)
\end{aligned} \tag{4.50}$$

Substituting these expressions into (4.35e) gives

$$\begin{aligned}
0 = {} & f_{U0} + f_{V0} \\
& + (f_{UU0} + 2f_{UV0} + f_{VV0})\left([n_1a_1 + n_2a_2] + \left[n_{11}a_1^2 + n_{12}a_1a_2 + n_{22}a_2^2\right]\right) \\
& + \frac{1}{6}f_{UUU0}\left([n_1a_1 + n_2a_2]^2 + a_1^2\frac{C_4(q_1)}{C_2(q_1)}\right) \\
& + \frac{1}{2}f_{UUV0}\left(3\left[n_1a_1 + n_2a_2\right]^2 + a_1^2C_2(q_1)\right) \\
& + \frac{1}{2}f_{UVV0}\left(3\left[n_1a_1 + n_2a_2\right]^2 + a_2^2C_2(q_2)\right) \\
& + \frac{1}{6}f_{VVV0}\left([n_1a_1 + n_2a_2]^2 + a_2^2\frac{C_4(q_2)}{C_2(q_2)}\right) \\
& + O(a_1^4a_2^{-1}) + O(a_1^3) + O(a_1^2a_2) + O(a_1a_2^2) + O(a_2^3) + O(a_1^{-1}a_2^4)
\end{aligned} \tag{4.51}$$

This equation is a polynomial in a_1 and a_2, so for the expression to be equal to zero the coefficients of each power of a must each be zero. Equating coefficients gives

$$a^0\colon\ 0 = f_{U0} + f_{V0} \tag{4.52a}$$

$$a_1^1\colon\ 0 = \left(f_{UU0} + 2f_{UV0} + f_{VV0}\right) n_1 \tag{4.52b}$$

$$a_2^1\colon\ 0 = \left(f_{UU0} + 2f_{UV0} + f_{VV0}\right) n_2 \tag{4.52c}$$

$$\begin{aligned} a_1^2\colon\ 0 = {} & \left(f_{UU0} + 2f_{UV0} + f_{VV0}\right) n_{11} \\ & + \frac{1}{6} f_{UUU0} \left(n_1^2 + \frac{C_4(q_1)}{C_2(q_1)}\right) + \frac{1}{2} f_{UUV0} \left(3n_1^2 + C_2(q_1)\right) \\ & + \frac{1}{2} f_{UVV0} \left(3n_1^2\right) + \frac{1}{6} f_{VVV0} \left(n_1^2\right) \end{aligned} \tag{4.52d}$$

$$\begin{aligned} a_1 a_2\colon\ 0 = {} & \left(f_{UU0} + 2f_{UV0} + f_{VV0}\right) n_{12} \\ & + \frac{1}{6} f_{UUU0} \left(2n_1 n_2\right) + \frac{1}{2} f_{UUV0} \left(6n_1 n_2\right) \\ & + \frac{1}{2} f_{UVV0} \left(6n_1 n_2\right) + \frac{1}{6} f_{VVV0} \left(2n_1 n_2\right) \end{aligned} \tag{4.52e}$$

$$\begin{aligned} a_2^2\colon\ 0 = {} & \left(f_{UU0} + 2f_{UV0} + f_{VV0}\right) n_{22} \\ & + \frac{1}{6} f_{UUU0} \left(n_2^2\right) + \frac{1}{2} f_{UUV0} \left(3n_2^2\right) \\ & + \frac{1}{2} f_{UVV0} \left(3n_2^2 + C_2(q_2)\right) + \frac{1}{6} f_{VVV0} \left(n_2^2 + \frac{C_4(q_2)}{C_2(q_2)}\right) \end{aligned} \tag{4.52f}$$

At this point consider the nature of the map. In steady flight, the aircraft is confined to the line $U = V$. Therefore, the optimal airspeed, which we will denote by V_*, is that point at which the component of the gradient in the direction of that line is zero. That is

$$\left.\frac{\partial f}{\partial U}\right|_{V_*} + \left.\frac{\partial f}{\partial V}\right|_{V_*} = f_{U*} + f_{V*} = 0 \tag{4.53}$$

Recall that the f_0 notation concerns the lift to drag ratio at the point (n_0, n_0). Assuming that along the line $U = V$ the map has a unique maximum, the a^0 equation requires that

$$n_0 = V_* \tag{4.54}$$

If the maximum is unique, then the curvature at that point along the line $U = V$ is non zero (specifically, negative). The curvature along this line is

$$\begin{aligned} & \frac{\partial}{\partial U}\left[\frac{\partial f}{\partial U}+\frac{\partial f}{\partial V}\right]\Big|_{V_*}+\frac{\partial}{\partial V}\left[\frac{\partial f}{\partial U}+\frac{\partial f}{\partial V}\right]\Big|_{V_*} \\ = & \left.\frac{\partial^2 f}{(\partial U)^2}\right|_{V_*}+2\left.\frac{\partial^2 f}{\partial U \partial V}\right|_{V_*}+\left.\frac{\partial^2 f}{(\partial V)^2}\right|_{V_*} \\ = & f_{UU*}+2f_{UV*}+f_{VV*}<0 \end{aligned} \tag{4.55}$$

Since $n_0 = V_*$, this means that f_0 is the same as f_*, and all derivatives are the same as well. Since the quantity in (4.55) is negative and therefore non-zero, it can be divided out of (4.52b) and (4.52c) to give

$$n_1 = 0 \tag{4.56}$$

$$n_2 = 0 \tag{4.57}$$

This simplifies the remaining equations in (4.52). They become

$$a_1^2\colon\ 0 = \left(f_{UU*}+2f_{UV*}+f_{VV*}\right)n_{11}+\frac{1}{6}f_{UUU*}\frac{C_4(q_1)}{C_2(q_1)}+\frac{1}{2}f_{UUV*}C_2(q_1) \tag{4.58a}$$

$$a_1a_2\colon\ 0 = \left(f_{UU*}+2f_{UV*}+f_{VV*}\right)n_{12} \tag{4.58b}$$

$$a_2^2\colon\ 0 = \left(f_{UU*}+2f_{UV*}+f_{VV*}\right)n_{22}+\frac{1}{2}f_{UVV*}C_2(q_2)+\frac{1}{6}f_{VVV*}\frac{C_4(q_2)}{C_2(q_2)} \tag{4.58c}$$

which gives

$$n_{11} = -\frac{f_{UUU*}C_4(q_1)+3f_{UUV*}\left(C_2(q_1)\right)^2}{6\left(f_{UU*}+2f_{UV*}+f_{VV*}\right)C_2(q_1)} \tag{4.59}$$

$$n_{12} = 0 \tag{4.60}$$

$$n_{22} = -\frac{3f_{UVV*}\left(C_2(q_2)\right)^2+f_{VVV*}C_4(q_2)}{6\left(f_{UU*}+2f_{UV*}+f_{VV*}\right)C_2(q_2)} \tag{4.61}$$

Substituting the obtained values of that n_0 n_1 n_2 n_{11} n_{12} and n_{22} back into the original Taylor expansion (4.36) gives a second order expression for the equilibrium value of v:

$$\begin{aligned} v = V_* & -\frac{f_{UUU*}C_4(q_1)+3f_{UUV*}\left(C_2(q_1)\right)^2}{6\left(f_{UU*}+2f_{UV*}+f_{VV*}\right)C_2(q_1)}a_1^2-\frac{3f_{UVV*}\left(C_2(q_2)\right)^2+f_{VVV*}C_4(q_2)}{6\left(f_{UU*}+2f_{UV*}+f_{VV*}\right)C_2(q_2)}a_2^2 \\ & +O(a_1^3)+O(a_1^2a_2)+O(a_1a_2^2)+O(a_2^3) \end{aligned} \tag{4.62}$$

Using the coefficients in (4.49) and (4.50) gives the equilibrium values of s_2 and s_3 as

$$\begin{aligned} s_2 = f_{U*} & \\ & - (f_{UU*} + f_{UV*}) \left[\frac{f_{UUU*} C_4(q_1) + 3 f_{UUV*} \left(C_2(q_1)\right)^2}{6 \left(f_{UU*} + 2 f_{UV*} + f_{VV*}\right) C_2(q_1)} a_1^2 \right. \\ & \left. + \frac{3 f_{UVV*} \left(C_2(q_2)\right)^2 + f_{VVV*} C_4(q_2)}{6 \left(f_{UU*} + 2 f_{UV*} + f_{VV*}\right) C_2(q_2)} a_2^2 \right] \\ & + \frac{1}{6} f_{UUU*} a_1^2 \frac{C_4(q_1)}{C_2(q_1)} + \frac{1}{2} f_{UVV*} a_2^2 C_2(q_2) \\ & + O(a_1^3) + O(a_1^2 a_2) + O(a_1 a_2^2) + O(a_2^3) + O(a_1^{-1} a_2^4) \end{aligned} \tag{4.63}$$

$$\begin{aligned} s_3 = f_{V*} & \\ & - (f_{UV*} + f_{VV*}) \left[\frac{f_{UUU*} C_4(q_1) + 3 f_{UUV*} \left(C_2(q_1)\right)^2}{6 \left(f_{UU*} + 2 f_{UV*} + f_{VV*}\right) C_2(q_1)} a_1^2 \right. \\ & \left. + \frac{3 f_{UVV*} \left(C_2(q_2)\right)^2 + f_{VVV*} C_4(q_2)}{6 \left(f_{UU*} + 2 f_{UV*} + f_{VV*}\right) C_2(q_2)} a_2^2 \right] \\ & + \frac{1}{2} f_{UUV*} a_1^2 C_2(q_1) + \frac{1}{6} f_{VVV*} a_2^2 \frac{C_4(q_2)}{C_2(q_2)} \\ & + O(a_1^4 a_2^{-1}) + O(a_1^3) + O(a_1^2 a_2) + O(a_1 a_2^2) + O(a_2^3) \end{aligned} \tag{4.64}$$

Using (4.53) the equilibrium value of s_1 is

$$s_1 = f + \frac{1}{2} \left[f_{UU*} a_1^2 C_2(q_1) + f_{VV*} a_2^2 C_2(q2) \right] + O(a_1^3) + O(a_1^2 a_2) + O(a_1 a_2^2) + O(a_2^3) \tag{4.65}$$

So the average system has an equilibrium point at

$$
\begin{aligned}
v = V_* &- \frac{f_{UUU*}C_4(q_1) + 3f_{UUV*}\left(C_2(q_1)\right)^2}{6\left(f_{UU*} + 2f_{UV*} + f_{VV*}\right)C_2(q_1)}a_1^2 \\
&- \frac{3f_{UVV*}\left(C_2(q_2)\right)^2 + f_{VVV*}C_4(q_2)}{6\left(f_{UU*} + 2f_{UV*} + f_{VV*}\right)C_2(q_2)}a_2^2 \\
&+ O(a_1^3) + O(a_1^2a_2) + O(a_1a_2^2) + O(a_2^3) \qquad (4.66a)
\end{aligned}
$$

$$
\begin{aligned}
s_1 = f_* &+ \frac{1}{2}\left[f_{UU*}a_1^2C_2(q_1) + f_{VV*}a_2^2C_2(q2)\right] \\
&+ O(a_1^3) + O(a_1^2a_2) + O(a_1a_2^2) + O(a_2^3) \qquad (4.66b)
\end{aligned}
$$

$$
\begin{aligned}
s_2 = f_{U*} &- \left(f_{UU*} + f_{UV*}\right)\left[\frac{f_{UUU*}C_4(q_1) + 3f_{UUV*}\left(C_2(q_1)\right)^2}{6\left(f_{UU*} + 2f_{UV*} + f_{VV*}\right)C_2(q_1)}a_1^2\right. \\
&\left. + \frac{3f_{UVV*}\left(C_2(q_2)\right)^2 + f_{VVV*}C_4(q_2)}{6\left(f_{UU*} + 2f_{UV*} + f_{VV*}\right)C_2(q_2)}a_2^2\right] \\
&+ \frac{1}{6}f_{UUU*}a_1^2\frac{C_4(q_1)}{C_2(q_1)} + \frac{1}{2}f_{UVV*}a_2^2C_2(q_2) \\
&+ O(a_1^3) + O(a_1^2a_2) + O(a_1a_2^2) + O(a_2^3) + O(a_1^{-1}a_2^4) \qquad (4.66c)
\end{aligned}
$$

$$
\begin{aligned}
s_3 = f_{V*} &- \left(f_{UV*} + f_{VV*}\right)\left[\frac{f_{UUU*}C_4(q_1) + 3f_{UUV*}\left(C_2(q_1)\right)^2}{6\left(f_{UU*} + 2f_{UV*} + f_{VV*}\right)C_2(q_1)}a_1^2\right. \\
&\left. + \frac{3f_{UVV*}\left(C_2(q_2)\right)^2 + f_{VVV*}C_4(q_2)}{6\left(f_{UU*} + 2f_{UV*} + f_{VV*}\right)C_2(q_2)}a_2^2\right] \\
&+ \frac{1}{2}f_{UUV*}a_1^2C_2(q_1) + \frac{1}{6}f_{VVV*}a_2^2\frac{C_4(q_2)}{C_2(q_2)} \\
&+ O(a_1^4a_2^{-1}) + O(a_1^3) + O(a_1^2a_2) + O(a_1a_2^2) + O(a_2^3) \qquad (4.66d)
\end{aligned}
$$

$$
\begin{aligned}
V_{cmd} = V_* &- \frac{f_{UUU*}C_4(q_1) + 3f_{UUV*}\left(C_2(q_1)\right)^2}{6\left(f_{UU*} + 2f_{UV*} + f_{VV*}\right)C_2(q_1)}a_1^2 \\
&- \frac{3f_{UVV*}\left(C_2(q_2)\right)^2 + f_{VVV*}C_4(q_2)}{6\left(f_{UU*} + 2f_{UV*} + f_{VV*}\right)C_2(q_2)}a_2^2 \\
&+ O(a_1^3) + O(a_1^2a_2) + O(a_1a_2^2) + O(a_2^3) \qquad (4.66e)
\end{aligned}
$$

To aid understanding, a lower order approximation of the equilibrium point is

given below.

$$v = V_* + O(a_1^2) + O(a_1 a_2) + O(a_2^2) \tag{4.67a}$$

$$s_1 = f_* + O(a_1^2) + O(a_1 a_2) + O(a_2^2) \tag{4.67b}$$

$$s_2 = f_{U*} + O(a_1^2) + O(a_1 a_2) + O(a_2^2) + O(a_1^{-1} a_2^3) \tag{4.67c}$$

$$s_3 = f_{V*} + O(a_1^3 a_2^{-1}) + O(a_1^2) + O(a_1 a_2) + O(a_2^2) \tag{4.67d}$$

$$V_{cmd} = V_* + O(a_1^2) + O(a_1 a_2) + O(a_2^2) \tag{4.67e}$$

Next, the stability of the equilibrium point is tested. The Jacobian of the average system in terms of the variables $(v, s_1, s_2, s_3, V_{cmd})$, evaluated at the equilibrium point $(v_{\rm eq}, v_{\rm eq})$, is

$$J = \begin{pmatrix} -\frac{1}{\tau} & 0 & 0 & 0 & \frac{1}{\tau} \\ J_{2,1} & -k_1 & 0 & 0 & 0 \\ J_{3,1} & 0 & -k_2 a_1^2 C_2(q_1) + \sigma_2 k_{ES} & \sigma_2 k_{ES} & 0 \\ J_{4,1} & 0 & \sigma_3 k_{ES} & -k_3 a_2^2 C_2(q_2) + \sigma_3 k_{ES} & 0 \\ 0 & 0 & k_{ES} & k_{ES} & 0 \end{pmatrix} \tag{4.68}$$

The expresssions for the remaining elements are

$$J_{2,1} = k_1 \frac{\partial}{\partial v} \left[\int_{-\infty}^{\infty} \int_{-\infty}^{\infty} f \mu(\mathrm{d}\eta_1) \mu(\mathrm{d}\eta_2) \right] \Bigg|_{v=v_{\rm eq}} \tag{4.69}$$

$$J_{3,1} = k_2 \frac{\partial}{\partial v} \left[\int_{-\infty}^{\infty} \int_{-\infty}^{\infty} a_1 \,\mathrm{sat}\, \eta_1 f \mu(\mathrm{d}\eta_1) \mu(\mathrm{d}\eta_2) \right] \Bigg|_{v=v_{\rm eq}} \tag{4.70}$$

$$J_{4,1} = k_3 \frac{\partial}{\partial v} \left[\int_{-\infty}^{\infty} \int_{-\infty}^{\infty} a_2 \,\mathrm{sat}\, \eta_2 f \mu(\mathrm{d}\eta_1) \mu(\mathrm{d}\eta_2) \right] \Bigg|_{v=v_{\rm eq}} \tag{4.71}$$

where the partial derivatives are evaluated at the equilibrium point. The charac-

teristic polynomial is

$$
\begin{aligned}
&\det(sI - J) \\
&= \begin{vmatrix}
s + \frac{1}{\tau} & 0 & 0 & 0 & -\frac{1}{\tau} \\
-J_{2,1} & s + k_1 & 0 & 0 & 0 \\
-J_{3,1} & 0 & s + k_2 a_1^2 C_2(q_1) - \sigma_2 k_{ES} & -\sigma_2 k_{ES} & 0 \\
-J_{4,1} & 0 & -\sigma_3 k_{ES} & s + k_3 a_2^2 C_2(q_2) - \sigma_3 k_{ES} & 0 \\
0 & 0 & -k_{ES} & -k_{ES} & s
\end{vmatrix} \\
&= (s + k_1) \Bigg\{ \\
&\quad s^4 \\
&\quad + \left[k_2 a_1^2 C_2(q_1) + k_3 a_2^2 C_2(q_2) - k_{ES} (\sigma_3 + \sigma_2) + \frac{1}{\tau} \right] s^3 \\
&\quad + \Bigg[k_2 k_3 a_1^2 a_2^2 C_2(q_1) C_2(q_2) - k_{ES} \left(\sigma_2 k_3 a_2^2 C_2(q_2) + \sigma_3 k_2 a_1^2 C_2(q_1) \right) \\
&\quad + \frac{1}{\tau} \left(k_2 a_1^2 C_2(q_1) + k_3 a_2^2 C_2(q_2) - k_{ES} (\sigma_3 + \sigma_2) \right) \Bigg] s^2 \\
&\quad + \Bigg[\frac{1}{\tau} \Big(k_2 k_3 a_1^2 a_2^2 C_2(q_1) C_2(q_2) \\
&\quad - k_{ES} \left(\sigma_2 k_3 a_2^2 C_2(q_2) + \sigma_3 k_2 a_1^2 C_2(q_1) + J_{3,1} + J_{4,1} \right) \Big) \Bigg] s \\
&\quad + \left[-\frac{1}{\tau} k_{ES} \left(J_{4,1} k_2 a_1^2 C_2(q_1) + J_{3,1} k_3 a_2^2 C_2(q_2) \right) \right] \Bigg\}
\end{aligned}
\tag{4.72}
$$

The $\dot{s}_1$ dynamics decouple from the rest of the system, leaving a fourth order polynomial. (The $\dot{s}_1$ dynamics are stable for any positive k_1.) The coefficients of the remaining fourth order polynomial must all be positive for the system to be stable. In addition, using the Routh-Hurwitz criteria to examine a polynomial of the form $s^4 + bs^3 + cs^2 + ds + e$ it can be shown that if the inequality $bcd > b^2 e + d^2$ holds, then the system is stable.

The s^3 and s^2 coefficients are positive if the gains k_2 k_3 and k_{ES} are chosen positive and the parameters σ_2 and σ_3 are chosen negative, but the remaining stability conditions depend on $J_{3,1}$ and $J_{4,1}$. In order to keep the analysis applicable to a general map, approximations are sought that are valid for small turbulence intensities.

Now the lift to drag ratio f is a function of U and V, but both U and V can be written as functions of v (see (4.37)). The lift to drag ratio can be approximated using a Taylor expansion around an arbitrary point (v, v):

$$\begin{aligned} f = f_v &+ \left[f_{Uv}\left(U-v\right) + f_{Vv}\left(V-v\right)\right] \\ &+ \frac{1}{2}\left[f_{UUv}\left(U-v\right)^2 + 2f_{UVv}\left(U-v\right)\left(V-v\right) + f_{VVv}\left(V-v\right)^2\right] \\ &+ O\left(\left(U-v\right)^3\right) \\ &+ O\left(\left(U-v\right)^2\left(V-v\right)\right) \\ &+ O\left(\left(U-v\right)\left(V-v\right)^2\right) \\ &+ O\left(\left(V-v\right)^3\right) \end{aligned} \tag{4.73}$$

Here, the notation f_v is used to refer to the value of f at the arbitrary point (v, v) as f_0 was used to refer to the value of f at the point (n_0, n_0) above; it does not denote a derivative with respect to v. Substituting (4.37) into (4.73) gives

$$\begin{aligned} f = f_v &+ \left[f_{Uv}\left(a_1 \operatorname{sat} \eta_1\right) + f_{Vv}\left(a_2 \operatorname{sat} \eta_2\right)\right] \\ &+ \frac{1}{2}\left[f_{UUv}\left(a_1 \operatorname{sat} \eta_1\right)^2 + 2f_{UVv}\left(a_1 \operatorname{sat} \eta_1\right)\left(a_2 \operatorname{sat} \eta_2\right) + f_{VVv}\left(a_2 \operatorname{sat} \eta_2\right)^2\right] \\ &+ O\left(\left(a_1 \operatorname{sat} \eta_1\right)^3\right) \\ &+ O\left(\left(a_1 \operatorname{sat} \eta_1\right)^2 a_2 \operatorname{sat} \eta_2\right) \\ &+ O\left(a_1 \operatorname{sat} \eta_1 \left(a_2 \operatorname{sat} \eta_2\right)^2\right) \\ &+ O\left(\left(a_2 \operatorname{sat} \eta_2\right)^3\right) \end{aligned} \tag{4.74}$$

Using this expression for f, the integrals in (4.70) and (4.71) can be evaluated. After simplification they reduce to

$$\begin{aligned} \int_{-\infty}^{\infty}\int_{-\infty}^{\infty} a_1 \operatorname{sat} \eta_1 f \mu(\mathrm{d}\eta_1)\mu(\mathrm{d}\eta_2) = f_{Uv}a_1^2 C_2(q_1) \\ + O\left(a_1^4\right) + O\left(a_1^3 a_2\right) + O\left(a_1^2 a_2^2\right) + O\left(a_1 a_2^3\right) \end{aligned} \tag{4.75}$$

$$\begin{aligned} \int_{-\infty}^{\infty}\int_{-\infty}^{\infty} a_2 \operatorname{sat} \eta_2 f \mu(\mathrm{d}\eta_1)\mu(\mathrm{d}\eta_2) = f_{Vv}a_2^2 C_2(q_2) \\ + O\left(a_1^3 a_2\right) + O\left(a_1^2 a_2^2\right) + O\left(a_1 a_2^3\right) + O\left(a_2^4\right) \end{aligned} \tag{4.76}$$

Now since U and V both vary directly with v, the partial derivative with respect to v can be expressed as the sum of the partial derivatives with respect to U and V:

$$\frac{\partial}{\partial v} = \frac{\partial}{\partial U}\frac{\partial U}{\partial v} + \frac{\partial}{\partial V}\frac{\partial V}{\partial v} = \frac{\partial}{\partial U} + \frac{\partial}{\partial V} \tag{4.77}$$

Taking these partial derivatives of the integrals (4.75) and (4.76) and evaluating at the equilibrium point $(v_{\text{eq}}, v_{\text{eq}})$ gives

$$\begin{aligned} J_{3,1} &= k_2 \frac{\partial}{\partial v}\left[\int_{-\infty}^{\infty}\int_{-\infty}^{\infty} a_1 \operatorname{sat}\eta_1 f\mu(\mathrm{d}\eta_1)\mu(\mathrm{d}\eta_2)\right]\Bigg|_{v=v_{\text{eq}}} \\ &= k_2\left(\frac{\partial}{\partial U}[f_{Uv}] + \frac{\partial}{\partial V}[f_{Uv}]\right)\Bigg|_{v=v_{\text{eq}}} a_1^2 C_2(q_1) \\ &\quad + O\left(a_1^4\right) + O\left(a_1^3 a_2\right) + O\left(a_1^2 a_2^2\right) + O\left(a_1 a_2^3\right) \\ &= k_2\left(f_{UU\text{eq}} + f_{UV\text{eq}}\right) a_1^2 C_2(q_1) + O\left(a_1^4\right) + O\left(a_1^3 a_2\right) + O\left(a_1^2 a_2^2\right) + O\left(a_1 a_2^3\right) \end{aligned} \tag{4.78a}$$

and similarly

$$J_{4,1} = k_3\left(f_{UV\text{eq}} + f_{VV\text{eq}}\right) a_2^2 C_2(q_2) + O\left(a_1^3 a_2\right) + O\left(a_1^2 a_2^2\right) + O\left(a_1 a_2^3\right) + O\left(a_2^4\right) \tag{4.78b}$$

Since these are already small a_1, a_2 approximation, note that the above expressions can be equivalently stated in terms of the second partial derivatives at the maximum of the map, since for small a_1, a_2 the equilibrium point approaches the maximum of the map. That is, since

$$v_{\text{eq}} = V_* + O(a_1^2) + O(a_1 a_2) + O(a_2^2) \tag{4.79}$$

we can say

$$f_{UU\text{eq}} = f_{UU*} + O(a_1^2) + O(a_1 a_2) + O(a_2^2) \tag{4.80}$$

and similarly with other derivatives. Then

$$J_{3,1} = k_2\left(f_{UU*} + f_{UV*}\right) a_1^2 C_2(q_1) + O\left(a_1^4\right) + O\left(a_1^3 a_2\right) + O\left(a_1^2 a_2^2\right) + O\left(a_1 a_2^3\right) \tag{4.81a}$$

$$J_{4,1} = k_3\left(f_{UV*} + f_{VV*}\right) a_2^2 C_2(q_2) + O\left(a_1^3 a_2\right) + O\left(a_1^2 a_2^2\right) + O\left(a_1 a_2^3\right) + O\left(a_2^4\right) \tag{4.81b}$$

With these approximations, the characteristic polynomial can be written for small a_1, a_2 as

$$
\begin{aligned}
&(s+k_1)\Bigg\{ \\
&s^4 \\
&+\left[-k_{ES}\left(\sigma_3+\sigma_2\right)+\frac{1}{\tau}+O\left(a_1^2\right)+O\left(a_2^2\right)\right]s^3 \\
&+\left[-\frac{k_{ES}}{\tau}\left(\sigma_3+\sigma_2\right)+O\left(a_1^2\right)+O\left(a_2^2\right)\right]s^2 \\
&+\Bigg[-\frac{k_{ES}}{\tau}\left(k_2\left(f_{UU*}+f_{UV*}+\sigma_3\right)a_1^2C_2(q_1)+k_3\left(f_{UV*}+f_{VV*}+\sigma_2\right)a_2^2C_2(q_2)\right) \\
&+O\left(a_1^4\right)+O\left(a_1^3a_2\right)+O\left(a_1^2a_2^2\right)+O\left(a_1a_2^3\right)+O\left(a_2^4\right)\Bigg]s \\
&+\Bigg[-\frac{1}{\tau}k_{ES}k_2k_3a_1^2a_2^2C_2(q_1)C_2(q_2)\left(f_{UU*}+2f_{UV*}+f_{VV*}\right) \\
&+O\left(a_1^5a_2\right)+O\left(a_1^4a_2^2\right)+O\left(a_1^3a_2^3\right)+O\left(a_1^2a_2^4\right)+O\left(a_1a_2^5\right)\Bigg]\Bigg\}
\end{aligned}
\tag{4.82}
$$

Now the stability criteria can be tested. Again, k_1 must be positive:

$$k_1 > 0 \tag{4.83a}$$

For small a_1, a_2, the s^3 and s^2 coefficients are positive provided k_{ES} is positive and the sum $(\sigma_3+\sigma_2)$ is negative:

$$k_{ES} > 0 \tag{4.83b}$$

$$(\sigma_3+\sigma_2) < 0 \tag{4.83c}$$

Similarly, the s^1 coefficient is positive provided that (in addition to k_{ES} being chosen positive) k_2 and k_3 are positive and σ_2, σ_3 are chosen sufficiently negative. Specifically, if

$$k_2 > 0 \tag{4.83d}$$

$$k_3 > 0 \tag{4.83e}$$

and

$$\sigma_3 < -\left(f_{UU*}+f_{UV*}\right) \tag{4.83f}$$

$$\sigma_2 < -\left(f_{UV*}+f_{VV*}\right) \tag{4.83g}$$

Note that the s^1 coefficient cannot be made positive by choosing k_{ES} small, since k_{ES} multiplies the entire coefficient (for the small a_1, a_2 approximation, at least). Finally, for small a_1, a_2, the s^0 coefficient is positive provided that k_{ES}, k_2, and k_3 are chosen positive. [Recall from (4.55) that since we assume a unique maximum point along the line $U = V$, it follows that $f_{UU*} + 2f_{UV*} + f_{VV*} < 0$.]

So in the analysis of the characteristic polynomial, the conditions under which all of the coefficients are positive have been found. For stability, it remains to be shown that (in terms of a polynomial of the form $s^4 + bs^3 + cs^2 + ds + e$) the inequality $bcd > b^2e + d^2$ holds. The stability criterion simplifies to

$$\begin{aligned}
&\left[-k_{ES}\left(\sigma_3 + \sigma_2\right) + \frac{1}{\tau}\right] \times \left[\frac{1}{\tau}\left(-k_{ES}\left(\sigma_3 + \sigma_2\right)\right)\right] \\
&\times \left[-\frac{k_{ES}}{\tau}\Big(k_2\left(f_{UU*} + f_{UV*} + \sigma_3\right) a_1^2 C_2(q_1)\right. \\
&\left. + k_3\left(f_{UV*} + f_{VV*} + \sigma_2\right) a_2^2 C_2(q_2)\Big)\right] > \\
&0 + O\left(a_1^4\right) + O\left(a_1^3 a_2\right) + O\left(a_1^2 a_2^2\right) + O\left(a_1 a_2^3\right) + O\left(a_2^4\right)
\end{aligned} \tag{4.84}$$

This criterion is satisfied for small a_1, a_2 under the criteria already required to ensure the coefficients of the characteristic polynomial are positive. The equilibrium (4.66) of the closed loop system (4.23) is stable for small a_1, a_2 under the conditions (4.83).

The conditions on σ_2, σ_3 can be simplified somewhat. Given from (4.55) that $f_{UU*} + 2f_{UV*} + f_{VV*} < 0$, the following inequalities hold:

$$\frac{1}{2}\left(f_{VV*} - f_{UU*}\right) < -\left(f_{UU*} + f_{UV*}\right) \tag{4.85a}$$

$$\frac{1}{2}\left(f_{UU*} - f_{VV*}\right) < -\left(f_{UV*} + f_{VV*}\right) \tag{4.85b}$$

If the parameters σ_2 and σ_3 are chosen according to

$$\sigma_3 < \frac{1}{2}\left(f_{VV*} - f_{UU*}\right) \tag{4.86a}$$

$$\sigma_2 < \frac{1}{2}\left(f_{UU*} - f_{VV*}\right) \tag{4.86b}$$

then (4.83c), (4.83f), and (4.83g) are satisfied.

This concludes the bulk of the analysis. The average system has a stable equilibrium at the point given in (4.66) which is within an $O(a_1^2)+O(a_1a_2)+O(a_2^2)$ neighborhood of the optimal endurance speed. The linearized average system is stable if the turbulence intensities a_1 and a_2 are small but non-zero, the gains k_1, k_2, k_3, k_{ES} are chosen positive, and the design parameters σ_2, σ_3 are chosen to satisfy the criteria given in (4.86). Stability of the linearized average system proves local exponential stability of the average system (4.34) by Corollary 4.3 in [25]. Stability of the average system proves weak stability of the closed loop system (4.23) under the stochastic perturbations η_1 and η_2, by the stochastic averaging results in [3]. This result is expressed in Theorem 2.

4.6 Simulations

4.6.1 Simple Simulation

Before proceeding to the high fidelity simulations, the results of a simpler simulation are presented. This simulation follows (4.23) closely. The parameters of the simulation are listed in Table 4.1. They are chosen roughly to represent a U-2 flying at maximum takeoff weight at 36,000 feet. The turbulence parameters are chosen to model isotropic turbulence with a root mean square intensity of 3 ft/s and a characteristic length of 1,750 feet. To align with the assumptions of the analysis, the turbulence is bounded to less than 100 ft/s. The lift to drag ratio is modeled assuming a quadratic drag polar and using the Prandtl-Glauert rule. Written as a function of equivalent steady state airspeed and airspeed, the lift to drag ratio is

$$f(U,V) = \frac{\frac{2mg}{U^2\rho S}}{C_{D0} + \frac{1}{\pi Ae}\left(\frac{2mg}{U^2\rho S}\right)^2\left(1-\left(\frac{V}{a}\right)^2\right)} \tag{4.87}$$

The constants in this formula are given Table 4.1. The controller gains and design parameters are also listed. The results of this simple simulation are shown in Fig. 4.2.

Table 4.1: Simulation parameters

Parameter	Value	Units
a_1	100	ft/s
a_2	100	ft/s
ϵ_1	4.00	s
ϵ_2	4.00	s
q_1	0.225	$s^{1/2}$
q_2	0.0424	$s^{1/2}$
mg	40000	lbf
C_{D0}	0.0106	-
A	10.6	-
e	1	-
S	1000	ft^2
ρ	0.00070449	$slug/ft^3$
a	968.08	ft/s
τ	5	s
k_1	0.200	1/s
k_2	1.98e-4	s/ft^2
k_3	0.00556	s/ft^2
k_{ES}	22.9	ft^2/s^3
σ_2	-6.53e-4	s^2/ft^2
σ_3	0.00	s^2/ft^2

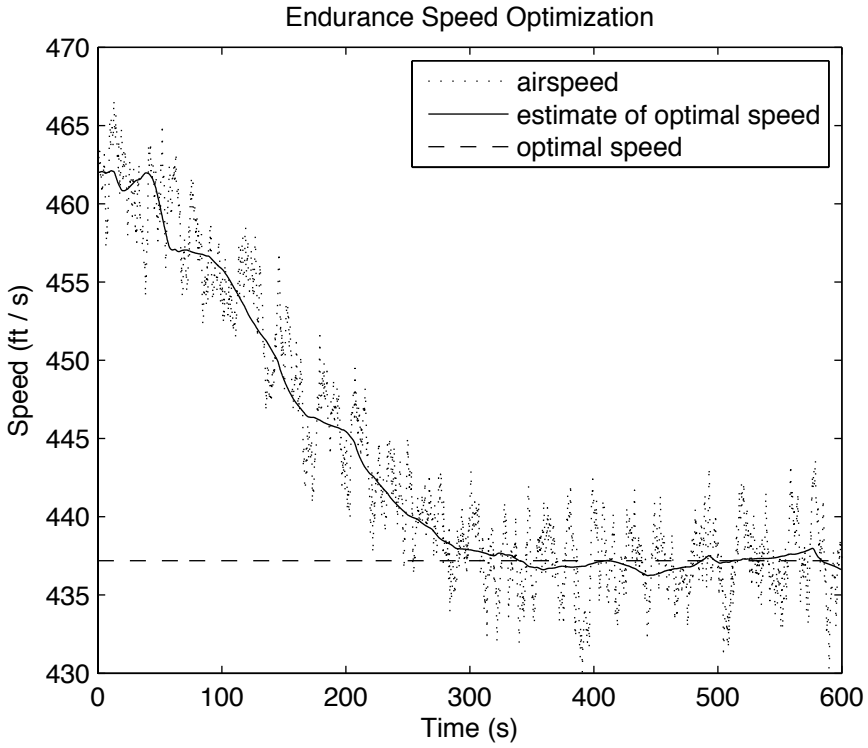

Figure 4.2: Results of a simulation closely following (4.23).

4.6.2 High-Fidelity Simulation Description

The software used for the following simulations is a six degree of freedom simulation routine developed by local industry. Because of the proprietary nature of the simulation, the simulation cannot be described in detail, but the simulation is highly realistic and has been validated by flight test data. It order to prevent disclosure of proprietary aircraft performance data, the numbers have been removed from all axes of figures showing high-fidelity simulation results.

4.6.3 Experiment Design

Two experiments are performed using the high-fidelity simulation software. The first is designed to test the extremum seeking algorithm. The simulation begins with the aircraft flying straight and level at its nominal loiter speed. The aircraft then encounters turbulence and the extremum seeking algorithm is activated; the aircraft adjusts its airspeed to the estimate of the optimal airspeed found by the algorithm. The turbulence encounter then ends and the extremum seeking control law is disengaged. From this point on, the airspeed command is set to maintain the same coefficient of lift as found by the extremum seeking algorithm. The simulation is then allowed to run for a short time to allow transients to settle. For comparison, the simulation is repeated without activating the extremum seeking algorithm. The steady fuel flow rate achieved by the extremum seeking algorithm is then compared to the steady fuel flow rate at the nominal loiter speed. A lower fuel flow rate corresponds to higher endurance.

The second experiment is designed to test the effectiveness of holding a constant coefficient of lift after the turbulence encounter ends. The experiment is similar to the first, with the following changes. The experiment runs for a much longer period of time, during which significant changes in aircraft weight occur, due to fuel being burned. The experiment is also run using settings of higher realism in the simulation software, which make for a good experiment but poor graphs, and as such are not used in the first experiment. Like the first experiment, the second experiment consists of two simulations that are identical, except that in one extremum seeking is active and in the other the aircraft remains at the

nominal loiter speed. The aircraft weight decreases in both simulations as fuel is burned. The difference between the aircraft weights indicates the net fuel savings from extremum seeking.

Note that because this is a computer simulation, the nominal loiter speed is expected to be at or very near the optimal endurance speed. The primary benefit of extremum seeking is that it is able to adapt to differences from the aerodynamic model that may exist in real flight. These simulations do not introduce any such differences, so the level of endurance achieved by extremum seeking is expected to be only as good as that achieved by the nominal loiter speed. The simulations test the ability of extremum seeking to achieve a level of endurance on par with that achieved by the nominal loiter speed in simulation, which provides a measure of confidence in the ability of the algorithm to find the true optimal endurance speed in real flight.

4.6.4 High-Fidelity Simulation Results

The results of the first experiment are shown in Fig. 4.3, Fig. 4.4, and Fig. 4.5. In these figures, results using the extremum seeking algorithm are shown in black; the results not using extremum seeking are shown in the background in gray. The small region boxed in Fig. 4.4 is shown enlarged in Fig. 4.5.

The results of the second experiment are shown in Fig. 4.6. The aircraft weight over the course of the simulations is plotted against the left axis, again in black for the results using extremum seeking and gray for the results not using extremum seeking. Because the curves overlap almost identically, the difference between the two curves is plotted in the same figure against the right axis, as a dashed line, on a much larger scale. Note that the difference is initially zero and becomes positive, indicating that weight of the aircraft using extremum seeking is greater than that of the aircraft at the nominal loiter speed.

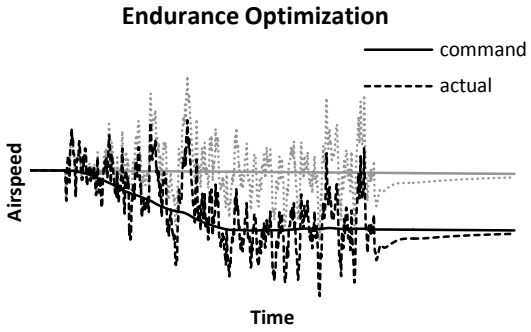

Figure 4.3: Airspeed optimization by extremum seeking.

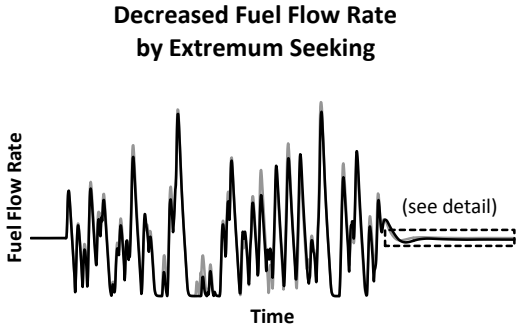

Figure 4.4: Fuel flow rate.

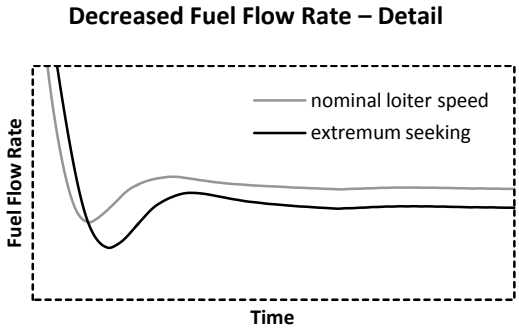

Figure 4.5: Fuel flow rate detail plot.

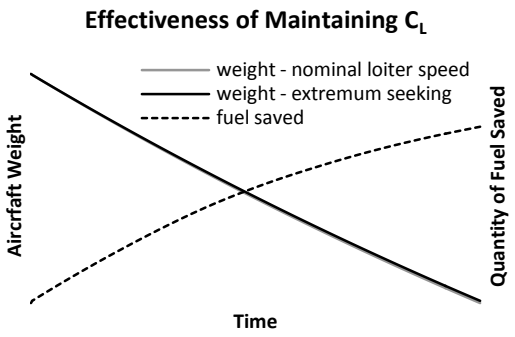

Figure 4.6: Net fuel savings over a long flight achieved by flying a constant C_L after exiting turbulence.

4.7 Discussion

The simulation results show that the extremum seeking algorithm matches the fuel economy of flight at the nominal loiter speed in simulation, without knowledge of the performance characteristics of the aircraft (see Fig. 4.4). The algorithm slightly exceeds the performance achieved at the nominal loiter speed; the difference is small but noticeable (Fig. 4.5). In simulations based on wind tunnel data, the nominal loiter speed should be close to the optimal endurance speed; the fact that the simulations show convergence to near the nominal loiter speed (with actually even slightly better performance) gives some confidence that the optimal speed may be found regardless of the aerodynamic characteristics of the aircraft. The benefit of the algorithm is not primarily in the slight performance improvements shown in these figures. Rather, the benefit is in the potentially more significant improvements that might be achieved in actual flight where the aerodynamic characteristics of the aircraft may differ from the wind tunnel data. Such differences may appear over time due to accumulated minor damage to the plane or due to environmental conditions such as structural icing. In such situations the endurance benefits from extremum seeking may become significant.

As shown in Fig. 4.6, the performance obtained by extremum seeking is maintained after exiting turbulence by adjusting the airspeed to fly a constant coefficient of lift. The difference between the aircraft weight in the simulation using

extremum seeking and the aircraft weight in the simulation at the nominal loiter speed, shown as the dashed line in Fig. 4.6, consistantly increases throughout the simulation. This indicates that the aircraft using extremum seeking continues to burn fuel at a slower rate than the aircraft at the nominal loiter speed throughout the flight, even though extremum seeking is only active for a short period of time at the beginning of the flight.

The simulation results also confirm the stability analysis performed above. This may lend some creedence to the modeling assumptions used in the analysis. A limitation of the result in Theorem 2 is that it speaks to the limiting case as the turbulence timescales (ϵ_1 and ϵ_2) approach zero. Stated another way, the theorem describes the behavior of the system when all timescales are slow compared to the turbulence timescales. As such the theorem does not make any claim regarding the behaviour of the system on timescales comparable to the turbulence. Since the high-fidelity simulation results are presented without units, the simple simulation results shown in Fig. 4.2 are presented to speak to the rate of convergence of the algorithm. (Again, to avoid inadvertently revealing any aircraft performance data, the parameters used in the simple simulations are not the same as those used in the high-fidelity simulations.)

Another limitation of the result in Theorem 2 is that it applies only when turbulence is small but non-zero. The controller cannot function in calm air and it is also possible that the controller could become unstable in unexpectedly heavy turbulence. While the intensity of turbulence can never be controlled, the design parameters can be adjusted to ensure stability in a worst-case turbulence encounter.

One area that remains to be addressed is operation in turning flight. The analysis and simulations above all assume straight and level flight, but loitering is commonly performed in a holding pattern, which involves portions of turning flight and portions of straight flight. The algorithm may require modification to be applicable to turning flight.

4.8 Conclusions

The extremum seeking algorithm stabilizes the aircraft to near the optimal endurance speed, accounting for both angle of attack and compressibility effects, using the excitation provided by atmospheric turbulence. Simulation results using a high-fidelity aircraft simulation routine show that the algorithm achieves a level of endurance slightly greater than that at the nominal loiter speed of the aircraft. This provides confidence that the optimal airspeed may be achieved in real flight where the aerodynamic characteristics of the aircraft are not known. The results validate the performance of the new form of gradient estimator used in the extremum seeking algorithm. After a turbulence encounter has ended, flying a constant coefficient of lift is an adequate means of maintaining the optimal airspeed as aircraft weight decreases.

4.9 Acknowledgements

This work was supported in part by the San Diego chapter of the ARCS Foundation. The authors would also like to thank the representatives of local industry who made possible the high-fidelity simulations.

Chapter 4 contains material that has been submitted for publication to the Journal of Guidance, Control, and Dynamics (Krieger, J., and Krstic, M.). The dissertation author was the primary investigator and author of this material.

References

[1] Ariyur, K. B., and Krstic, M., "SISO Scheme and Linear Analysis," *Real-Time Optimization by Extremum-Seeking Control*, John Wiley & Sons, Inc., Hoboken, NJ, 2003.

[2] Tan, Y., Moase, W. H., Manzie, C., Nesic, D., and Mareels, I. M. Y., "Extremum Seeking from 1922 to 2010," *Proceedings of the 29th Chinese Control Conference*, IEEE Publ., Piscataway, NJ, 2010, pp. 14–26.

[3] Liu, S.-J., and Krstic, M., "Stochastic Averaging in Continuous Time and Its Applications to Extremum Seeking," *IEEE Transactions on Automatic Control*, Vol. 55, No. 10, Oct. 2010, pp. 2235–2250.
doi:10.1109/TAC.2010.2043290

[4] Carnevale, D., Astolfi, A., Centioli, C., Podda, S., Vitale, V., and Zaccarian, L., "A New Extremum Seeking Technique and Its Application To Maximize RF Heating on FTU," *Fusion Engineering and Design*, Vol. 84, No. 2-6, 2009, pp. 554–558.
doi:10.1016/j.fusengdes.2008.12.032

[5] Wang, H.-H., and Krstic, M., "Extremum Seeking for Limit Cycle Minimization," *IEEE Transactions on Automatic Control*, Vol. 45, No. 12, Dec. 2000, pp. 2432–2436.
doi:10.1109/9.895589

[6] Choi, J.-Y., Krstic, M., Ariyur, K. B., and Lee, J. S., "Extremum Seeking Control for Discrete-Time Systems," *IEEE Transactions on Automatic Control*, Vol. 47, No. 2, Feb. 2002, pp. 318–323.
doi:10.1109/9.983370

[7] Tan, Y., Nesic, D., and Mareels, I., "On the Choice of Dither in Extremum Seeking Systems: A Case Study," *Automatica*, Vol. 44, No. 5, 2008, pp. 1446–1450.
doi:10.1016/j.automatica.2007.10.016

[8] Manzie, C., and Krstic, M., "Extremum Seeking with Stochastic Perturbations," *IEEE Transactions on Automatic Control*, Vol. 54, No. 3, Mar. 2009, pp. 580–585.
doi:10.1109/TAC.2008.2008320

[9] Tanelli, M., Astolfi, A., and Savaresi, S. M., "Non-Local Extremum Seeking Control for Active Braking Control Systems," *Proceedings of the 2006 IEEE International Conference on Control Applications*, IEEE Publ., Piscataway, NJ, 2006, pp. 891–896.
doi:10.1109/CACSD-CCA-ISIC.2006.4776763

[10] Schuster, E., Xu, C., Torres, N., Morinaga, E., Allen, C., and Krstic, M., "Beam Matching Adaptive Control via Extremum Seeking," *Nuclear Instruments and Methods in Physics Research Section A: Accelerators, Spectrometers, Detectors and Associated Equipment*, Vol. 581, No. 3, 2007, pp. 799–815.
doi:10.1016/j.nima.2007.07.154

[11] Wang, H.-H., Yeung, S., and Krstic, M., "Experimental Application of Extremum Seeking on an Axial-Flow Compressor," *IEEE Transactions on Control Systems Technology*, Vol. 8, No. 2, Mar. 2000, pp. 300–309.
doi:10.1109/87.826801

[12] Banaszuk, A., Ariyur, K. B., Krstic, M., and Jacobson, C. A., "An Adaptive Algorithm for Control of Combustion Instability," *Automatica*, Vol. 40, No. 11, 2004, pp. 1965–1972.
doi:10.1016/j.automatica.2004.06.008

[13] Moeck, J. P., Bothien, M. R., Paschereit, C. O., Gelbert, G., and King, R., "Two-Parameter Extremum Seeking for Control of Thermoacoustic Instabilities and Characterization of Linear Growth," AIAA Paper 2007-1416, Jan. 2007.

[14] Becker, R., King, R., Petz, R., and Nitsche, W., "Adaptive Closed-Loop Separation Control on a High-Lift Configuration Using Extremum Seeking," *AIAA Journal*, Vol. 45, No. 6, 2007, pp. 1382–1392.
doi:10.2514/1.24941

[15] Bastin, G., Nešić, D., Tan, Y., and Mareels, I., "On Extremum Seeking in Bioprocesses with Multivalued Cost Functions," *Biotechnology Progress*, Vol. 25, No. 3, 2009, pp. 683–689.
doi:10.1002/btpr.87

[16] Ou, Y., Xu, C., Schuster, E., Luce, T. C., Ferron, J. R., Walker, M. L., and Humphreys, D. A., "Design and Simulation of Extremum-Seeking Open-Loop Optimal Control of Current Profile in the DIII-D Tokamak," *Plasma Physics*

and Controlled Fusion, Vol. 50, No. 11, 2008, Paper 115001.
doi:10.1088/0741-3335/50/11/115001

[17] Binetti, P., Ariyur, K. B., Krstic, M., and Bernelli, F., "Formation Flight Optimization Using Extremum Seeking Feedback," *Journal of Guidance, Control, and Dynamics*, Vol. 26, No. 1, 2003, pp. 132–142.
doi:10.2514/2.5024

[18] Sachs, G., "Optimization of Endurance Performance," *Progress in Aerospace Sciences*, Vol. 29, No. 2, 1992, pp. 165–191.
doi:10.1016/0376-0421(92)90006-4

[19] Sachs, G., Lenz, J., and Holzapfel, F., "Periodic Optimal Flight of Solar Aircraft with Unlimited Endurance Performance," *Applied Mathematical Sciences*, Vol. 4, No. 76, 2010, pp. 3761–3778.

[20] Chen, R. H., and Speyer, J. L., "Improved Endurance of Optimal Periodic Flight," *Journal of Guidance, Control, and Dynamics*, Vol. 30, No. 4, 2007, pp. 1123–1133.
doi:10.2514/1.27313

[21] Chen, R. H., and Speyer, J. L., "Optimization and Mechanization of Periodic Flight," US Patent Application Publication US 2009/0177339 A1, 9 Jul. 2009, p. 1.

[22] Phillips, W. F., "Aircraft Performance," *Mechanics of Flight*, John Wiley & Sons, Inc., Hoboken, NJ, 2004.

[23] Roskam, J., and Lan, C. E., "Airplane Drag," *Airplane Aerodynamics and Performance*, DARcorporation, Lawrence, KS, 1997.

[24] "Flying Qualities of Piloted Airplanes," Military Specification MIL-F-8785C, 1980.

[25] Khalil, H. K., *Nonlinear Systems*, 3rd ed., Prentice Hall, Upper Saddle River, NJ, 2002, p. 166.

[26] Stankovic, M. S., and Stipanovic, D. M., "Extremum Seeking Under Stochastic Noise and Applications to Mobile Sensors," *Automatica*, Vol. 46, No. 8, 2010, pp. 1243–1251.
doi:10.1016/j.automatica.2010.05.005

[27] Moase, W. H., Manzie, C., and Brear, M. J., "Newton-Like Extremum-Seeking for the Control of Thermoacoustic Instability," *IEEE Transactions on Automatic Control*, Vol. 55, No. 9, 2010, pp. 2094–2105.
doi:10.1109/TAC.2010.2042981

[28] Tan, Y., Nesic, D., and Mareels, I., "On Non-Local Stability Properties of Extremum Seeking Control," *Automatica*, Vol. 42, No. 6, 2006, pp. 889–903. doi:10.1016/j.automatica.2006.01.014

[29] Liu, S.-J., and Krstic, M., "Stochastic Source Seeking for Nonholonomic Unicycle," *Automatica*, Vol. 46, No. 9, 2010, pp. 1443–1453. doi:10.1016/j.automatica.2010.05.025

[30] Ghaffari, A., Krstic, M., and Nesic, D., "Multivariable Newton-Based Extremum Seeking," *Automatica*, 2012.

[31] Ryan, J., and Speyer, J., "Peak-Seeking Control Using Gradient and Hessian Estimates," *2010 American Control Conference*, IEEE Publ., Piscataway, NJ, 2010, pp. 611–616.

[32] Guay, M., and Zhang, T., "Adaptive Extremum Seeking Control of Nonlinear Dynamic Systems with Parametric Uncertainties," *Automatica*, Vol. 39, No. 7, 2003, pp. 1283–1293. doi:10.1016/S0005-1098(03)00105-5

[33] Adetola, V., and Guay, M., "Parameter Convergence in Adaptive Extremum-Seeking Control," *Automatica*, Vol. 43, No. 1, 2007, pp. 105 – 110. doi:10.1016/j.automatica.2006.07.021

[34] Krieger, J. P., and Krstic, M., "Extremum Seeking Based on Atmospheric Turbulence for Aircraft Endurance," *Journal of Guidance, Control, and Dynamics*, Vol. 34, No. 6, 2011, pp. 1876–1885. doi:10.2514/1.53825

[35] Sherman, J., and Morrison, W. J., "Adjustment of an Inverse Matrix Corresponding to a Change in One Element of a Given Matrix," *The Annals of Mathematical Statistics*, Vol. 21, No. 1, 1950, pp. 124–127. doi:10.1214/aoms/1177729893

[36] Rotea, M. A., "Analysis of Multivariable Extremum Seeking Algorithms," *Proceedings of the American Control Conference*, IEEE Publ., Piscataway, NJ, 2000, pp. 433–437. doi:10.1109/ACC.2000.878937

[37] Kim, K., Kasnakoglu, C., Serrani, A., and Samimy, M., "Extremum-Seeking Control of Subsonic Cavity Flow," *AIAA Journal*, Vol. 47, No. 1, 2009, pp. 195–205. doi:10.2514/1.38180

[38] Creaby, J., Li, Y., and Seem, J. E., "Maximizing Wind Turbine Energy Capture using Multivariable Extremum Seeking Control," *Wind Engineering*, Vol. 33, No. 4, 2009, pp. 361–387.
doi:10.1260/030952409789685753

[39] Stankovic, M., Johansson, K., and Stipanovic, D., "Distributed Seeking of Nash Equilibria with Applications to Mobile Sensor Networks," *IEEE Transactions on Automatic Control*, Vol. PP, No. 99, 2011, p. 1.
doi:10.1109/TAC.2011.2174678

[40] Zhang, C., Arnold, D., Ghods, N., Siranosian, A., and Krstic, M., "Source Seeking with Non-Holonomic Unicycle Without Position Measurement and with Tuning of Forward Velocity," *Systems & Control Letters*, Vol. 56, No. 3, 2007, pp. 245 – 252.
doi:10.1016/j.sysconle.2006.10.014

[41] Cochran, J., and Krstic, M., "Nonholonomic Source Seeking with Tuning of Angular Velocity," *IEEE Transactions on Automatic Control*, Vol. 54, No. 4, 2009, pp. 717–731.
doi:10.1109/TAC.2009.2014927

[42] Zhang, X., Dawson, D., Dixon, W., and Xian, B., "Extremum-Seeking Nonlinear Controllers for a Human Exercise Machine," *IEEE/ASME Transactions on Mechatronics*, Vol. 11, No. 2, 2006, pp. 233–240.
doi:10.1109/TMECH.2006.871896

[43] Li, Y., Rotea, M., Chiu, G.-C., Mongeau, L., and Paek, I.-S., "Extremum Seeking Control of a Tunable Thermoacoustic Cooler," *IEEE Transactions on Control Systems Technology*, Vol. 13, No. 4, 2005, pp. 527–536.
doi:10.1109/TCST.2005.847334

[44] Killingsworth, N. J., and Krstic, M., "PID Tuning Using Extremum Seeking: Online, Model-Free Performance Optimization," *IEEE Control Systems*, Vol. 26, No. 1, 2006, pp. 70–79.
doi:10.1109/MCS.2006.1580155

[45] Moran, J., "Compressible Potential Flow past Airfoils," *An Introduction to Theoretical and Computational Aerodynamics*, Dover, Mineola, NY, 2003.